MICROCOPY RESOLUTION TEST CHART

LEVEL

ESL-TR-80-39

ATMOSPHERIC CHEMISTRY OF HYDRAZINES: GAS PHASE KINETICS AND MECHANISTIC STUDIES

JAMES N. PITTS, JR.

ERNESTO C. TUAZON, WILLIAM P. CARTER, ARTHUR M. WINER,
GEOFFREY W. HARRIS, ROGER ATKINSON, RICHARD A. GRAHAM

STATEWIDE AIR POLLUTION RESEARCH CENTER
UNIVERSITY OF CALIFORNIA
RIVERSIDE, CALIFORNIA 92521

AUGUST 1980

FINAL REPORT
SEPTEMBER 1978 - JUNE 1980

DTIC
ELECTE
JAN 7 1981
S D
A

ENGINEERING & SERVICES LABORATORY
AIR FORCE ENGINEERING & SERVICES CENTER
TYNDALL AIR FORCE BASE, FLORIDA 32403

AD A093486

DDC FILE COPY

81 1 06 019

NOTICE

Please do not request copies of this report from
HQ AFESC/RD (Engineering and Services Laboratory).
Additional copies may be purchased from:

National Technical Information Service
5285 Port Royal Road
Springfield, Virginia 22161

Federal Government agencies and their contractors
registered with Defense Technical Information Center
should direct requests for copies of this report to:

Defense Technical Information Center
Cameron Station
Alexandria, Virginia 22314

REPORT DOCUMENTATION PAGE		READ INSTRUCTIONS BEFORE COMPLETING FORM
1. REPORT NUMBER AFESC/ESL-TR-80-39	2. GOVT ACCESSION NO. AD-A092 486	3. RECIPIENT'S CATALOG NUMBER
4. TITLE (and Subtitle) ATMOSPHERIC CHEMISTRY OF HYDRAZINES: GAS PHASE KINETICS AND MECHANISTIC STUDIES		5. TYPE OF REPORT & PERIOD COVERED Final Report September 1978—June 1980
		6. PERFORMING ORG. REPORT NUMBER
7. AUTHOR(s) James N. Pitts, Jr., Ernesto C. Tuazon, William P. L. Carter, Arthur M. Winer, Geoffrey W. Harris, Roger Atkinson, Richard A. Graham		8. CONTRACT OR GRANT NUMBER(s) F08635-78-C-0307
9. PERFORMING ORGANIZATION NAME AND ADDRESS Statewide Air Pollution Research Center University of California Riverside, California 92521		10. PROGRAM ELEMENT, PROJECT, TASK AREA & WORK UNIT NUMBERS Program Element 62601F Project 19002015
11. CONTROLLING OFFICE NAME AND ADDRESS AIR FORCE ENGINEERING AND SERVICES CENTER Tyndall Air Force Base, Florida 32403		12. REPORT DATE August 1980
		13. NUMBER OF PAGES 88
14. MONITORING AGENCY NAME & ADDRESS(if different from Controlling Office)		15. SECURITY CLASS. (of this report) UNCLASSIFIED
		15a. DECLASSIFICATION/DOWNGRADING SCHEDULE

16. DISTRIBUTION STATEMENT (of this Report)

Approved for public release; distribution unlimited.

17. DISTRIBUTION STATEMENT (of the abstract entered in Block 20, if different from Report)

18. SUPPLEMENTARY NOTES

Availability of this report is specified on verso of front cover.

19. KEY WORDS (Continue on reverse side if necessary and identify by block number)

Hydrazine	Environmental Simulation
Oxidation	Environmental Quality
Ozone	Missile Fuels
Nitrogen Oxides	

20. ABSTRACT (Continue on reverse side if necessary and identify by block number)

Relatively little work has been done on the atmospheric chemistry of nitrogen-containing compounds such as amines and hydrazines, which are widely used in industrial and military applications. However the discovery of compounds such as N-nitrosamines in the environment and concern regarding their impact on man indicate the need to further elucidate the role of nitrogenous compounds in the atmosphere.

The Air Force is presently assessing the environmental impact of the Space

DD FORM 1473 EDITION OF 1 NOV 68 IS OBSOLETE

20. ABSTRACT (CONCLUDED)

Transportation System which uses hydrazine as one of the fuels. In addition, hydrazine is used as a propellant in the F-16 for emergency power. Both uses will result in potential atmospheric releases which should be controlled to a degree dictated by the impact of hydrazines on ambient air quality. Thus, the present study was designed to experimentally evaluate the atmospheric fate of unsubstituted hydrazine (N_2H_4), monomethylhydrazine (MMH), and unsymmetrical dimethylhydrazine (UDMH).

Because of the need for detailed information on the gas phase chemistry of selected hydrazines, the following specific studies were undertaken: flash photolysis-resonance fluorescence measurements of the absolute rate constants for the reaction of hydrazines with OH radicals; a study of the rates and products of the dark reactions of ozone with N_2H_4, MMH, and UDMH; and an investigation of the NO_x-photooxidation of these same hydrazines under simulated atmospheric conditions. The latter two studies were conducted using a 30,000-liter outdoor irradiation chamber equipped with a 10-meter basepath optical system coupled to a Fourier transform-infrared (FT-IR) spectrometer.

Not unexpectedly the hydrazines were found to be very reactive. Extensive product analysis by FT-IR spectroscopy has permitted proposal of detailed mechanisms for the reactions of OH and O_3 with hydrazine, MMH, and UDMH.

The results of the studies reported here show that, upon release into the atmosphere, all three of the hydrazines investigated could be rapidly consumed by reaction either with ozone (O_3) or with hydroxyl radicals (OH) present in the atmosphere, depending upon the nature of the atmosphere into which the emissions occur. With respect to reaction with OH, the tropospheric half-life for hydrazine is expected to range from < 1 hour in polluted urban atmospheres to up to 3 to 6 hours in unpolluted atmospheres, with substituted hydrazines being consumed at about the same rate.

With respect to reaction with O_3, the half-life for unsubstituted hydrazine would range from less than 10 minutes during O_3 pollution episodes to less than 2 hours in the natural troposphere, with the half-lives for the substituted hydrazines (MMH and UDMH) being at least a factor of 10 shorter. Therefore, under most conditions, reaction with ozone will be the major fate of hydrazines released into the atmosphere.

In terms of long-range impact, beyond the toxicity of the hydrazines themselves, the release of N_2H_4 or MMH will probably have relatively little effect on the levels of NO_x, nitrates, or other forms of active nitrogen in the atmosphere, since the hydrazine nitrogen appears to be efficiently converted to N_2. A qualification to this, however, is that a major release of MMH in an area of high O_3 pollution, particularly during late afternoon or early evening hours, could subject any industrial environment or nearby downwind region to possibly significant levels of potentially toxic methylhydroperoxide and methyldiazene, as well as highly poisonous diazomethane.

A similar scenario for UDMH and other unsymmetrically disubstituted hydrazines could have even more far-reaching health implications, since their reactions with O_3 would form high yields of nitrosamines, species which are known to be very potent carcinogens. Although nitrosamines react in sunlight to form the relatively more stable nitramines, the latter class of compounds may also be classified as a health hazard since dimethylnitramine has been demonstrated to induce carcinogenic activity in test animals.

PREFACE

This report documents work performed during the period September 1978 through June 1980 under Program Element 62601F, Project 1900, Subtask 2015. The work was carried out at the Statewide Air Pollution Research Center (SAPRC) of the University of California, Riverside, California under the direction of the Principal Investigator and Director of SAPRC, Dr. James N. Pitts, Jr. The senior research personnel on this program were Drs. Ernesto C. Tuazon, William P. L. Carter, Arthur M. Winer, Geoffrey W. Harris, Roger Atkinson, and Richard A. Graham. The assistance provided by Mr. Richard Brown in carrying out the experimental program is appreciated. We are also indebted to Dr. Hiromi Niki of Ford Motor Company for providing us with a calibrated infrared spectrum of methylhydroperoxide prior to its publication. The authors also wish to thank Dr. Marian Carpelan and Ms. Yvonne Katzenstein for technical editing and assistance in many other aspects of the preparation of this report.

We gratefully acknowledge the support and contributions to the conduct of this program by Dr. Daniel A. Stone, Project Officer, and LtCol Michael G. MacNaughton, Chief of the Environmental Sciences Division.

This report has been reviewed by the Public Affairs Office (PA) and is releasable to the National Technical Information Service (NTIS). At NTIS it will be available to the general public, including foreign nationals.
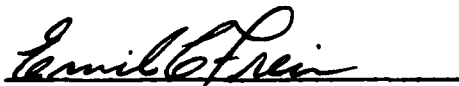
This technical report has been reviewed and is approved for publication.

DANIEL A. STONE
Project Officer

MICHAEL G. MACNAUGHTON,LtCol,USAF,BSC
Project Manager

EMIL C. FREIN,LtCol,USAF
Chief, Environics Division

FRANCIS B. CROWLEY III,Colonel,USAF
Director, Engineering and Services
Laboratory

i
(The reverse of this page is blank)

TABLE OF CONTENTS

LIST OF FIGURES

LIST OF FIGURES (CONCLUDED)

LIST OF TABLES

SECTION I

INTRODUCTION

Prior to the 1970s the atmospheric chemistry of nitrogen-containing compounds such as amines and hydrazines, which have wide industrial and military applications, has received comparatively little attention. However, within the past five years several developments have brought a greatly increased demand for information concerning the chemical transformations and atmospheric fate of these compounds and their photooxidation products.

Among these developments has been the recognition of the need to further elucidate the role of nitrogenous compounds in the stratosphere and troposphere, discovery of the occurrence of N-nitrosamines in the environment, and growing concern regarding the direct and indirect impact of these species on man and his environment. An explicit expression of this concern is the directive to the Administrator of the U.S. Environmental Protection Agency (EPA) in the new Clean Air Act Amendments (1977) to specifically formulate air quality criteria relating to a wide spectrum of nitrogenous compounds (see Section 104.6 of the Clean Air Act Amendments).

The U.S. Air Force is presently assessing the environmental impact of the Space Transportation System which uses hydrazine (N_2H_4) as one of the fuels. In addition, hydrazine is used as a propellant in the F-16 fighter plane for emergency power and monomethylhydrazine (MMH) is commonly employed as a propellant for small thrusters in space vehicles. A 50-50 mixture of N_2H_4 and unsymmetrical dimethylhydrazine (UDMH), known as Aerozine-50, is a fuel for the Titan missile. These uses, along with the attendant transport and storage of large quantities of these compounds, can potentially lead to atmospheric releases of hydrazines that can impact on ambient air quality. Thus, the present study was designed to experimentally evaluate the atmospheric fate of hydrazine, MMH, and UDMH.

Since the hydrazines do not photolyze in the actinic region ($\lambda < 290$ nm), their likely reaction pathways in the atmosphere are reaction with the hydroxyl (OH) radical and attack by ozone (O_3), both of which are produced in NO_x-photooxidation systems. Very few investigations have been done concerning reactions of hydrazines in atmospheric systems, although there

1

have been extensive studies in liquid solutions (References 1 and 2) and at high temperatures (References 3 and 4) as well as studies (Reference 5) of the gas phase stability of N_2H_4 and UDMH.

To answer the need for detailed information on the gas phase atmospheric chemistry of selected hydrazines, the following specific studies were undertaken: flash photolysis-resonance fluorescence measurements of the absolute rate constants for the reaction of hydrazines with OH radicals; a study of the rates and products of the dark reactions of ozone with N_2H_4, MMH, and UDMH; and an investigation of the NO_x-photooxidation of these same hydrazines under simulated atmospheric conditions. The latter two studies were conducted using a 30,000-liter outdoor irradiation chamber equipped with a 10-meter basepath optical system coupled to a Fourier transform-infrared (FT-IR) spectrometer. Not unexpectedly, the hydrazines were found to be very reactive. Extensive product analysis by FT-IR spectroscopy has permitted detailed mechanisms to be proposed for the reactions of OH and O_3 with the hydrazines.

SECTION II

KINETICS OF THE REACTIONS OF THE HYDROXYL RADICAL (OH)
WITH SELECTED HYDRAZINES

It became recognized during the 1970s that the hydroxyl radical plays a dominant role in the chemistry of the troposphere (References 6 through 10), and is, in many cases, the primary reactive intermediate depleting compounds introduced into the troposphere from either natural or anthropogenic sources.

Hydrazine and its derivatives methylhydrazine and 1,1-dimethylhydrazine are presently used as rocket fuels; hence, the rate constants for the reactions of hydrazines with OH radicals are needed for any assessment of the atmospheric chemistry of these compounds following possible release into the biosphere. Absolute rate constants are reported here over the temperature range of 298 to 424 K, determined using a flash photolysis-resonance fluorescense technique, for the reaction of OH radicals with hydrazine and methylhydrazine. The use of these data for predicting the value of the rate constant for the reaction of OH radicals with unsymmetrical dimethylhydrazine (UDMH) is also described. Because of severe handling difficulties encountered for UDMH, it is believed that more confidence can be placed in the deduced rate constant than could be placed in data obtained by direct techniques.

EXPERIMENTAL

The apparatus and techniques used have been described in the literature (Reference 11). OH radicals were produced by the pulsed vacuum ultraviolet photolysis of H_2O at wavelengths longer than the CaF_2 cutoff ($\geq$ 1250 Å). OH radical concentrations were monitored as a function of time after the flash by resonance fluorescence using a cooled EMI 9659QA photomultiplier fitted with an interference filter transmitting the 3064 Å band of $OH(A^2\Sigma^+$, $v' = 0 \rightarrow X^2\Pi$, $v'' = 0$). The intersection of the detection system aperture and the resonance radiation beam defined a fluorescence viewing zone at the center of the reaction vessel whose cross-section was ~2 cm in diameter. This region was well separated from the reaction vessel walls, minimizing heterogeneous losses of the OH radicals. The reaction cell was enclosed in a

3

furnace which could be held constant to greater than ± 1 K over the temperature range from 295 to 475 K, the gas temperature being measured by a Chromel/Alumel thermocouple mounted inside the reaction vessel.

The flash lamp was typically operated at discharge energies of 10 to 20 joules per flash at repetition rates of one flash every three seconds. Signals were obtained by photon counting in conjunction with multichannel scaling. Decay curves of OH radicals were accumulated from 118 to 2120 flashes depending on the signal strengths. OH radical half-lives ranged from 1.24 to 50.6 msec, and the concentrations were followed over at least three half-lives. In all cases the flash duration ($\leq$ 1 μsec) was negligible in comparison with the OH radical half-lives encountered.

In order to avoid the accumulation of photolysis or reaction products and to avoid wall losses of the hydrazines, all experiments were carried out under flow conditions so that the gas mixture in the reaction vessel was replenished every few flashes. The partial pressure of H_2O in the reaction cell ranged from 0.01 to 0.03 torr. The argon and reactants used had purity levels, according to the manufacturers, of: Ar $\geq$ 99.998%; N_2H_4 $\geq$ 97% (Matheson, Coleman and Bell); and CH_3NHNH_2 $\geq$ 98% (Aldrich).

A known fraction of the total argon flow was saturated with hydrazine or methylhydrazine vapor at 273 K and the reactant partial pressures in this fraction of the argon flow were determined by ultraviolet absorption spectroscopy using a Cary 15 spectrophotometer. The system was calibrated using known pressures of N_2H_4 and CH_3NHNH_2 as measured by an MKS Baratron capacitance manometer. All gas flows were monitored by calibrated flowmeters, and the gases were premixed before entering the reaction vessel.

RESULTS AND DISCUSSION

The reactions of OH radicals with N_2H_4 and CH_3NHNH_2 were studied over the temperature range from 298 to 424 K with 25 to 50 torr of argon as the diluent gas. Under experimental conditions where the reactant concentrations were in large excess over the initial OH radical concentrations (estimated to be $\leq 10^{11}$ molecule cm^{-3}), the pseudo-first order decays of the OH radical concentrations are given by the integrated rate expression

$$[OH]_0/[OH]_t = S_0/S_t = \exp[(k_0 + k_1 [\text{reactant}]) (t-t_0)] \qquad (1)$$

4

where $[OH]_0$ and $[OH]_t$ are the concentrations of OH at times t_0 and t, respectively, S_0 and S_t are the corresponding resonance fluorescence intensities, k_0 is the first order rate for removal of OH in the absence of added reactant (primarily attributed to diffusion out of the viewing zone and to reaction with impurities), and k_1 is the rate constant for the reaction of OH radicals with hydrazine or methylhydrazine.

In all experiments, exponential decays of the resonance fluorescence signal were observed, and the measured OH radical decay rates, defined as $R = (t-t_0)^{-1} \ln S_0/S_t$, were found to depend linearly on the concentration of added hydrazine or methylhydrazine. For both reactants, a variation of a factor of 2 in the flash energy produced no variation in the rate constants within the experimental errors, indicating that secondary reactions were negligible under these conditions. Furthermore, a variation from 25 torr to 50 torr total pressure of argon at 298 K for hydrazine and at 424 K for methylhydrazine had no effect on the rate constants within the experimental errors.

Figure 1 shows plots of the OH radical decay rate against hydrazine concentrations for the three temperatures studied (298 ± 1, 355 ± 1 and 424 ± 1 K), while Table 1 gives the rate constants k_1 obtained from such

TABLE 1. RATE CONSTANTS FOR THE REACTION OF OH RADICALS WITH HYDRAZINE AND METHYLHYDRAZINE

Reactant	Temperature (K)	$10^{11} \times k_1$ cm^3 molecule^{-1} sec^{-1}[a]
Hydrazine	298 ± 1	6.5 ± 1.0
	355 ± 1	5.9 ± 0.9
	424 ± 1	5.8 ± 0.9
Methylhydrazine	298 to 424	6.5 ± 1.3

[a]The quoted errors include twice the standard deviation of the slopes in Figures 1 and 3 plus the estimated error in the measurements of flow rates, total pressures, and ultraviolet absorption calibrations.

plots by least squares analysis. Figure 2 shows the rate constants k_1 for hydrazine plotted in Arrhenius form, and a least squares analysis of the
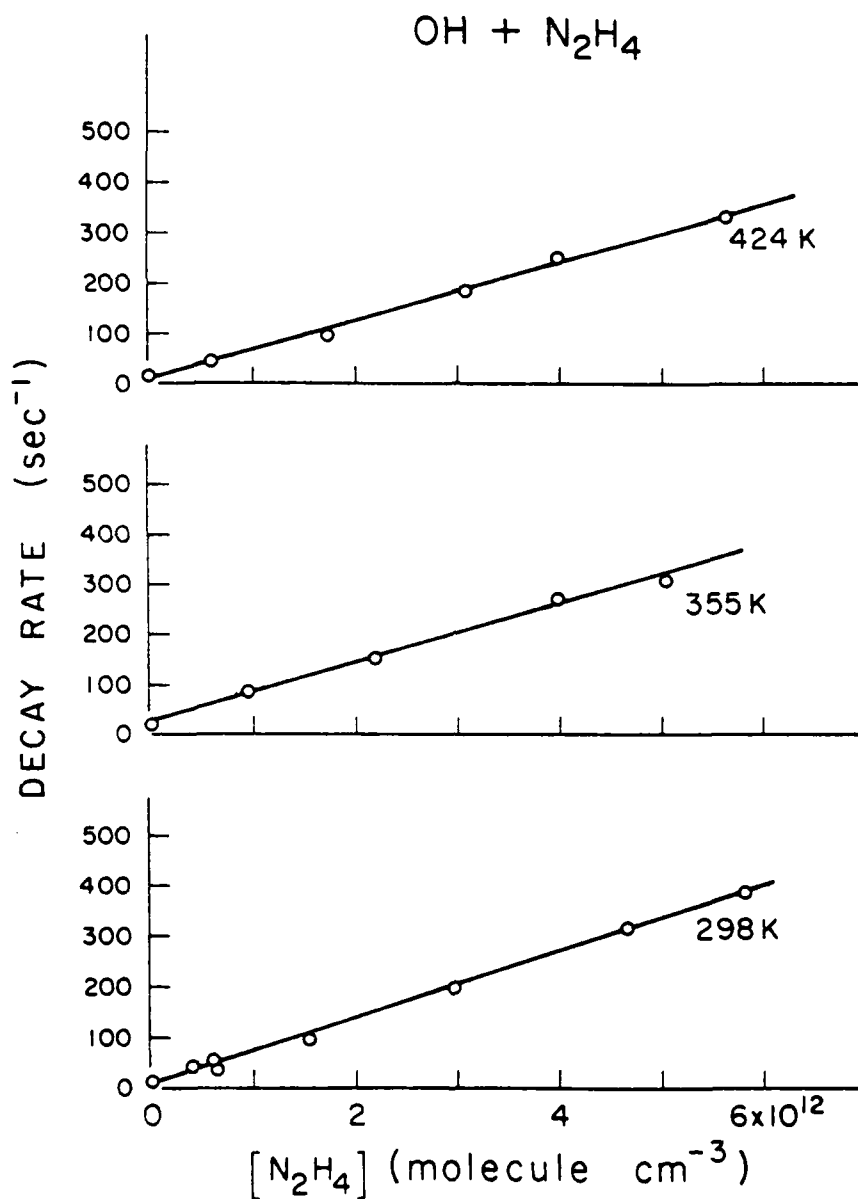
Figure 1. Plots of the OH Radical Decay Rates Against Hydrazine Concentration at 298, 355, and 424 K

data yields the Arrhenius expression

$$k_1(N_2H_4) = 4.4 \times 10^{-11} e^{(230 \pm 350)/RT} \text{ cm}^3 \text{ molecule}^{-1} \text{ sec}^{-1}$$

where the indicated error in the activation energy is the estimated overall

ARRHENIUS PLOT FOR OH + HYDRAZINE
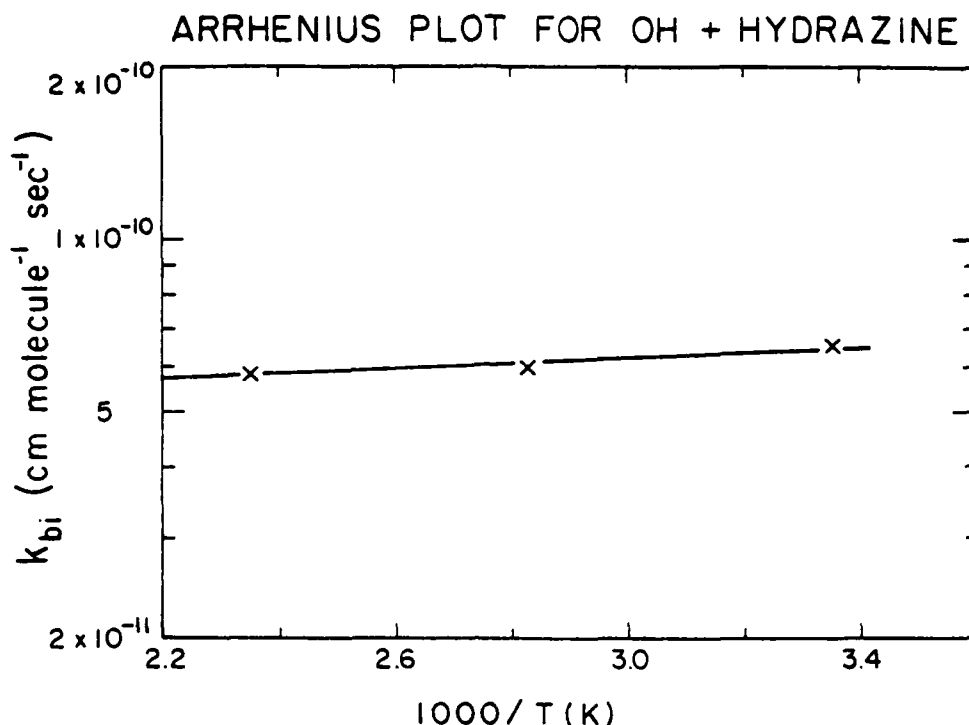
Figure 2. Arrhenius Plot of Log of the Bimolecular Rate Constant, $k_1(N_2H_4)$, Against 1000/T (K)

error limit. However, within these error limits, the data are as well represented by the temperature independent rate constant

$$k_1(N_2H_4) = (6.1 \pm 1.0) \times 10^{-11} \text{ cm}^3 \text{ molecule}^{-1} \text{ sec}^{-1} \quad (T = 298-424 \text{ K}).$$

This zero or slightly negative temperature dependence (equivalent to $T^{-0.35\pm0.5}$) is in accord with the previous measurements from this laboratory on the reaction of hydroxyl radicals with a series of amines (References 12 and 13) and with CH_3SH (Reference 12) and CH_3SCH_3 (Reference 14) and probably reflects a slightly temperature-dependent preexponential factor (References 12 through 14).

The only previously reported measurement of the rate constant for the reaction of OH radicals with hydrazine [$k_1(N_2H_4) = 2.2 \times 10^{-11} \text{ cm}^3 \text{ molecule}^{-1} \text{ sec}^{-1}$ at 298 K] (Reference 15) was obtained in a discharge flow-epr (electron

7

paramagnetic resonance) study and is lower by a factor of ~3 than the present value. The possibility that the present value of k_1 is high due to the participation of hydrazine-water complexes can be discounted on the basis of the study of analogous $NH_3 \cdot H_2O$ complexes by Hamilton and Naleway (Reference 16). The amount of H_2O in the present system is very low (0.01 to 0.03 torr), and the ratio of its concentration to that of hydrazine varied by over an order of magnitude with no observable effect on the rate constant. Hence, the reason for the discrepancy between the present value and that of Hack et al (Reference 15) is not clear, but it is possible that heterogeneous loss processes occurring in their discharge flow system could lead to errors in understanding the stoichiometry of the reaction system.

For methylhydrazine it was found necessary to allow several hours for the methylhydrazine partial pressure, as monitored in the ultraviolet absorption cell, to stabilize before beginning the acquisition of data. The decomposition products of methylhydrazine on surfaces are likely to include amines, and since these react rapidly with the OH radical (References 12 and 13) wider error limits were placed on the measured rate constants for methylhydrazine than for hydrazine. For hydrazine, the decomposition products are NH_3 (observed by ultraviolet absorption in the present work at the lowest hydrazine flow rates) and N_2, and NH_3 is less reactive than hydrazine towards the OH radical by a factor of ~400 (Reference 17). In view of these accuracy limits the temperature dependence of the reaction of OH radicals with methylhydrazine was investigated by measurement of only a few first order decay rates at the higher temperatures to confirm that the temperature dependence, as expected from the hydrazine data, was essentially zero. The OH radical decay rates as a function of methylhydrazine concentration are shown in Figure 3, and it can be seen that the data at the three temperatures studied are well represented by the temperature independent rate constant

$$k_1(CH_3NHNH_2) = (6.5 \pm 1.3) \times 10^{-11} \text{ cm}^3 \text{ molecule}^{-1} \text{ sec}^{-1} \quad (T = 298-424 \text{ K})$$

The magnitude and lack of temperature and pressure effects for these two rate constants indicate that the reactions proceed by means of H atom abstraction from the very weak N-H bonds [N-H bond strength ~76 kcal mole^{-1} in hydrazine (Reference 18)]. In going from hydrazine to methylhydrazine,

8
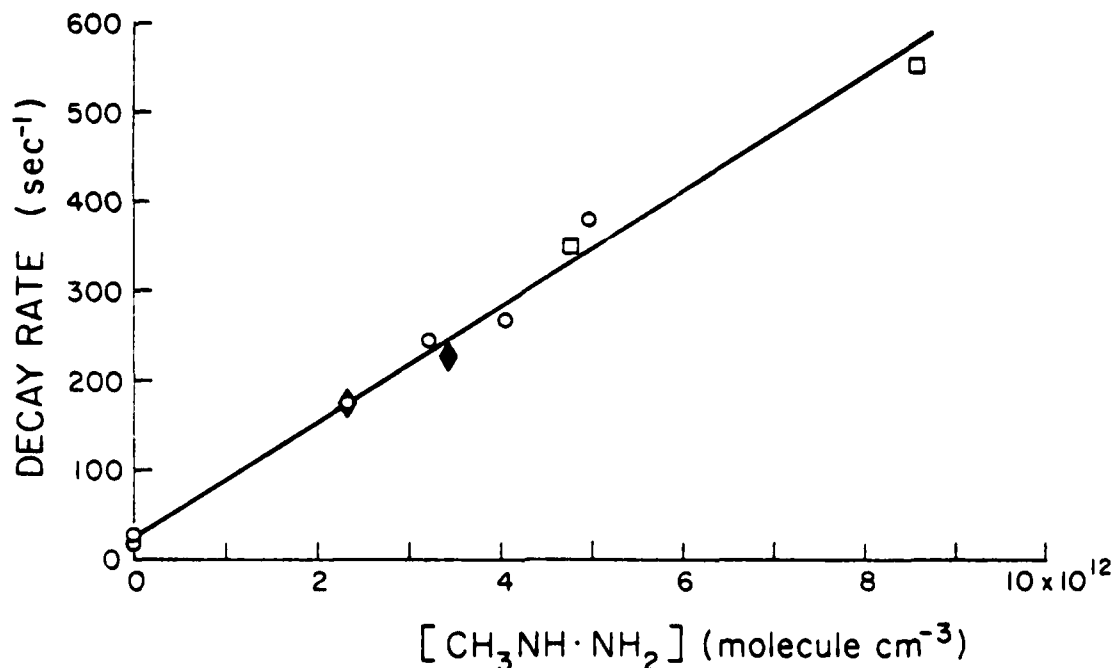
Figure 3. Plot of the OH Radical Decay Rates Against Methylhydrazine Concentration at ○ 298 K, ◆ 355 K, and □ 424 K

the reaction rate with OH radicals would be expected to drop somewhat because of the lower number of N-H bonds, but the compensation of the electron donating effect of the methyl group will result in a weaker bond to one of the hydrogen atoms and the net magnitude of these effects can be seen from the data to be approximately zero.

An attempt to further study these trends by measuring the rate constant for the reaction of hydroxyl radicals with 1,1-dimethylhydrazine (UDMH) failed because of very severe handling problems encountered for this compound. In this system, the compound appeared to decompose rapidly to gaseous products, with the decomposition occurring fast enough to provide a significant pressure differential acting against the direction of the bulk flow. It may be that a gas handling system of different design using glass

capillaries instead of needle valves to provide pressure flow rate regulation might ameliorate this problem to some extent. Consideration of the data already obtained for hydrazine and methylhydrazine, of the trends in bond strength, and of the number of H atoms available for extraction leads to the conclusion that the rate constant for reaction of OH radicals with UDMH lies in the range $(5 \pm 2) \times 10^{-11}$ cm^3 molecule^{-1} sec^{-1}, independent of temperature in the range 298 to 424 K.

It is unlikely that direct data could be obtained which would produce smaller uncertainties in the values of this rate constant, and use of the above estimate is recommended for atmospheric modeling purposes.

If an average OH radical concentration of $\sim 10^6$ cm^{-3} is taken for the lower troposphere, the rate constants reported here allow calculation of tropospheric half-lives of ~ 3 hours for all three hydrazines. The half-life may be 2 to 5 times longer in otherwise pristine atmospheres and < 1 hour in polluted urban atmospheres.

SECTION III

REACTIONS OF SELECTED HYDRAZINES WITH OZONE AND OXIDES OF NITROGEN

Hydrazines do not photolyze in the actinic region ($\lambda > 290$ nm); thus, their likely reaction pathways in the atmosphere are reaction with the hydroxyl (OH) radical and attack by ozone (O_3), both of which are produced in NO_x-photooxidation systems. In the experimental evaluation of the atmospheric fate of hydrazine (N_2H_4), monomethylhydrazine (MMH), and unsymmetrical dimethylhydrazine (UDMH), an investigation was undertaken of the rates and products of the dark reactions of O_3 with N_2H_4, MMH, and UDMH as well as a study of the NO_x-photooxidation of these same hydrazines under simulated atmospheric conditions. These two studies were conducted using a 30,000-liter outdoor irradiation chamber equipped with a 10-meter basepath optical system coupled to a Fourier transform-infrared spectrometer. Based on extensive product analysis by FT-IR spectroscopy, detailed mechanisms for reactions of hydrazines with OH and O_3 were developed and are reported in this section.

EXPERIMENTAL

Chamber Construction. The outdoor chamber, multiple-reflection optics, and FT-IR spectrometer employed in this study are illustrated in Figure 4. The reaction chamber is essentially a large Teflon® bag of triangular cross-section held semi-rigidly by a framework of steel pipes. The 50 μ (2-mil) thick Teflon® wall provides excellent transmission (> 98%) of solar actinic radiation. Depending on the degree of inflation, the chamber's volume ranges from ~30,000 to 33,000 liters as measured by injection of a calibration gas. The experiments are usually conducted with an initial slight overpressure (at ~32,000 liters) inside the chamber such that, even with a small degree of leakage, concentrations would remain essentially unaffected. The outer frame supports a two-section white tarpaulin shield which could be removed readily by rollers to expose the chamber to solar radiation. The tarpaulin transmits $\leq 0.1\%$ of noon sunlight (as verified with a radiometer) and is therefore employed also as an opaque cover for dark experiments.
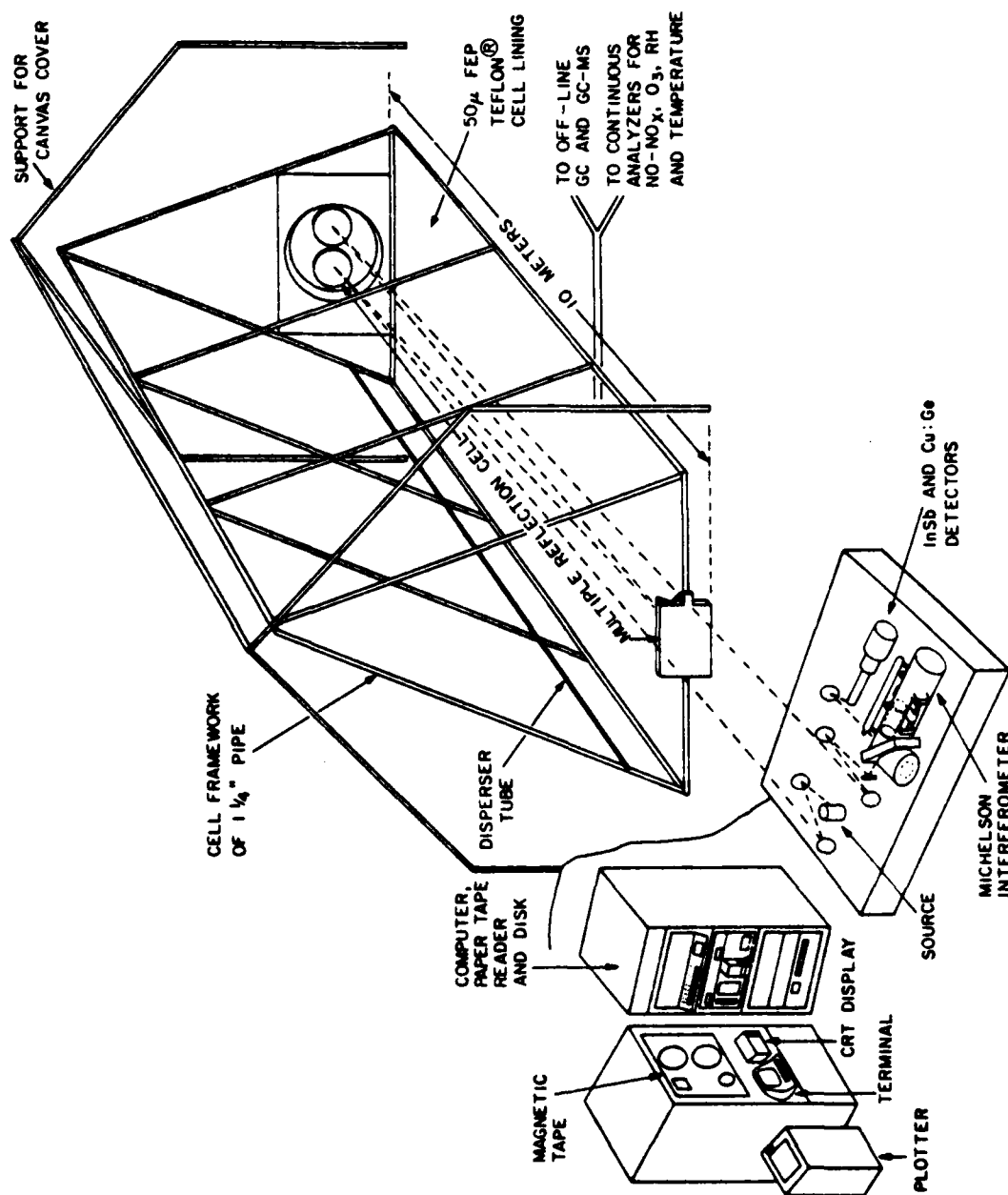
Figure 4. Fourier Transform-Infrared Spectrometer and 30,000-Liter Outdoor Chamber
Facility with In Situ Multiple Reflection Optics

12

Provisions for sample injection and gas sampling are situated in the middle section of the chamber and consist of a disperser bulb, several glass tubes with sealed fittings, and a Teflon® disperser tube which runs the length of the cell. A Teflon®-coated panel making up each of the chamber's end sections attaches to the mirror assembly by a cylindrical tube of Teflon® film, thereby reducing to a minimum the vibration transmitted by the chamber to the cell optics. The end panels also provide the attachments for the mixing fans and the purge inlet and exhaust ports.

In its initial form, the outdoor chamber consisted of a cylindrical Teflon® bag (~40,000 liters) enclosed in an outer shell of Teflon®. The laminar flow of air between these two chambers created an overpressure which effectively protected the inner (reaction) chamber from wind abrasion. However, employing a black polyethylene cover over the inner chamber during dark experiments caused the temperature in the reaction chamber to rise to 45 to 50°C even when the existing ambient temperature was only ~20°C. Due to the excessive heat build-up inside the reaction chamber, this design was abandoned after a few experiments.

Long-Path Optics. The mirror assembly consists of two 30-cm-diameter collecting mirrors and a 15-cm x 25-cm rectangular mirror at the in-focus end with a common radius of curvature of 10 meters. The in-focus mirror is modified with the addition of a corner reflector (Reference 19) which returns the output beam for additional sets of reflections, thereby doubling the number of passes obtainable with the conventional White design. Pathlengths in excess of 1 km can be achieved with the use of high-reflectivity ($\geq$ 99.0%) fresh gold coating on the mirrors. The kinematic mounts employed in this system have provided satisfactory alignment stability during actual operation over ambient temperature variations of up to $\pm$ 15°C.

FT-IR Spectrometer. Interfaced to the multiple-reflection optics is a rapid-scan Midac interferometer with a maximum resolution capability of 0.06 cm^{-1}. It is equipped with a dual-element Cu:Ge and InSb detector cooled with a closed-cycle refrigeration unit. The interferometer and data system are housed in a 3.6-m x 3.6-m air-conditioned building immediately adjacent to the outdoor chamber. Data collection and processing is performed with a Computer Automation LSI-2/20 minicomputer with 32 K

13

words and a special fast Fourier transform (FFT) processor. System peripherals include a 2.5-M word dual-disk drive, raster plotter, line printer, oscilloscope display, CRT terminal, and magnetic tape unit.

Materials. Anhydrous hydrazine (stated purity 97+%, Matheson, Coleman and Bell), methylhydrazine (98%, Aldrich Chemical Company), and 1,1-dimethylhydrazine (99+%, Aldrich Chemical Company) were further purified by collecting the middle fraction of a 20-ml sample of each compound by slow room-temperature distillation in a vacuum line. For each experiment a small fraction of the stored sample was topped off and discarded prior to transfer of vapors into glass bulbs. Even with these precautions, NH_3 was found to be an unavoidable impurity in the final sample introduced into the reaction chamber.

Samples of nitric oxide (commercial purity 99.0%, Matheson, Coleman and Bell) were drawn directly in glass syringes which were pre-flushed with N_2 gas to prevent immediate conversion to NO_2 prior to injection into the chamber.

Ozone was produced in a Welsbach Laboratory ozonizer and collected into 2- and 5-liter glass bulbs. Depending on the experiment's requirements, samples with 0.8 to 1.5% ozone were obtained by appropriate adjustments of O_2 gas flow and/or voltage applied to the electrodes. The O_3 being flushed into the glass bulb flowed through a 10-cm cell equipped with KBr windows and its concentration verified by its infrared absorption at ~1055 cm^{-1}.

Methods of Procedure. Vapors of the hydrazine sample were measured into a 5-liter glass bulb in a vacuum line using an MKS Baratron capacitance manometer. The total pressure was brought to 1 atmosphere with N_2 gas and immediately flushed through the disperser bulb into the reaction chamber with rapid mixing by fans. The hydrazine was usually observed for a certain period of time in the dark before injection of either O_3 or NO_x. The predetermined amount of O_3 in a 5-liter glass bulb or NO_x (initially measured as NO) in a glass syringe was then flushed and stirred into the chamber through the Teflon® disperser tube. Uniform mixing of reactants was verified to be complete within 2 minutes.

NO and NO_2 were monitored by a Bendix chemiluminescent instrument. The NO_2 readings of this type of instrument have been known to include those of HNO_3, HONO, and other organic compounds bearing the groups -NO and $-NO_2$.

14

The growth and decay of all other species (including O_3) were monitored by FT-IR spectroscopy. A total pathlength of 460 meters and resolution of 1 cm^{-1} were employed throughout this study. Each spectrum (700 to 3000 cm^{-1}) was adequately covered by the response of the Cu:Ge detector. The 32 interferograms co-added for each spectrum generally took ~40 seconds to collect. By pre-storing successive sets of co-added interferograms, a convenient 1-minute time resolution was attained for monitoring the fast initial stage of certain reactions (e.g., N_2H_4 + O_3). Slower events (e.g., dark decays) were covered by co-adding 64 interferograms for improved signal-to-noise ratio, followed by immediate calculation of each spectrum.

Reactant and product analyses were obtained from intensities of infrared absorption bands by spectral desynthesis (i.e., successive subtraction of absorptions by known species). Low-noise reference spectra for the hydrazines and several reaction products were generated for this purpose so as to minimize the increase in the noise level of the residual spectrum with each stage of subtraction. Appendix A provides a summary of the absorption coefficients, detection limits, and a brief discussion of the problems encountered in the analysis.

RESULTS

Dark Decay of Hydrazines in the Chamber

The individual hydrazines were mixed into purified matrix air, and their decay in the reaction chamber was monitored by FT-IR spectroscopy for periods of 3 to 5 hours. The results are summarized in Table 2. The N_2H_4 decay experiments were the first runs carried out in the initial chamber (double-shell design) and were conducted during winter evening hours; hence, low average temperatures prevailed. Two experiments were carried out for each compound: one was with the driest output of the air purification system, and the second was with water content approximately corresponding to that of air at 20°C and 50 percent relative humidity.

As seen in Table 2, the decay rate of hydrazine (N_2H_4) showed a pronounced dependence on humidity, being about 3 times faster in humid air than in dry air. It should be noted that the first-order plot obtained for the decay rate of N_2H_4 in dry air exhibited a noticeable curvature, more typical of second-order behavior, during the first 60 minutes, but followed

15

TABLE 2. DARK DECAY OF HYDRAZINES IN THE CHAMBER

Compound	Initial Concentration (ppm)	Average Temperature ($^\circ$C)	Relative Humidity (%)	Approximate Half-Life (hrs)
N_2H_4	2.85	15	16	4.4 - 5.7
	3.77	14	85	1.8
MMH	3.16	40	4	4.2
	3.65	40	15	3
UDMH	4.37	41	4	9
	2.48	40	15	5.9

a straight line for the remainder of the 4-hour experiment. The higher value of the range of half-lives reported in Table 2 corresponds to the straight-line portion of the first-order plot. The dependence of decay on humidity is significantly less for monomethylhydrazine (MMH) and unsymmetrical dimethylhydrazine (UDMH), the rates being ~1.5 times faster in humidified air than in dry air for both compounds.

The known stability of UDMH (References 5 and 20) over N_2H_4 and MMH is reflected in these observed half-lives. Due to the difference in temperature between the respective experiments and the observed initial curvature in the first-order plot of N_2H_4, it is not certain whether the difference in the half-lives found for N_2H_4 and MMH in dry air is significant. The rough order of stabilities observed at the relatively low concentrations used and prevailing ambient temperatures is in marked contrast to those found in studies at high temperatures and high initial concentrations of the hydrazines. A study (Reference 21) of the gas-phase decomposition of the hydrazines in an adiabatic flow reactor in the temperature range 800 to 1000 K found that UDMH decomposition is fastest, that of N_2H_4 is slowest, and the MMH decomposition rate is intermediate. The same study found that the rate of decomposition of N_2H_4 in $N_2H_4-H_2O$ mixtures is slower than that of anhydrous N_2H_4 by approximately a factor of 10. These contrasting results

16

point out the danger of comparing values obtained from widely different concentration regimes and experimental conditions.

Ammonia (NH_3) was observed to form during the decay of the hydrazines but accounts for only 5 to 10% of the N_2H_4 or UDMH lost. The NH_3 produced in the MMH decomposition in dry air was considerably higher, amounting to as much as 50% of the MMH which disappeared during the first few minutes and 20% at the half-life; the corresponding values observed for NH_3 formation in humidified air were only about one-third that observed in dry air. Nitrous oxide (N_2O) was also detected as a minor product of N_2H_4 decomposition, accumulating after 3 hours to approximately 3% (0.04 ppm) and 1% (0.02 ppm) of N_2H_4 lost for runs in dry and humidified air, respectively. About 0.02 ppm of N_2O formed after 3 hours in the MMH decomposition in dry air but was below detection limit (< 0.014 ppm) in the same period of time for MMH in humidified air. The formation of methyldiazene ($CH_3N=NH$) in the MMH decay experiments was also established by the growth of its infrared absorptions (Reference 22) at 845.2 cm^{-1} and ~1140 cm^{-1}, but its absolute concentrations could not be determined due to lack of reliable absorption coefficients. The relative yield of $CH_3N=NH$ in humidified air was estimated to be about twice that in dry air.

Reactions of Selected Hydrazines with Ozone

The Reaction of Hydrazine (N_2H_4) with Ozone. The reaction of N_2H_4 with O_3 in the dark proceeded at a rapid rate to produce hydrogen peroxide (H_2O_2). Apart from ammonia (NH_3), the only other minor product clearly observed by FT-IR spectroscopy was nitrous oxide (N_2O). This is illustrated by the spectra (Figure 5) and detailed results (Table 3) for the experiment which was carried out using the initial chamber design (double-shell) with dry matrix air at an average temperature of 44°C. Approximately equimolar quantities of N_2H_4 (2.5 ppm) and O_3 (2.4 ppm) were employed. A similar run at a much lower average temperature of 21°C (see Table 4 for detailed results) was conducted using the new chamber (Figure 4) with initial concentrations of ~1.6 ppm each of N_2H_4 and O_3. The small increase in NH_3 concentration over its initial level as an impurity was presumably due to N_2H_4 decomposition (Reference 5). Readings from the chemiluminescent analyzer indicated that no significant levels of NO_x were formed.

17
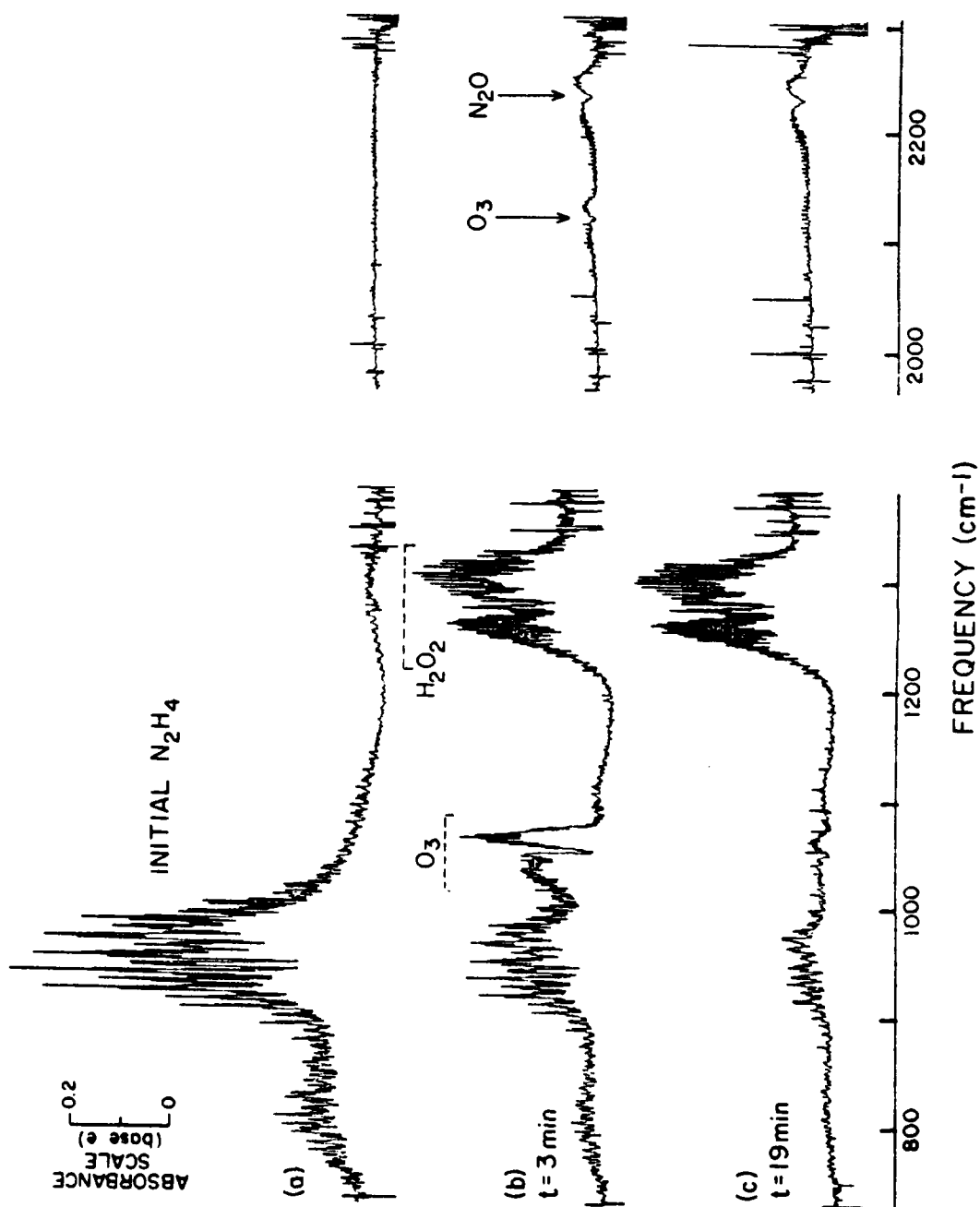
Figure 5. Fourier Transform-Infrared Spectra of $N_2H_4 + O_3$ Dark Reaction (44°C): Resolution = 1 cm^{-1}, Pathlength = 460 m; O_3 Injection at t = 0 (see Table 3)

18

TABLE 3. CONCENTRATIONS OF REACTANTS AND PRODUCTS VERSUS TIME IN N_2H_4 $+O_3$ DARK REACTION (1 FEBRUARY 1980). T (AVE.) = 44°C, %RH (AVE.) = 1

Elapsed Time (min)	Concentration (ppm)				
	N_2H_4	O_3	H_2O_2	N_2O	NH_3
-15	2.50				-[c]
-5	2.37				-
0[a]		~2.4[b]			
3	0.951	0.617	0.68	0.035	-
10	0.521	0.228	0.80	0.039	0.023
15	0.329	0.128	0.77	0.043	0.037
19	0.293	0.095	0.75	0.043	0.033
25	0.208	0.071	0.73	0.044	0.042
35	0.184	0.040	0.71	0.047	0.031
57	0.095	-	0.62	0.049	0.038
85	-	-	0.48	0.062	0.043

TABLE 4. CONCENTRATIONS OF REACTANTS AND PRODUCTS VERSUS TIME IN N_2H_4 $+O_3$ DARK REACTION (2 APRIL 1980). T (AVE.) = 21°C, %RH (AVE.) = 12

Elapsed Time (min)	Concentration (ppm)				
	N_2H_4	O_3	H_2O_2	N_2O	NH_3
-18	1.69				0.088
-7	1.54				0.108
0[a]		~1.6[b]			
3	0.826	1.17	0.29	0.027	0.113
5	0.682	0.969	0.40	0.027	0.116
7	0.542	0.806	0.43	0.027	0.108
9	0.407	0.711	0.48	0.029	0.110
14	0.214	0.477	0.46	0.032	0.126
19	0.203	0.388	0.54	0.032	0.126
24	0.137	0.348	0.53	0.033	0.124
29	0.092	0.332	0.53	0.035	0.126
41	-[c]	0.251	0.47	0.041	0.125

[a]Time of O_3 injection   [b]Calculated initial O_3 concentration

[c]Dash means below FT-IR detection sensitivity; blank means no measurement was made

The time-concentration profiles of reactants for the higher temperature run (Figure 6) indicate a faster rate of reaction during the initial few minutes. However, the time-concentration curves for the latter stage of the reaction are essentially parallel. For both the 44°C and 21°C experiments, > 90% of N_2H_4 was consumed in ~30 minutes. Within experimental error, the O_3/N_2H_4 ratio during the reaction was essentially 1:1.

A third experiment was carried out at an average temperature of ~24°C using an initial excess of O_3 ($O_3/N_2H_4 \simeq 2$), followed by a second addition of N_2H_4 to the unreacted O_3 (Table 5). The decay of N_2H_4 with excess O_3 was determined to be approximately exponential and allowed an estimate of the N_2H_4 + O_3 rate constant to be made (see Discussion, this section).

The Reaction of Unsymmetrical Dimethylhydrazine (UDMH) with Ozone. Figure 7 illustrates the dark reaction between UDMH and O_3 at initial concentrations of 1.7 ppm and 2 ppm, respectively. The first infrared spectrum recorded at 2 minutes after O_3 injection showed no measureable O_3 left and indicates that ~77% of the initial amount of UDMH had been consumed. The major product formed in this instantaneous reaction was N-nitrosodimethylamine [$(CH_3)_2N-NO$], positively identified by its infrared absorptions at 1296, 1016, and 848 cm^{-1} (Figure 7). The nitrosamine and formaldehyde (HCHO) formed during the first 2 minutes account for ~60% and ~15%, respectively, of the UDMH consumed (Table 6).

The reaction mixture was further observed in the dark for 1 hour with little change noted in the nitrosamine concentration. During this period, HCHO was seen to decrease by ~60% along with a smaller decrease (~30%) in NH_3. The output of the chemiluminescent analyzer indicated a negligible rise of the NO concentration above background level. The increase in the NO_2 readings is likely to be primarily due to the nitrosamine being detected as NO_2 after passage through the catalytic converter of the analyzer.

On subsequent exposure of the chamber to sunlight, a decrease in the intensities of the nitrosamine absorptions was observed and was accompanied by growth of the absorption bands at 1307 and 980 cm^{-1} (Figure 7). This observation confirmed that N-nitrosodimethylamine was being converted to dimethylnitramine [$(CH_3)_2N-NO_2$], a reaction which has been studied previously (References 23 and 24). Destruction of the nitrosamine was complete

20
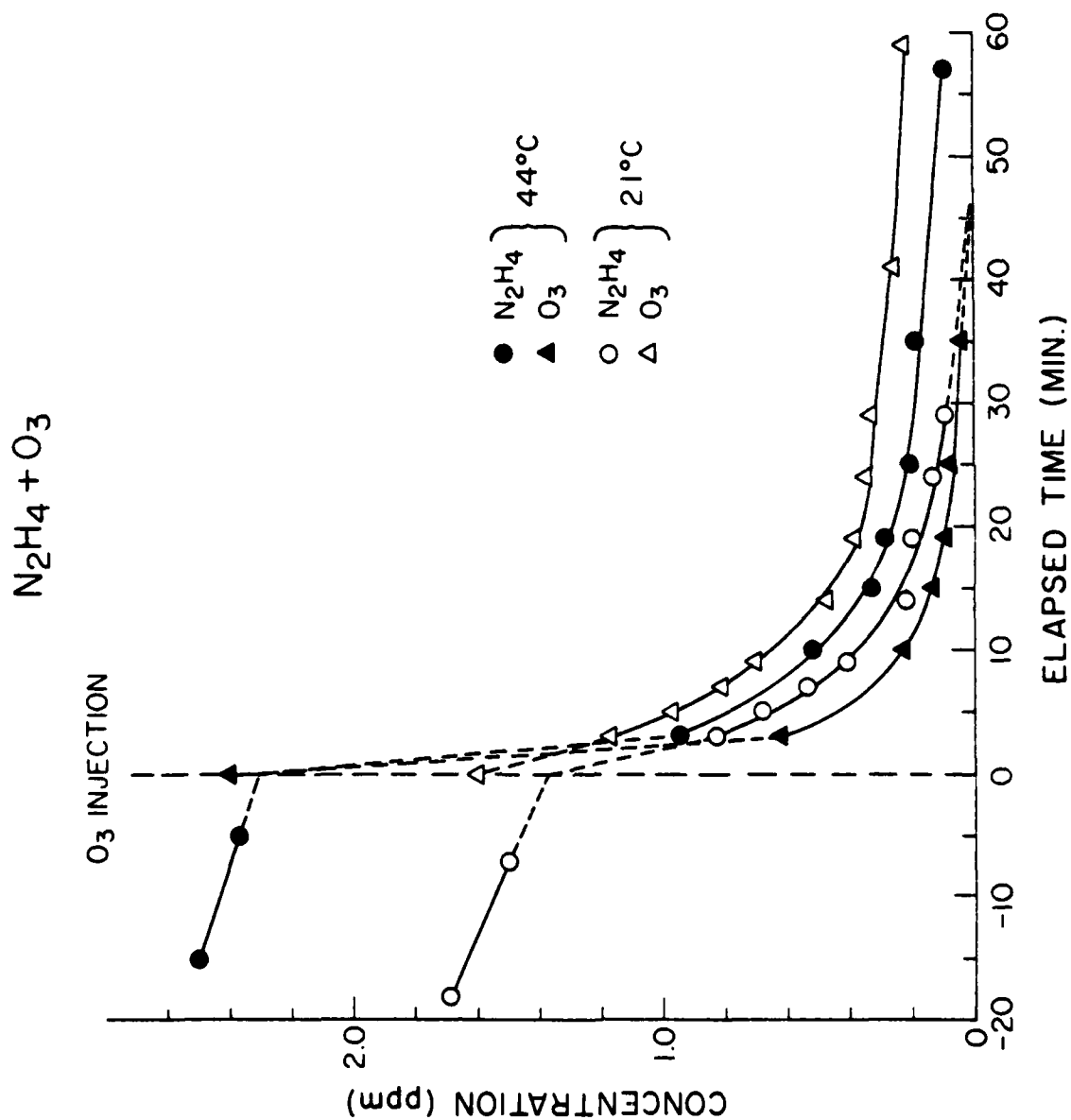
Figure 6. Decay Curves of Reactants in Two $N_2H_4 + O_3$ Experiments at Different Temperatures (see Tables 3 and 4)

TABLE 5. CONCENTRATIONS OF REACTANTS AND PRODUCTS VERSUS TIME IN $N_2H_4 + O_3$ DARK REACTION (7 MAY 1980). T (AVE.) = 24°C, %RH (AVE.) = 8

Elapsed Time (min)	Concentration (ppm)				
	N_2H_4	O_3	H_2O_2	N_2O	NH_3
-15	1.13				0.585
- 2	1.09				0.646
0		~2.1 (calculated initial O_3 conc.)			
2	0.235	2.00	0.29	≤0.014	0.657
3	0.202	1.91	0.34		0.640
4	0.122	1.74	0.36		0.658
5	0.082	1.73	0.36		0.661
6	0.074	1.67	0.37		0.652
8	-[a]	1.60	0.37		0.643
14	-	1.46	0.34	≤0.014	0.625
22	-	1.46	0.31		0.586
31	-	1.33	0.29		0.567
41	-	1.34	0.24		0.533
51	-	1.27	0.20	0.020	0.506
71	-	1.24	0.19	0.022	0.476
79		~1.5 (calculated N_2H_4 conc., 2nd injection)			
82	1.10	0.95	0.28	0.023	0.632
83	0.923	0.84	0.33	0.024	0.610
85	0.791	0.72	0.38	0.027	0.635
88	0.638	0.53	0.41	0.024	0.619
92	0.424	0.39	0.45	0.024	0.644
97	0.275	0.30	0.44	0.023	0.644
102	0.163	0.22	0.43	0.022	0.653
108	0.133	0.16	0.39		0.647
116	0.077	0.15	0.37		0.642
126	-	-	0.30	0.027	0.636
141	-	-	0.25	0.024	0.595

[a]Dash means below FT-IR detection sensitivity; blank means no measurement was made
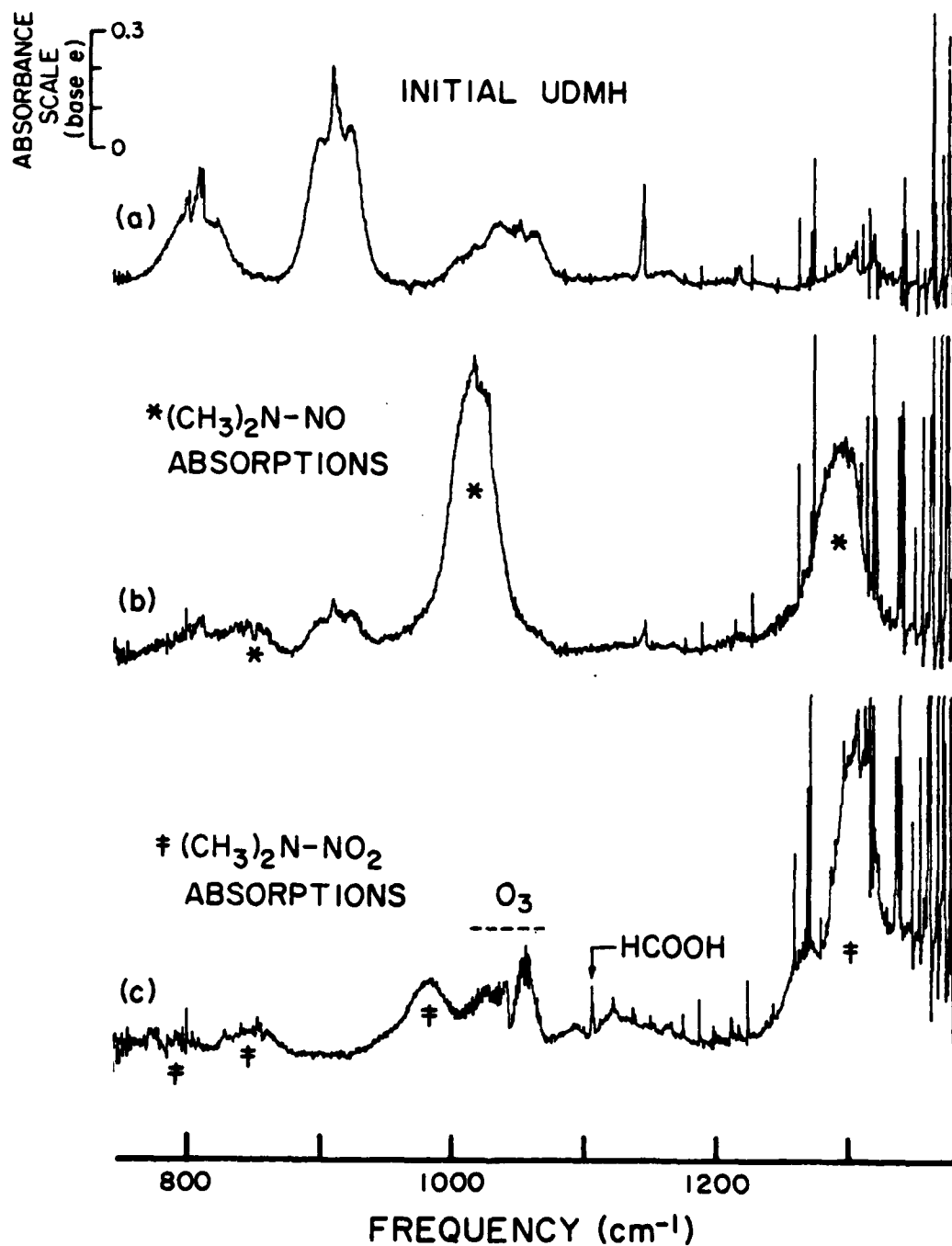
Figure 7. Fourier Transform-Infrared Spectra of UDMH + O_3
Reaction: (a) UDMH Spectrum, (b) 2 Minutes After
O_3 Injection, (c) ~1 Hour Into Sunlight Irradiation
of Reaction Mixture (see Table 6). NH_3 Absorptions
Subtracted from (a) and (b). Resolution = 1 cm^{-1},
Pathlength = 460 m.

23

TABLE 6. CONCENTRATIONS OF REACTANTS AND PRODUCTS[a] VERSUS TIME IN UDMH + O_3 REACTION (9 MAY 1980).
T (AVE.) = 21°C AND %RH (AVE.) = 10 DURING THE DARK PART OF THE EXPERIMENT

Elapsed Time (min)	UDMH	O_3	$(CH_3)_2NNO$	H_2O_2	HCHO	Concentration (ppm) NH_3	NO	NO_2	$(CH_3)_2NNO_2$	HCOOH	HONO
-12	1.76					0.114	0.026	0.015			
-7	1.71					0.116	0.030	0.021			
0		-2.0 (calculated initial O_3 conc.)									
2	0.386	-[b]	0.81	0.14	0.19	0.106	0.045				0.023
4	0.371	-	0.79	0.13	0.18	0.097	0.060				0.025
8	0.346	-	0.81	0.15	0.19	0.089	0.047	0.86			0.040
28	0.247	-	0.82	0.10	0.13	0.089	0.042	0.92			0.052
61	0.170	-	0.78	0.08	0.08	0.079	0.045	0.92			0.062
69	Start of Sunlight Irradiation (1401 PDT)										
79	-	-	0.41	0.07	0.34	0.077	0.138	0.86	0.15	-	0.19
98	-	0.17	0.18	-	0.61	0.030	0.041	0.86	0.38	0.027	0.14
128	-	0.51	-	-	0.50	-	0.012	0.68	0.48	0.043	-

[a]Other products detected at end of irradiation: CO
N_2O (0.015 ppm max. conc.)
CH_3ONO_2 (0.05 ppm max. conc.)

[b]Dash means below FT-IR detection sensitivity; blank means no measurement was made

24

within 2 hours under the partly cloudy sky which prevailed during the afternoon irradiation. Significant quantities of HONO were observed during the initial stage of the irradiation. In addition to the products listed in Table 6 (i.e., nitramine, O_3, HCHO, NO_x, and HCOOH), CO and traces of CH_3ONO_2 were also found at the end of the irradiation. In contrast with the case of N_2H_4 plus O_3 reaction, N_2O was not detected during the dark part of the experiment but formed to a maximum of 0.035 ppm by the end of the irradiation.

A second experiment was carried out under dark conditions using two O_3 injections to completely deplete UDMH (Table 7). The results of the first O_3 injection essentially parallel those of the dark reaction in the previous experiment. The second injection introduced excess O_3 into the system with near quantitative conversion of the remaining UDMH to the nitrosamine compound. The amount of O_3 consumed in this second step was closely accounted for by the additional nitrosamine and HCHO formed. An unidentified weak absorption band at ~952 cm^{-1} was detectable ~1 hour after the first O_3 injection, and immediately increased in intensity when excess O_3 was introduced. The NO output recorded by the chemiluminescent analyzer might have indicated the presence of some interferences since the instrument's readings with UDMH alone in the chamber were considerably above typical background values and the readings under conditions of excess O_3 were appreciably higher than zero. The NO_2 values could also account for the nitrosamine and HONO formed, but a positive interference similar to that which apparently occurred for NO might be present.

N-nitrosodimethylamine has been reported previously as an oxidation product of UDMH but under experimental conditions markedly different from those used in the present study. It was observed in the liquid phase as a minor product after prolonged (10 days) bubbling of oxygen through UDMH (Reference 25). It was also found to constitute 60 to 80% of the liquid products (Reference 2) when stoichiometric quantities of UDMH and N_2O_4 were reacted at $-20^\circ C$ in CCl_4.

In both experiments here, the O_3/UDMH ratio of the fast initial reaction was ~1.5 which suggests that some O_3 was being consumed in another step which possibly produced HCHO as well as other products not detected by infrared spectroscopy.

TABLE 7. CONCENTRATIONS OF REACTANTS AND PRODUCTS[a] VERSUS TIME IN UDMH + O_3 DARK REACTION (8 MAY 1980). T (AVE.) = 21°C, %RH (AVE.) = 10

Elapsed Time (min)	Concentration (ppm)								
	UDMH	O_3	$(CH_3)_2NNO$	H_2O_2	HCHO	NH_3	NO[c]	NO_2[c]	HONO
-27	1.97					0.079			
-19	1.93					0.102	0.063	0.082	
-9	1.93					0.116	0.064	0.106	
0		-2.0[b] (1st O_3 injection)							
3	0.479	-[d]	0.82	0.13	0.17	0.099	0.068	0.76	-
7	0.463	-	0.81	0.11	0.18	0.088	0.110	0.79	0.029
13	0.432	-	0.80	0.11	0.15	0.084	0.105	0.79	0.031
32	0.386	-	0.79	0.10	0.10	0.086	0.103	0.82	0.031
73	0.293	-	0.77	0.045	0.051	0.069	0.095	0.83	0.052
84		-2.0[b] (2nd O_3 injection)							
88	-	1.47	1.09	0.13	0.21	-	0.087	1.42	0.066
100	-	1.17	1.10	0.13	0.22	-	0.081	1.30	0.054
120	-	1.09	1.11	0.15	0.22	-	0.075	0.22	0.058

[a] Other minor products detected at end of experiment: CO; N_2O (0.033 ppm max. conc.)
[b] Calculated initial O_3 concentration
[c] Positive interferences on output of chemiluminescent instrument might be present (see text)
[d] Dash means below FT-IR detection sensitivity; blank means no measurement was made

26

The Reaction of Monomethylhydrazine (MMH) with Ozone. In contrast with the apparent simplicity of the products generated in the N_2H_4 plus O_3 and UDMH plus O_3 systems, those seen in the MMH plus O_3 reaction present a more complicated case. Intermediate products were formed which further reacted with excess O_3 to form a variety of products, some of which have not been identified.

The first MMH plus O_3 dark reaction was carried out with approximately equimolar amounts (1.4 ppm each) of MMH and O_3 (Table 8). The second run consisted of a higher initial concentration of MMH (~3.6 ppm) with two separate injections (~2.8 ppm each) of O_3 (Table 9). For both experiments, the initial phase was characterized by instantaneous complete consumption of either MMH or O_3. The products identified were diazomethane (CH_2N_2), methyldiazene ($CH_3N=NH$), methylhydroperoxide (CH_3OOH) and methanol (CH_3OH). N_2O was not observed to form during this initial stage, but small amounts were detected later in the experiment.

The product spectra for the high concentration experiment are presented in Figure 8. The absorptions of NH_3 have been subtracted in each case for clarity. The spectrum recorded at 2 minutes after the first O_3 injection (Figure 8b) clearly shows the formation of CH_2N_2 (2102.0 cm^{-1}), H_2O_2 (resolved structures at ~1260 cm^{-1}), and $CH_3N=NH$ (Q-branch at 845.2 cm^{-1} and overlapped fundamental bands at ~1120 and ~1140 cm^{-1}). The absorption region for HCHO (analytical bands at 2778.9 and 2781.3 cm^{-1}), an important product of the reaction, is not shown in Figure 8. The Q-branch absorption at 1034.1 cm^{-1} is due to CH_3OH. Its P-R wings are overlapped by absorption band(s) of methylhydroperoxide (CH_3OOH) centered at ~1028 cm^{-1}. During the 30 minutes after the first O_3 injection, MMH was seen to decay rapidly; slower decreases were observed for $CH_3N=NH$ and HCHO. CH_2N_2, CH_3OH, and CH_3OOH remained essentially unchanged during this period (see Table 9).

Within 2 minutes after the second injection of excess O_3, both CH_2N_2 and $CH_3N=NH$ were completely consumed (Figure 8c). The CH_3OH Q-branch approximately doubled in intensity along with an apparent comparable increase in intensity of the underlying P-R branches.

The identification of CH_3OOH as a product of the MMH plus O_3 reaction presented a special difficulty. Its absorption envelope at ~1028 cm^{-1}

TABLE 8. CONCENTRATIONS OF REACTANTS AND PRODUCTS[a] VERSUS TIME IN THE MMH + O$_3$ DARK REACTION (28 MAY 1980). T (AVE.) = 22°C, %RH (AVE.) = 12

Elapsed Time (min)	MMH	O$_3$	CH$_2$N$_2$	H$_2$O$_2$	HCHO	NH$_3$	NO	NO$_2$	CH$_3$OH	CH$_3$OOH	Absorbance[b] CH$_3$NNH
-16	1.57					0.357					
-5	1.35					0.381					
0	--	~1.4 (calculated initial O$_3$ conc.)									
2	--c	0.24	0.16	0.18	0.20	0.382	0.003	0.005	0.086	0.93	0.056
4	--	0.15	0.16	0.19	0.22	0.369	0.008	0.063	0.089	1.0	0.054
6	--	0.06	0.16	0.18	0.21	0.370	0.009	0.059	0.086	1.0	
10	--	-	0.15	0.13	0.20	0.343	0.007	0.057	0.097	1.0	
14	--	-	0.14	0.13	0.17	0.325	0.007	0.057	0.11	1.0	0.044
18	--	-	0.14	0.14	0.16	0.312	0.006	0.059	0.12	1.0	
33	--	-	0.12	0.11	0.12	0.275	0.007	0.061	0.12	1.0	0.043
53	--	-	0.10	0.086	0.081	0.229	0.009	0.064	0.11	1.0	
78	--	-	0.089	0.070	0.065	0.197	0.013	0.064	0.11	1.0	
98	--	-	0.072	0.052	0.049	0.173	0.011	0.066	0.11	0.90	0.038

[a] Other products: N$_2$O, 0.019 ppm max. conc. formed at end of experiment

CH$_3$ONO$_2$, small amounts formed could not be measured due to interference by CH$_3$N=NH

[b] Q-branch intensity (base e) of CH$_3$N=NH at 845.2 cm^{-1}

[c] Dash means below FT-IR detection sensitivity; blank means no measurement was made

28

TABLE 9. CONCENTRATIONS OF REACTANTS AND PRODUCTS[a] VERSUS TIME IN THE MMH + O₃ DARK REACTION (16 JUNE 1980). T (AVE.) = 41.5°C, %RH (AVE.) = 4

Elapsed Time (min)	MMH	O₃	CH₂N₂	H₂O₂	HCHO	Concentration (ppm) NH₃	NO	NO₂	CH₃OH	CH₃OOH	Absorbance[c] CH₃NNH
-8	3.68					0.655	0.010	0.013			
0		-2.8[b] (1st O₃ injection)									
2	0.661	–	0.40	0.51	0.29	0.753	0.019	0.113	0.11	1.5	0.205
9	0.524	–	0.40	0.44	0.25	0.774	0.020	0.113	0.12	1.5	0.198
16	0.480	–	0.40	0.41	0.23	0.783	0.030	0.114	0.12	1.6	0.191
23	0.435	–	0.40	0.37	0.22	0.777	0.030	0.116	0.13	1.6	0.184
30	0.460	–	0.40	0.32	0.19	0.770	0.031	0.113	0.13	1.6	0.175
38		-2.8[b] (2nd O₃ injection)									
40	–[d]	2.37	–	0.41	0.59	0.661	0.013	0.174	0.26	2.5	–
47	–	2.13	–	0.38	0.60	0.581	0.011	0.166	0.27	2.6	–
54	–	1.99	–	0.37	0.60	0.513	0.011	0.180	0.30	2.6	–
61	–	1.84	–	0.35	0.59	0.449	0.010	0.160	0.29	2.5	–
68	–	1.75	–	0.34	0.58	0.398	0.010	0.162	0.30	2.4	–
80	–	1.61	–	0.33	0.61	0.350	0.010	0.148	0.30	2.4	–
91	–	1.54	–	0.29	0.57	0.302	0.010	0.145	0.30	2.4	–

[a] Other products: N₂O, 0.022 ppm max. conc. formed at end of experiment; CH₃ONO₂, 0.05 ppm at t = 40 min. to 0.07 ppm at t = 91 min; presence of CH₃N=NH before 2nd O₃ injection interfered with its measurement

[b] Calculated initial O₃ concentration

[c] Q-branch intensity (base e) of CH₃N=NH at 865.2 cm⁻¹

[d] Dash means below FT-IR detection sensitivity; blank means no measurement was made

29
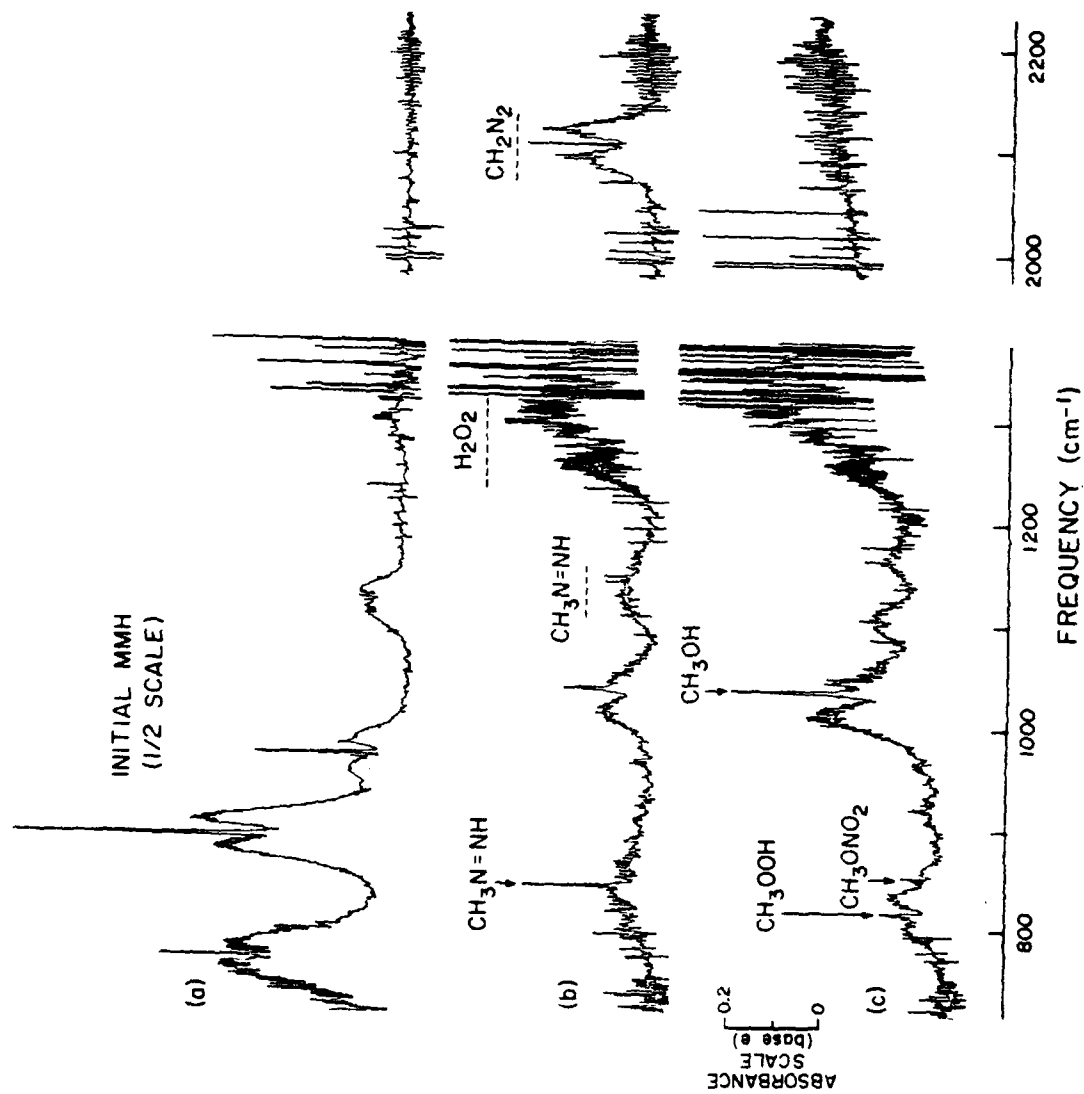
Figure 8. Fourier Transform-Infrared Spectra of MMH + O_3 Dark Reaction: (a) MMH Spectrum, (b) 2 Minutes After First O_3 Injection, (c) 2 Minutes After Second O_3 Injection (see Table 6). NH_3 Absorptions Subtracted from (a) and (b); NH_3 and O_3 Absorptions Subtracted from (c). Resolution = 1 cm^{-1}, Pathlength = 460 m.

heavily overlaps with the 1034.1 cm^{-1} fundamental band of CH_3OH. The stability of CH_3COOH (even under sunlight irradiation), together with its concentration increase and apparent constant ratio with CH_3OH in several experiments, created the impression of a single end-product being formed. Only through consideration of a possible reaction mechanism (see Discussion, this section), and the clear appearance of weaker CH_3OOH absorptions at 821.5 cm^{-1} and ~1165 cm^{-1} in the high-concentration run, was its formation suspected and verified. Subtraction of the CH_3OH absorption brought out the similarity of the band contour of the ~1028 cm^{-1} band with that of a published spectrum (Reference 26) of CH_3OOH.

Other unknown absorptions (Figure 8c) which developed after the second O_3 injection are the medium intensity bands at ~1106 cm^{-1} (overlapped by the 1105.5 cm^{-1} Q-branch from a trace amount of HCOOH) and a weak doublet Q-branch feature at 921.8 and 923.3 cm^{-1}. The other Q-doublet at 853.4 and 855.8 cm^{-1} is due to the formation of a small amount of CH_3ONO_2.

From the data of Tables 8 and 9, it is seen that there is an approximate 1:1 correspondence in the consumption of MMH and O_3 whether equimolar initial quantities of reactants or excess MMH are used. The observed ratio 1:1 is probably fortuitous since the initial products CH_2N_2 and CH_3NNH have been demonstrated to be consumed equally rapidly upon the introduction of excess O_3.

Although the large yield of CH_3OOH was surprising, its amount measured immediately after the second O_3 injection (t = 40 minutes, Table 9), along with the amounts of CH_3OH, HCHO, and CH_3ONO_2, add up to a satisfying carbon balance, accounting for ~91% of the initial MMH. [The quantitative evaluation of CH_3OOH was made possible by a carefully calibrated high-resolution (1/16 cm^{-1}) spectrum provided by Dr. Hiromi Niki of the Ford Motor Company Research Laboratories, Dearborn, Michigan. Estimates of the CH_3OOH yields were made through comparison of the broader features of the absorption bands, e.g., the P branch of the 821.5 cm^{-1} band.] Unfortunately, the only spectrum of $CH_3N=NH$ found in the literature (Reference 22) is not sufficiently quantitative to permit a reliable estimate of its yield.

31

Reactions of Selected Hydrazines with Nitrogen Oxides

Reaction of Hydrazine (N_2H_4) with NO_x. A mixture of 1.4 ppm of N_2H_4 with ~1 ppm NO_x (initial readings of 0.64 ppm NO and 0.34 ppm NO_2) was observed in the dark for 4 hours; the half-life of N_2H_4 during this experiment was ~2 hours with no observed change in the total NO_x level. At the end of 4 hours, 78% of N_2H_4 was lost with 95% of the initial NO_x still remaining. The total increase in NH_3 concentration above its initial impurity level could account for only ~8% of the N_2H_4 which disappeared. The total amount of N_2O formed at the end of the run was estimated to be 0.018 ppm. Thus, virtually no reaction between N_2H_4 and NO_x occurred in the dark at the low initial concentrations used. The major loss process of N_2H_4 in this experiment appears to be its decomposition to N_2 and H_2O.

Similar initial concentrations of N_2H_4 (1.3 ppm) and NO_x (0.87 ppm NO and 0.12 ppm NO_2) were employed in a second experiment in which the reactants were subsequently exposed to sunlight. The results presented in Table 10 show that the ~0.87 ppm and N_2H_4 remaining at the start of the afternoon irradiation was rapidly depleted in 30 minutes. An increase in N_2O was observed throughout the irradiation experiment. Figure 9 depicts the concentration versus time profiles for the reactants and products. It can be seen that the decay of NH_3 parallels that of NO_2 and coincides with the rise in O_3 concentration.

The observed progressive decrease in the infrared transmission at the high frequency end (> 2000 cm^{-1}) of the spectrum during irradiation was indicative of scattering of the source light due to particulate formation. The residual spectrum (Figure 10a) at the end of irradiation shows structureless absorption bands at 827, 964, and 1102 cm^{-1} along with indication of a very strong band (under heavy interference by H_2O bands) located above 1300 cm^{-1}.

A comparison with the product spectrum from the vapor-phase reaction of N_2H_4 and HNO_3 (Figure 10b) confirmed that the nitric acid salt of hydrazine ($N_2H_4 \cdot xHNO_3$) was formed during the irradiation experiment. The amount of hydrazinium nitrate formed could not be estimated since this compound presumably occurred largely in the aerosol phase. NH_4NO_3 was certainly formed during the irradiation, but the only spectral feature that could be

TABLE 10. REACTANT AND PRODUCT CONCENTRATIONS VERSUS TIME DURING IRRADIATION OF N_2H_4/NO_x MIXTURE (17 APRIL 1980). T (AVE.) = 40°C, %RH (AVE.) = 5

Elapsed Time (min)	Concentration (ppm)					
	N_2H_4	NO	NO_2	N_2O	NH_3	O_3
-12	1.32	0.008	-[a]		0.480	
- 4	1.16	0.008	-		0.502	
0 →	NO_x injection					
5	1.03	0.866	0.123		0.526	
10	1.02	0.855	0.138		0.543	
21	0.935	0.855	0.148		0.533	
31	0.879	0.851	0.157	0.021	0.548	
36 →	Start of sunlight irradiation (1436 PDT)					
38	0.796	0.830	0.165	0.026	0.561	-
40	0.782	0.800	0.184	0.029	0.573	-
43	0.684	0.760	0.227	0.027	0.559	-
47	0.623	0.670	0.288	0.032	0.576	-
53	0.503	0.523	0.430	0.035	0.593	-
59	0.360	0.317	0.601	0.038	0.586	-
65	0.094	0.099	0.691	0.035	0.586	0.107
72	-	-	0.736	0.039	0.507	0.233
80	-	-	0.650	0.043	0.409	0.354
96	-	-	0.559	0.043	0.303	0.277
105	-	-	0.510	0.046	0.209	0.297

[a]Dash means below FT-IR detection sensitivity; blank means no measurement was made
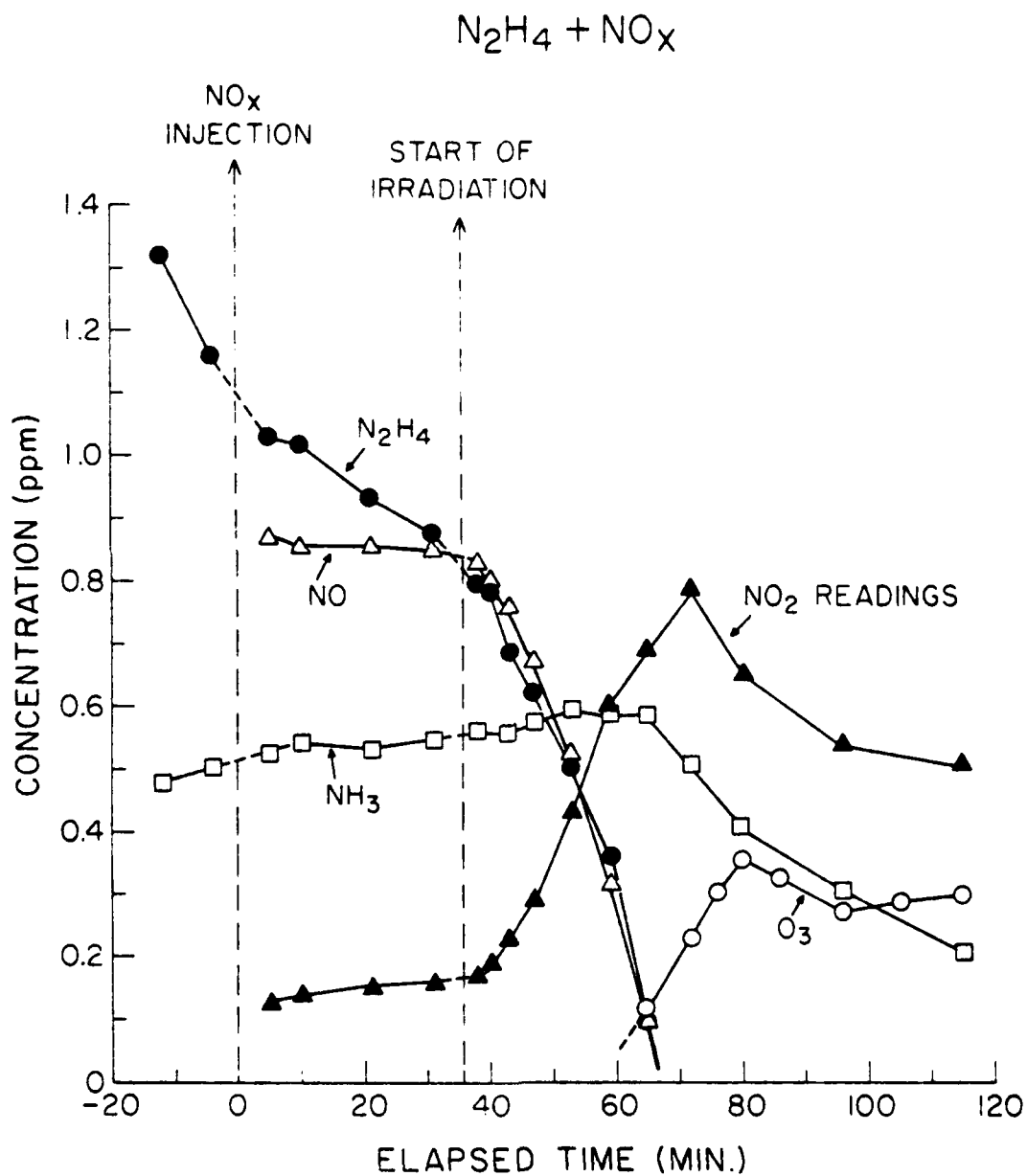
Figure 9. Time-Concentration Profile of Reactants and Some Products of $N_2H_4 + NO_x$ Reaction (see Table 10)

34
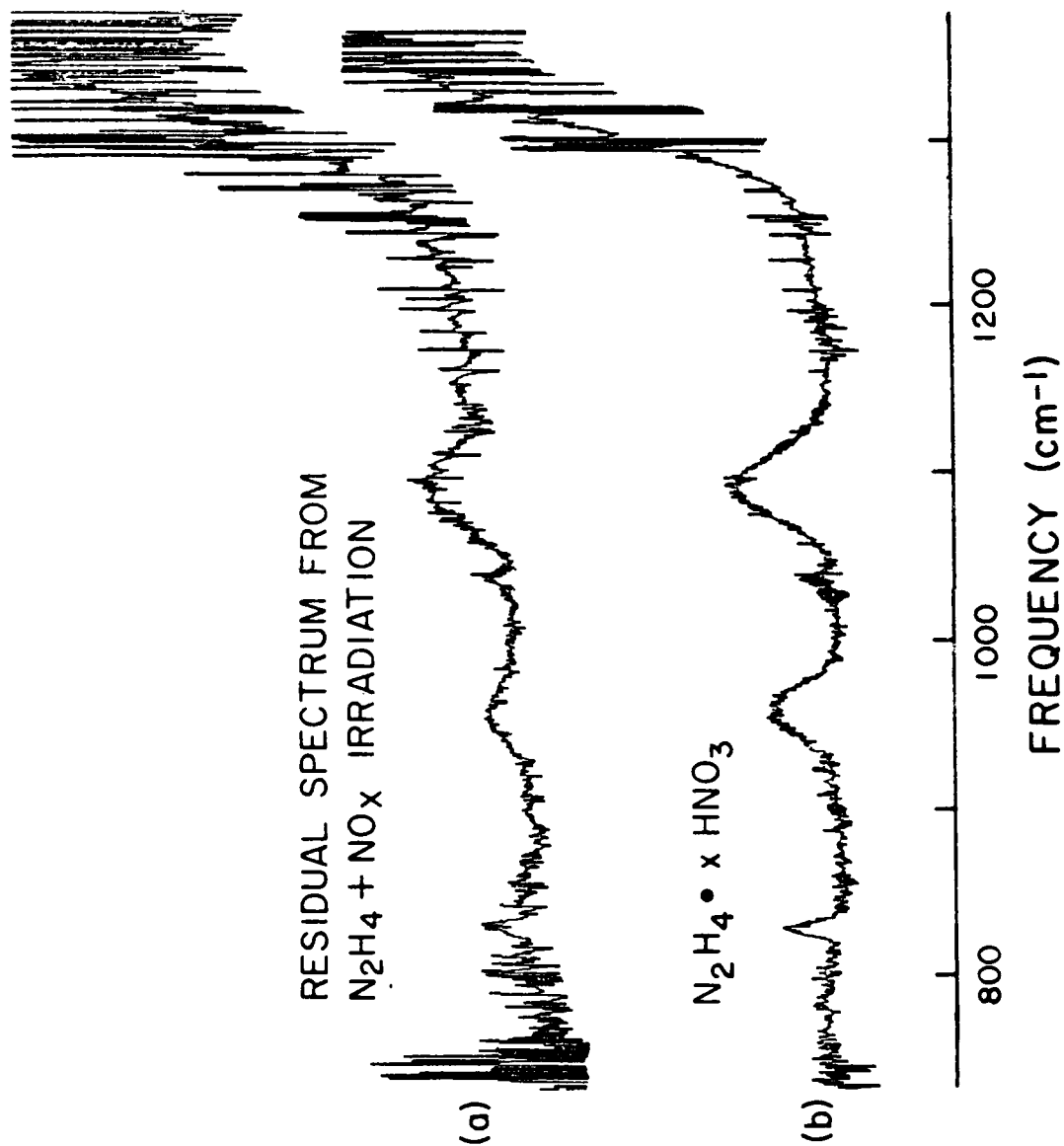
Figure 10. (a) Product Spectrum at End of $N_2H_4 + NO_x$ Irradiation (NH_3 and O_3 Absorptions Subtracted); (b) Spectrum of Product Obtained by Direct Reaction of N_2H_4 and HNO_3 in the Vapor-Phase

observed under the experimental conditions used is the 827 cm^{-1} band common to all inorganic nitrates. Hydrazinium nitrate was also reported to be a major product in the reaction of N_2H_4 with N_2O_4 in CCl_4 solvent at $-20^{\circ}C$ (Reference 2).

Reaction of Unsymmetrical Dimethylhydrazine (UDMH) with NO_x. A mixture of 1.3 ppm UDMH with an approximately equal amount of NO_x was observed in the dark for 3 hours. About 70% of UDMH remained at the end of this period and a comparatively negligible increase in NH_3 over its initial concentration was observed. Along with the expected build-up in HONO concentration (up to ~0.16 ppm), significant quantities of N_2O were formed (up to 0.07 ppm) together with the growth of an unidentified product(s) characterized by its broad infrared absorption at ~994 cm^{-1} (Figure 1'a).

In an additional experiment, a mixture of UDMH plus NO_x was irradiated with sunlight (Table 11). The reactant concentrations at the start of irradiation were approximately 1.5 ppm UDMH and 1.9 ppm NO_x (1.8 ppm NO and 0.14 ppm NO_2). During the first 40 minutes, UDMH was consumed rapidly; during the next 10 minutes it suddenly dropped in concentration from ~0.5 ppm to below detection limit (Figure 12). This abrupt depletion of UDMH was followed by a large jump in the chemiluminescent monitor's readings for NO_2, which probably reflected the presence of both NO_2 and organic compounds bearing the -NO and -NO_2 moieties (Reference 27). As expected, the NO concentration dropped quickly, followed by rapid O_3 formation. HCHO reached a maximum and began to show a decrease at this point. Even under sunlight irradiation, HONO concentration gradually built to a maximum just before O_3 was detected. This was also the approximate period at which NH_3 (mostly introduced as impurity) was consumed rapidly, presumably by the HNO_3 being generated. In contrast with the UDMH plus O_3 reaction where N_2O was negligibly formed, the reaction of UDMH with NO_x under irradiation yielded N_2O as a major product (the highest yield among the three hydrazine plus NO_x systems studied).

During the initial stage of irradiation, the infrared absorption at ~994 cm^{-1} of the unknown product(s) which was observed in the previous 3-hour dark experiment also developed in intensity. It is shown in the residual spectrum of Figure 11b (at 19 minutes from start of irradiation)

36
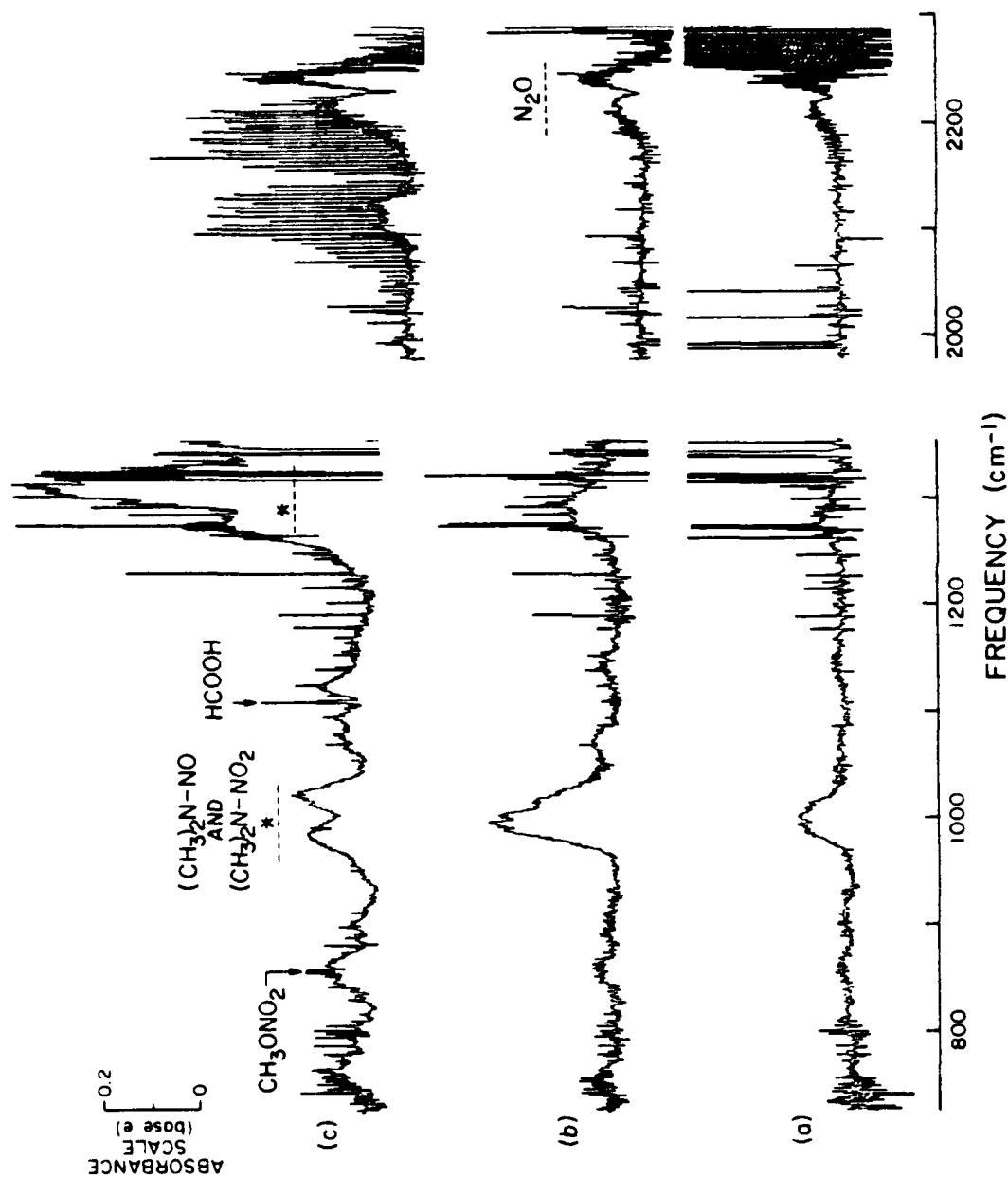
Figure 11. (a) Residual Spectrum Depicting Unknown ~994 cm^{-1} Absorption, UDMH + NO$_x$ in the Dark at 3 Hours. (b) and (c) Are From a Separate UDMH + NO$_x$ Irradiation Experiment (see Table 11): (b) is Residual Spectrum at 19 Minutes Into Irradiation, (c) is Residual Spectrum at 200 Minutes of Irradiation

TABLE 11. REACTANT AND PRODUCT[a] CONCENTRATIONS VERSUS TIME DURING IRRADIATION OF UDMH/NO$_x$ MIXTURE (13 MAY 1980). T (AVE.) = 38°C, %RH (AVE.) = 4

Elapsed Time (min)	Concentration (ppm)											
	UDMH	NO	NO$_2$	N$_2$O	NH$_3$	Nitros-amine[b]	Nitra-mine[c]	HCHO	HCOOH	O$_3$	HONO	HNO$_3$
-16	1.75	0.008	0.031		0.133							
-8	1.67	0.008	0.010		0.141							
0	NO$_x$ injection											
6	1.54	1.80	0.134		0.144						0.10	
15	1.52	1.80	0.139		0.143						0.14	
22	Start of sunlight irradiation (1202 PDT)											
25	1.45	1.80	0.147	0.055	0.147						0.15	
27	1.35	1.78	0.144	0.055	0.141						0.15	
31	1.17	1.74	0.153	0.061	0.136			-			0.14	
35	1.05	1.70	0.152	0.074	0.131			0.070			0.16	
41	0.87	1.57	0.169	0.088	0.126			0.093			0.14	
48	0.70	1.47	0.227	0.099	0.119			0.15			0.20	
56	0.58	1.28	0.295	0.12	0.113			0.20			0.21	
70	-	0.895	0.820	0.18	0.074			0.45	-		0.32	
80	-	0.565	0.952	0.19	0.035			0.67	0.006		0.34	
90	-	0.320	1.05	0.20	-[e]	0.29[d]	0.27[d]	0.77	0.020	-	0.29	-
100	-	0.162	0.958	0.21		0.24	0.36	0.82	0.031	0.170	0.21	0.041
120	-	0.045	0.839	0.25		0.18	0.44	0.74	0.040	0.364	-	0.140
140	-	0.035	0.740	0.24		0.15	0.48	0.60	0.048	0.528	-	0.215
160	-	0.030	0.658	0.25		0.13	0.50	0.55	0.056	0.651	-	0.265
180	-	0.028	0.602	0.25		0.12	0.52	0.51	0.061	0.717	-	0.277
200	-	0.026	0.602	0.23		0.11	0.53	0.48	0.067	0.796	-	0.290

[a] Other products of irradiation: CO; CH$_3$ONO$_2$, 0.05 ppm at t = 80 min. to 0.13 ppm at t = 200 min.
[b] (CH$_3$)$_2$N-NO
[c] (CH$_3$)$_2$N-NO$_2$
[d] Measurements at earlier times interfered with by unknown absorption at 994 cm^{-1}
[e] Dash means below FT-IR detection sensitivity; blank means no measurement was made

38
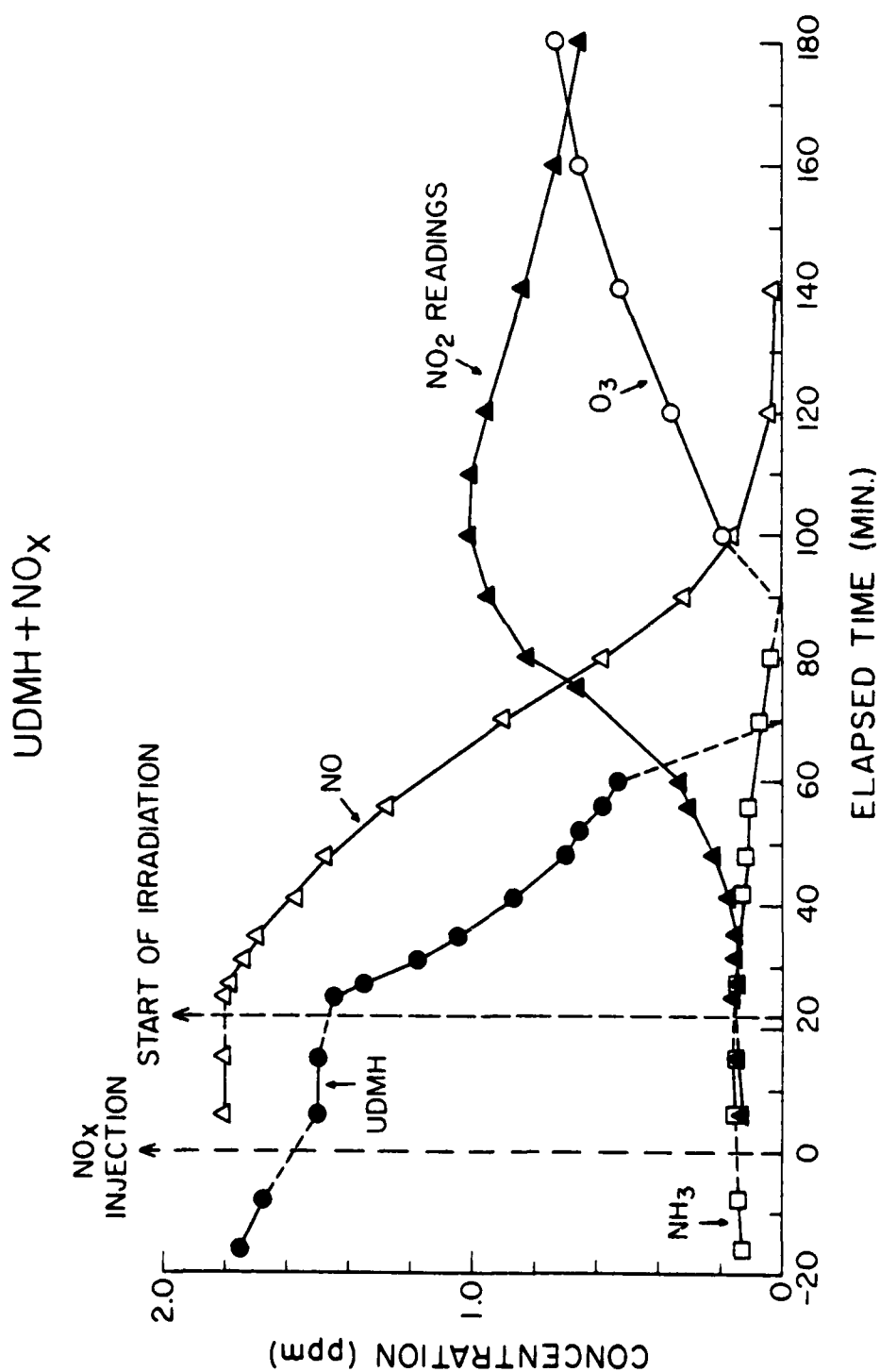
Figure 12. Time-Concentration Profile of Reactants and Some Products of UDMH + NO$_x$ Reaction (see Table 11)

with the superimposed 1016 cm^{-1} band of the $(CH_3)_2NNO$ being formed. This unknown absorption was further masked later in the reaction by the 980 cm^{-1} band of $(CH_3)_2NNO_2$. The 994 cm^{-1} absorption disappeared much later in the irradiation and thus allowed estimates of the amounts of the nitrosamine and nitramine compounds to be made (Figure 11c). Other stable irradiation products are CO and CH_3ONO_2. In addition, another unknown product, whose band envelope is situated underneath the CO P-branch at ~2110 cm^{-1} (Figure 11c) also started to form at the time the UDMH concentration abruptly dropped to zero. Its maximum concentration did not appear to change during the latter stages of irradiation which suggests that it has an appreciable photolytic life.

The Reaction of Monomethylhydrazine (MMH) with NO$_x$. A mixture of ~1.3 ppm initial MMH and an approximately equal amount of NO$_x$ (1.1 ppm NO and 0.32 ppm NO$_2$) was observed in the dark for 84 minutes and then exposed to sunlight (Table 12); at the end of the dark period, only the expected HONO growth and the formation of $CH_3N=NH$ (Figure 13a) were clearly observed in the infrared spectra. Approximately 60% of MMH decayed during this period. The increase in NH$_3$ concentration could account for only ~7% of the MMH depletion. As in the case of the N$_2$H$_4$ plus NO$_x$ system, a negligible amount of total NO$_x$ (~5%) was consumed during the dark part of the experiment. The formation of $CH_3N=NH$ is most likely due to autooxidation in air since this product was also observed in previous experiments in which MMH alone was mixed into purified matrix air to measure its half-life in the chamber. $CH_3N=NH$ has also been reported as one component of the complex mixture of products obtained in a reaction system of MMH and excess oxygen (Reference 28).

Upon exposure to sunlight the remaining ~0.5 ppm of MMH was virtually gone in less than 8 minutes. The sudden burst of chemical activity during this short period (Figure 14) was characterized by an equally rapid depletion of NO, an increase in NO$_2$ readings, and immediate formation of O$_3$ and HCHO. NH$_3$ was presumably rapidly stabilized to NH$_4$NO$_3$ as its disappearance was followed by a large build-up of HNO$_3$ near the end of irradiation.

Figure 13b is the residual spectrum (after subtraction of O$_3$ and HNO$_3$ absorptions) at the end of the irradiation experiment. CO, HCOOH, and

TABLE 12. REACTANT AND PRODUCT[a] CONCENTRATIONS VERSUS TIME DURING IRRADIATION OF MMH/NO_x MIXTURE (29 MAY 1980). T (AVE.) = 32°C, %RH (AVE.) = 8

Elapsed Time (min)	Concentration (ppm)										Absorbance[b]
	MMH	NO	NO_2	N_2O	NH_3	HCHO	HCOOH	O_3	HONO	HNO_3	CH_3NNH
-15	1.37	-[c]	0.011		0.289						
-6	1.26	-	0.010		0.321						
0 →	NO injection										
2	1.16	1.09	0.324	0.021	0.333						-
10	1.13	1.07	0.369	0.027	0.342				0.13		-
20	0.956	1.01	0.425	0.033	0.359				0.11		-
30	0.856	0.950	0.475	0.035	0.361				0.14		0.039
44	0.772	0.864	0.551	0.019	0.369				0.19		0.059
64	0.630	0.733	0.646	0.018	0.366				0.22		0.079
84	0.499	0.599	0.746	0.019	0.374	-		-	0.27		0.090
90 →	Start of sunlight irradiation (1556 PDT)										
94	0.034	0.059		0.041	0.333	0.24	-	0.181	0.32	-	0.098
98	-	0.016	1.06	0.046	0.156	0.38	-	0.428	0.27	-	-
106	-	0.010	0.825	0.050	-	0.45	0.014	0.757	0.17	0.060	-
116	-	0.014	0.610	0.056	-	0.44	0.021	0.912	0.13	0.193	-
131	-	0.013	0.416	0.064	-	0.41	0.025	1.01	-	0.314	-
151	-	0.010	0.310	0.071	-	0.39	0.031	1.01	-	0.380	-

[a] Other products of irradiation: CO; CH_3ONO_2, 0.04 ppm at t = 98 min. to 0.12 ppm at t = 151 min.

[b] Intensity (base e) of the 845.2 cm^{-1} Q-branch of CH_3N-NH

[c] Dash means below FT-IR detection sensitivity; blank means no measurement was made

41
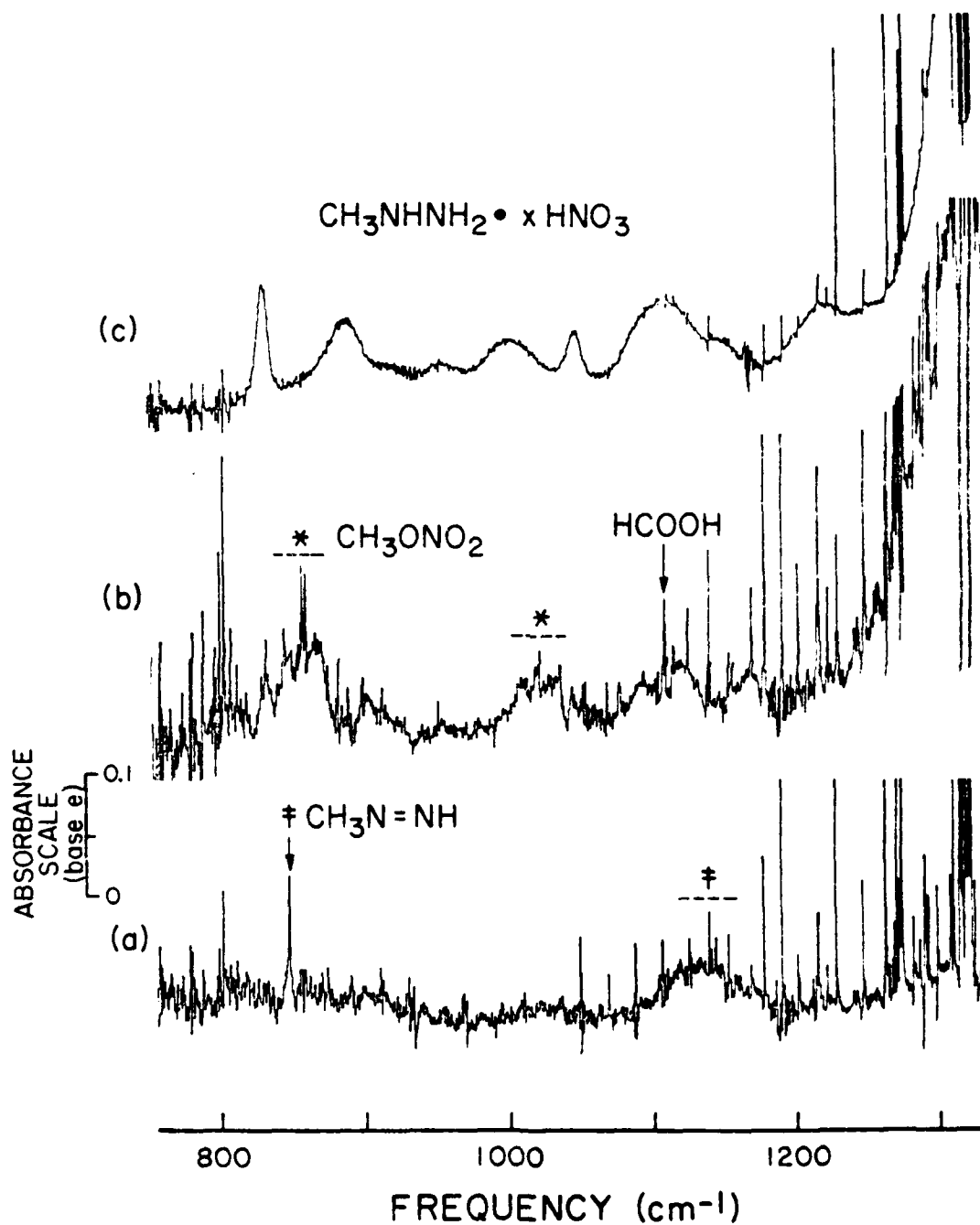
Figure 13. Product Spectra of MMH + NO_x Reaction: (a) at 84 Minutes in the Dark (MMH, NH_3, and HONO Absorptions Subtracted), (b) at ~1 Hour of Irradiation (O_3 and HNO_3 Absorptions Subtracted) (see Table 12), and (c) Spectrum of Product Obtained in the Vapor-Phase Reaction of MMH and HNO_3
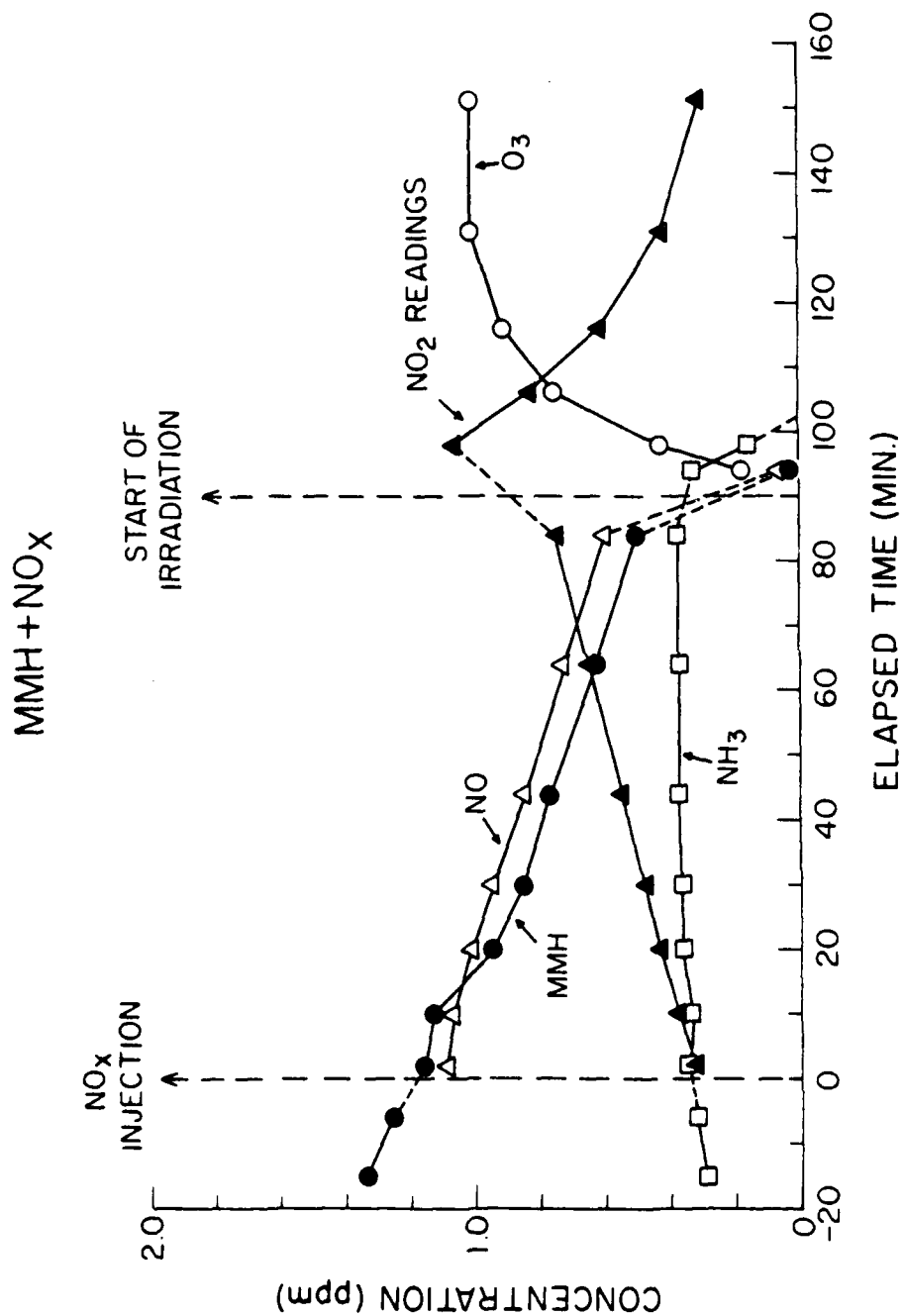
Figure 14. Time-Concentration Profile of Reactants and Some Products of MMH + NO$_x$ Reaction (see Table 12)

43

CH_3ONO_2 are other products of the irradiation. The significant attenuation of transmission at the high frequency region (> 2000 cm^{-1}) of the infrared spectrum indicated aerosol build-up during irradiation. It could not be ascertained upon comparison of Figure 13b with the spectrum (Figure 13c) of methylhydrazinium nitrate ($CH_3NHNH_2 \cdot xHNO_3$) whether the latter was formed. However, the appearance of the 827 cm^{-1} peak is indicative of the formation of salts of nitric acid.

DISCUSSION

Atmospheric Reactions of Hydrazine

Information was obtained in this study on the reaction of hydrazine in pure air, in air in the presence of NO_x, in air in the presence of ozone, and in NO_x-air photolyses. As expected, hydrazine is very reactive in atmospheric systems; the results and possible mechanisms accounting for them are discussed below.

When NO and NO_2 were added to a dry hydrazine-air mixture, the N_2H_4 decay was found to have a half-life of ~2 hours, about one-half that observed for hydrazine alone in dry air. Although there was apparently some acceleration in N_2H_4 loss, no products were observed by infrared spectroscopy other than NH_3 and N_2O in amounts comparable to those formed in the absence of NO_x. The experimental data were insufficient to permit an unambiguous determination as to whether some intermediates possibly formed in the $N_2H_4-O_2$ system interacted with NO_x.

Hydrazine + O_3 Dark Reaction. The results of three experiments in which hydrazine was reacted with O_3 are given in Tables 3, 4 and 5. In the 7 May 1980 (T = 24°C, Table 5) experiment, where O_3 was in excess (average O_3 concentration = 1.81 $\pm$ 0.14 ppm), the N_2H_4 decay was reasonably exponential. The observed decay rate corresponded to an N_2H_4 plus O_3 apparent rate constant of (1.3 $\pm$ 0.1) x 10^{-16} cm^3 molecule^{-1} sec^{-1}. The rates of N_2H_4 and O_3 decay in the 2 April 1980 (T = 21°C, Table 4) run are in reasonable agreement with the 7 May 1980 rate constant, but the apparent rate constant in the 1 February 1980 (T = 44°C, Table 3) run was approximately 50% higher, which could be caused by the reaction having a 3.5 to 5 kcal/mole activation energy. These rate constant estimates are

empirical in nature, and because of the possibility of secondary reactions consuming both O_3 and hydrazine, they must be considered only as upper limits for the elementary O_3 plus hydrazine reaction.

The major product observed in the N_2H_4-O_3 system is H_2O_2 with N_2O formed in minor amounts. The yields of these products appear to be independent of the amount of O_3 initially in excess. Hydrogen peroxide (H_2O_2) accounts for only 16 to 20% of the initial hydrogen, while N_2O accounts for < 3% of the initial nitrogen in the system. The missing nitrogen and hydrogen are most likely accounted for by formation of N_2, H_2O, or H_2 decomposition products, which could not be monitored by FT-IR spectroscopy. Significant increases in the concentrations of NH_3 and NO_x were not observed. Nitric acid formation is unlikely since a decrease in NH_3, with which it would have reacted, was not observed. Significant formation of other nitrogen- and hydrogen-containing products can be ruled out either on the basis of chemical reasonableness or non-detection by infrared spectroscopy.

An overall scheme of possible reactions to account for the observations reported here is given in Figure 15. It is unlikely that all pathways are significant, and some can be discarded on the basis of inconsistency with the available data. The reactions and considerations relating to them are discussed below.

There are four possible reactions which could account for the initial attack of O_3 on hydrazine:

$$H_2N\text{-}NH_2 + O_3 \rightarrow H_2N\text{-}\overset{\bullet}{N}H + HO_3 \tag{1}$$

$$H_2N\text{-}NH_2 + O_3 \rightarrow H_2N\text{-}\overset{\bullet}{N}H + HO + O_2 \tag{2}$$

$$H_2N\text{-}NH_2 + O_3 \rightarrow H_2N\text{-}\overset{\bullet}{N}H + HO_2 + O \tag{3}$$

$$H_2N\text{-}NH_2 + O_3 \rightarrow H_2N\text{-}\overset{\overset{O}{\uparrow}}{\underset{H}{N}}\text{-}H + O_2 \tag{4}$$
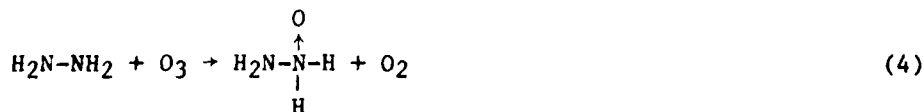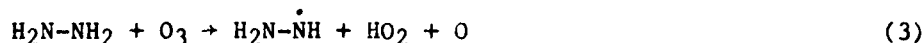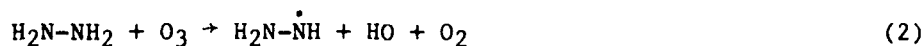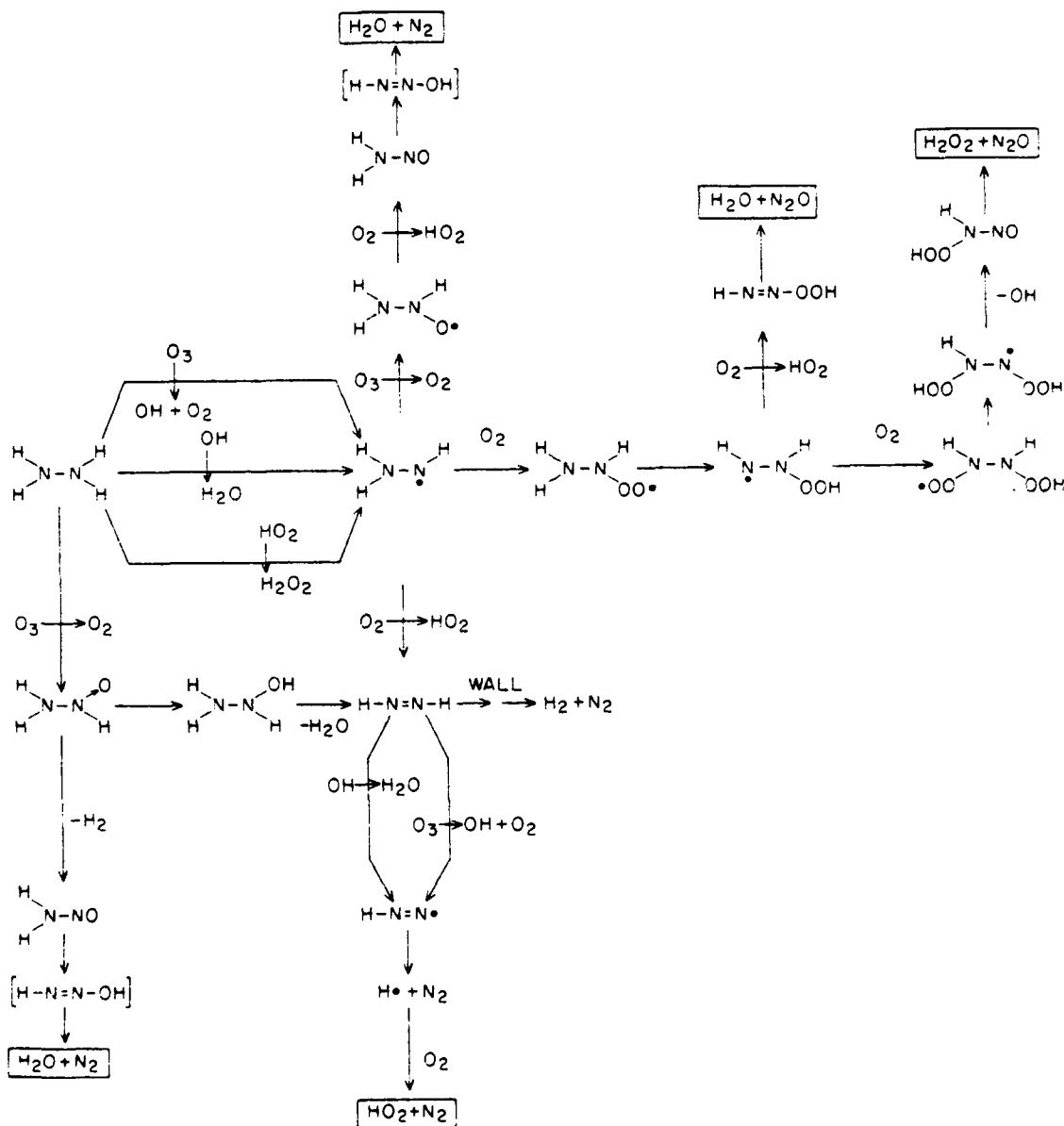
Figure 15. Possible Mechanisms for Reactions of Ozone with Hydrazine

Reactions (1) and (3) can be eliminated, since they are estimated to be highly endothermic, based on the published hydrazine N-H bond strength of 76 ± 2 kcal/mole (References 29 and 30) and the heats of formation of N_2H_4, OH, HO_2, and HO_3 given by Benson (Reference 31). Reaction (2) is roughly thermoneutral; if hydrogen abstraction occurs, it must involve the simultaneous fragmentation to OH and O_2. Reaction (4) is highly speculative and its thermochemistry is unknown, but it could be considered to be analogous to the known, rapid oxygen atom transfer reactions between O_3 and NO,

$$NO + O_3 \rightarrow NO_2 + O_2$$
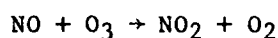
which occur at rates roughly comparable to the hydrazine-O_3 reactions reported here.

If reaction (4) occurs, the N-oxide formed may either eliminate H_2 to form nitrosamine [reaction (5)] or rearrange and eliminate H_2O to form diimide [reaction (6)]

$$\begin{array}{c} \text{H} \quad \text{O} \qquad \text{H} \\ \diagdown \uparrow \qquad \diagdown \\ \text{N-N-H} \rightarrow \quad \text{N-NO} + \text{H}_2 \\ \diagup \quad | \qquad \diagup \\ \text{H} \quad \text{H} \qquad \text{H} \end{array} \qquad (5)$$

$$\begin{array}{c} \text{H} \quad \text{O} \qquad \text{H} \quad \text{OH} \\ \diagdown \uparrow \qquad \diagdown \diagup \\ \text{N-N-H} \rightarrow \quad \text{N-N} \qquad \text{H}_2\text{O} + \text{H-N=N-H} \\ \diagup \quad | \qquad \diagup \diagdown \\ \text{H} \quad \text{H} \qquad \text{H} \quad \text{H} \end{array} \qquad (6)$$
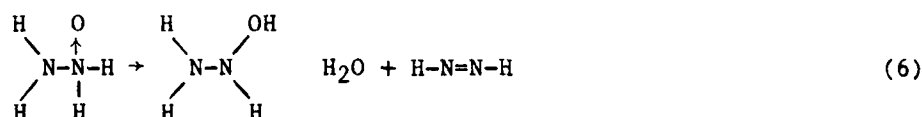
Nitrosamine is known to be unstable, and if formed is expected to decompose to form $H_2O + N_2$ (Reference 32). Diimide is not observed; if formed it would either decompose to $H_2 + N_2$ or react with O_3 (see below). The observed 1:1 O_3/N_2H_4 stoichiometry implies that if diimide is formed by reaction (6), it cannot undergo a secondary reaction to consume ozone significantly. Therefore, if N-oxide formation occurred, the major overall process would be fragmentation forming $N_2 + H_2 + H_2O$, regardless of the exact decomposition pathways. Such a process does not account for the high yields of H_2O_2 observed; thus, it is unlikely that N-oxide formation is the dominant initial mode of O_3 attack on N_2H_4.

47

It is probable that the major initial process is H-abstraction [reaction (2)], resulting in the formation of N_2H_3 and OH radicals. The OH radical is expected to react rapidly with another hydrazine molecule [the OH-hydrazine reaction is fast (see Section II and Reference 33) and would dominate over the reaction (Reference 34) of OH with O_3] yielding an additional N_2H_3 radical:

$$H_2N-NH_2 + OH \rightarrow H_2O + H_2N-\overset{\bullet}{N}H \tag{7}$$

The N_2H_3 radical formed in reactions (2) or (7) could react with either O_2 or O_3:

$$H_2N-\overset{\bullet}{N}H + O_2 \overset{M}{\rightarrow} H_2N-\overset{\overset{OO^\bullet}{|}}{N}H \tag{8}$$

$$H_2N-\overset{\bullet}{N}H + O_2 \rightarrow HO_2 + HN=NH \tag{9}$$

$$H_2N-\overset{\bullet}{N}H + O_3 \rightarrow H_2N-\overset{\overset{O^\bullet}{|}}{N}H + O_2 \tag{10}$$

Amino radicals are also known to react rapidly with NO and NO_2 (Reference 35) but since significant levels of NO_x are not observed in these runs, such reactions will not be considered.

If the N_2H_3 radicals reacted with ozone (reaction 10), ultimate formation of HO_2, N_2, and H_2O is expected.

$$\underset{H}{\overset{H}{\diagdown}}N-N\underset{O^\bullet}{\overset{H}{\diagup}} + O_2 \rightarrow HO_2 + \underset{H}{\overset{H}{\diagdown}}N-NO \tag{11}$$

$$\underset{H}{\overset{H}{\diagdown}}N-NO \rightarrow [H-N=NOH] \rightarrow H_2O + N_2 \tag{12}$$
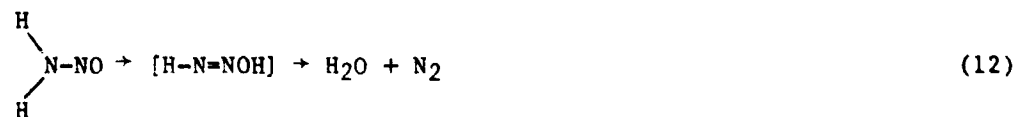
Under the conditions of these runs the major fate of HO_2 is expected to be self-reaction [reaction (13)], or reaction with hydrazine [reaction (14)]:

48

$$HO_2 + HO_2 \rightarrow H_2O_2 + O_2 \tag{13}$$

$$HO_2 + \underset{H}{\overset{H}{\diagdown}}N\text{--}N\underset{H}{\overset{H}{\diagup}} \rightarrow H_2O_2 + \underset{H}{\overset{H}{\diagdown}}N\text{--}N\overset{H}{\diagup}_{\textbf{.}} \tag{14}$$
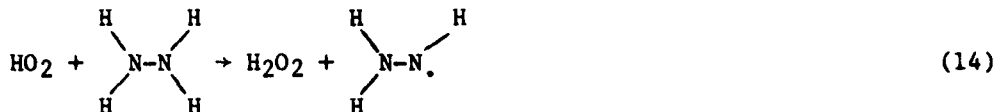
If reactions (2), (7), and (10) through (14) are the major processes in the O_3-N_2H_4 system, then the 1:1 O_3/N_2H_4 stoichiometry indicates that reaction (14) is significant, resulting in a radical chain mechanism with HO_2 as a carrier; if reaction (14) is negligible, the reaction sequence yields a predicted 3:2 O_3/N_2H_4 stoichiometry. Although this mechanism is consistent with most of the observed results in the O_3-N_2H_4 system, the observation of high yields of methyldiazene in the O_3-monomethylhydrazine system suggests that its parent analogue, diimide (more recently called diazene), may play a significant role in the hydrazine-O_3 system, which is inconsistent with the mechanism just considered.

Diimide formation is expected to result from the abstraction reaction of O_2 with N_2H_3 [reaction (9)], a reaction analogous to the O_2 plus dimethylamine radical reaction

$$(CH_3)_2N\cdot + O_2 \rightarrow HO_2 + H_2C\text{=}N\text{--}CH_3 \tag{15}$$

observed by Lindley and coworkers (Reference 36), or to the known CH_3O plus O_2 reaction (Reference 37), both of which occur at significant rates for atmospheric systems. Diimide undergoes heterogeneous decomposition (Reference 38) to H_2 and N_2 and could also react with OH, resulting in the formation of H_2O, N_2, and HO_2 (see Figure 15). However, if diimide formation by means of reaction (9) is the major fate of N_2H_3, it is necessary to assume that the diimide formed reacts primarily with O_3 in order to be consistent with the 1:1 O_3/N_2H_4 stoichiometry.

There are a number of possible mechanisms for the reaction of O_3 with diimide:

$$HN\text{=}NH + O_3 \rightarrow HN\text{=}N\cdot + OH + O_2 \overset{O_2}{\rightarrow\rightarrow} HO_2 + N_2 + OH + O_2 \tag{16}$$

49

$$\text{HN=NH} + O_3 \rightarrow \overset{\displaystyle O}{\underset{\displaystyle \text{H-N-N-H}}{\overset{\displaystyle /\backslash}{\overset{\displaystyle O\ \ O}{|\ \ |}}}} \tag{17}$$

$$\overset{O}{\underset{\text{H-N-N-H}}{\overset{/\backslash}{\overset{O\ O}{|\ |}}}} \rightleftharpoons \left[\overset{O\cdot}{\underset{\text{H-N-N-H}}{\overset{|}{\overset{O\ O}{|\ |}}}}\right] \rightarrow \overset{\text{HOO}}{\underset{H}{\diagdown}} \text{N-NO} \rightarrow H_2O_2 + N_2O \tag{18}$$

$$\overset{O}{\underset{\text{H-N-N-H}}{\overset{/\backslash}{\overset{O\ O}{|\ |}}}} \rightarrow \text{HNO} + \text{H}\overset{\bullet}{\text{N}}-\text{O}\overset{\bullet}{\text{O}} \tag{19}$$

$$\text{HNO} + O_2 \rightarrow HO_2 + \text{NO}$$

$$\text{NO} + O_3 \rightarrow NO_2$$

$$\text{H}\overset{\bullet}{\text{N}}\text{O}\overset{\bullet}{\text{O}} \rightarrow \left[\text{H-N}\overset{O}{\underset{O}{\diagdown\!\!\diagup}}\right] \rightarrow \text{HN}\overset{O}{\underset{O}{\diagup\diagdown}} \overset{O_2}{\rightarrow} \rightarrow HO_2 + NO_2$$
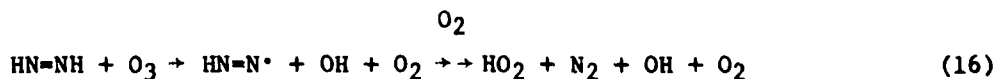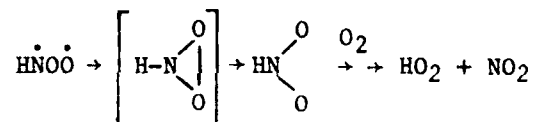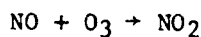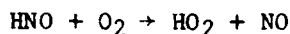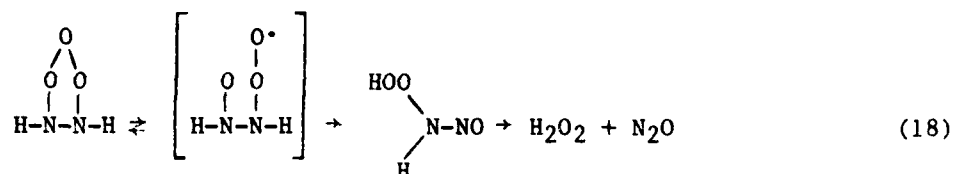
Only reaction (16) is consistent with the results of this study, since
N_2O [predicted by reactions (17) and (18)] is observed only in low yields
which are independent of the initial O_3/N_2H_4 ratios, and NO_2 [predicted
by reactions (17) and (19)] is not observed. If diimide formation followed
by reaction (16) is important, then the $O_3 + N_2H_4$ mechanism consisting
of reactions (2), (7), (9), (13), and (16) would be a chain reaction with
OH as the chain carrier. This mechanism is also consistent with the ob-
served O_3/N_2H_4 stoichiometry and, except for minor formation of N_2O, with
most of the product data. It also has the additional advantage of being
consistent with the mechanism proposed for the products observed in the
MMH + O_3 system.

It is also possible that addition of O_2 to N_2H_3 radicals [reaction
(8)] occurs to some extent. The most probable subsequent reactions of the
N-peroxy radical formed (shown in Figure 15) would result in the formation

of N_2O. The reactions are speculative in nature but have reasonable transition states and should be exothermic; most are analogous to known reactions in other systems. The observation that N_2O is a minor product in the O_3 + N_2H_4 system (maximum yield $\simeq$ 3%) suggests that reaction (8) is a minor pathway. Also, from the fact that the addition of O_2 to amino radicals is extremely slow ($<3 \times 10^{-8}$ cm^3 molecule^{-1} sec^{-1} at 500 K (Reference 39) and thus negligible at 300 K), it is reasonable to expect reaction (8) likewise to be negligible. However, N_2O formation following reaction (8) can account for the observed formation of N_2O, and the fact that its yield does not increase when excess O_3 is present.

Despite the relative simplicity of the products observed, it is clear that the chemistry of the O_3 + hydrazine systems is complex, with at least two reasonable radical chain mechanisms being able to account for the observations. The currently available data are not sufficient to positively determine the exact mechanism, although the MMH-O_3 data suggest that diimide plays a major role. In view of the probability that chain reactions occur, the rate of the initial O_3 plus hydrazine reaction may be considerably slower than the empirical rate of hydrazine loss observed in these experiments.

Hydrazine-NO$_x$ Photolysis. Although hydrazine does not significantly react in the dark with NO$_x$, when hydrazine-NO$_x$-air mixtures are irradiated hydrazine is rapidly consumed, NO is converted to NO_2 at a rate approximately equal to that of hydrazine decay, and O_3 is formed following NO consumption (see Figure 9 and Table 10). The only nitrogen-containing product observed was N_2O in trace amounts. NO$_x$ apparently is not a major product, since there is no increase in NO$_x$ concentration over the period hydrazine is consumed.

The initial consumption of hydrazine can be attributed primarily to reaction with hydroxyl radicals [reaction (7)], since OH is formed in NO$_x$-air irradiations, and the OH-hydrazine reaction has been shown to be fast (see Section II and Reference 33). After O_3 is formed, the rapid O_3-hydrazine reaction appears to dominate.

Since the reaction of N_2H_4 with OH, like that with O_3, initially forms the N_2H_3 radical, the overall mechanism for these two systems should be

51

similar. The conversion of one molecule of NO to NO_2 per molecule of hydrazine consumed can be attributed to HO_2 being formed in reaction (9) and then reacting with NO.

$$HO_2 + NO \rightarrow OH + NO_2 \tag{20}$$

The fact that only one molecule of NO is converted to NO_2 per molecule consumed means that reaction of NO with $N_2H_3O_2$ (reaction 21)

$$\begin{matrix} H & & OO\cdot \\ & \diagdown & \diagup \\ & N-N & \\ & \diagup & \diagdown \\ H & & H \end{matrix} + NO \rightarrow \begin{matrix} H & & O\cdot \\ & \diagdown & \diagup \\ & N-N & \\ & \diagup & \diagdown \\ H & & H \end{matrix} + NO_2 \tag{21}$$

followed by

$$\begin{matrix} H & & O\cdot \\ & \diagdown & \diagup \\ & N-N & \\ & \diagup & \diagdown \\ H & & H \end{matrix} + O_2 \rightarrow HO_2 + \begin{matrix} H & \\ & \diagdown \\ & N-NO \\ & \diagup \\ H & \end{matrix} \tag{22}$$
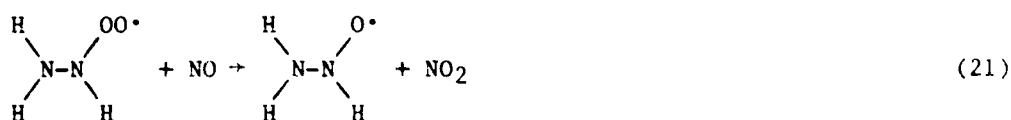
is probably not important, since the HO_2 formed in reaction (22) would convert a second molecule of NO to NO_2, which is inconsistent with the results.

The reaction of HO_2 with NO competes with the formation of H_2O_2 from HO_2 and can account for the fact that H_2O_2, observed in large yields in the $N_2H_4-O_3$ system, is not observed in the $N_2H_4-NO_x$ irradiation. Furthermore, the fact that H_2O_2 is not formed in the irradiation is consistent with the assumption that the H_2O_2 observed in the $N_2H_4-O_3$ system is formed from HO_2, and not from some type of molecular rearrangement.

During the initial stages of the reaction, when O_3 is absent, the diimide formed could be consumed by photolysis [reaction (23)] or by reaction with OH [reaction (24)].

$$HN=NH + h\nu \xrightarrow[\quad]{O_2} N_2 + 2HO_2 \tag{23}$$

52

$$HN{=}NH + OH \rightarrow H_2O + HNN \overset{O_2}{\rightarrow} \rightarrow N_2 + HO_2 + H_2O \qquad (24)$$
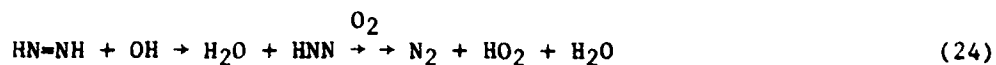
If photolysis of diimide is the dominant pathway, the fact that reaction (23) is chain branching would cause the overall N_2H_4 oxidation process to be self-initiating, which was not observed. Therefore, it is probable that the major fate of diimide is reaction with OH, at least until O_3 is formed.

In the presence of NO_x the possibility of two additional reactions of the N_2H_3 radical must be considered:

$$\begin{array}{c}
H \\ \diagdown \\ \diagup N{-}N \diagup \\ H \bullet
\end{array}
\begin{array}{c} H \\ \diagup \end{array}
+ NO \overset{M}{\rightarrow}
\begin{array}{c}
H H \\ \diagdown \diagup \\ N{-}N \\ \diagup \diagdown \\ H NO
\end{array}
\qquad (25)$$

$$\begin{array}{c}
H \\ \diagdown \\ \diagup N{-}N \diagup \\ H \bullet
\end{array}
\begin{array}{c} H \\ \diagup \end{array}
+ NO_2 \overset{M}{\rightarrow}
\begin{array}{c}
H H \\ \diagdown \diagup \\ N{-}N \\ \diagup \diagdown \\ H NO_2
\end{array}
\qquad (26)$$

Reaction (25), if it occurs, would probably be of negligible effect since it is expected to be rapidly reversed by photolysis, but the fate of the product formed in reaction (26) is uncertain. It may decompose to form diimide and HONO [reaction (27)] which, because of the rapid photolysis of HONO, would be chain propagating.

$$\begin{array}{c}
H H \\ \diagdown \diagup \\ N{-}N \\ \diagup \diagdown \\ H NO_2
\end{array}
\rightarrow
\left[
\begin{array}{c}
H H \\ \diagdown \diagdown \\ N{-}N \\ \vdots \diagdown \\   N{-}O \\ H_{\cdot \cdot} \diagup \\ {\cdot \cdot} O
\end{array}
\right]
\rightarrow HN{=}NH + HONO
\qquad (27)$$

$$HONO + h\nu \rightarrow OH + NO \qquad (28)$$
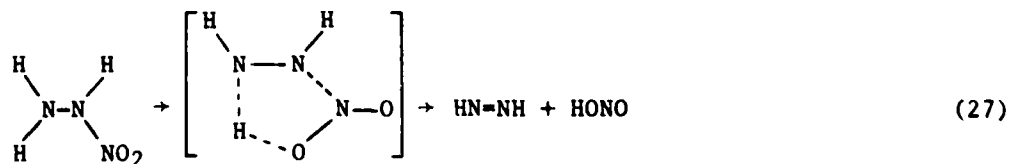
The net effect of reactions (26 through 28) would be conversion of NO_2 to NO, which is the opposite of what is observed; but if the diimide formed were to undergo rapid photolysis [reaction (23)], the two molecules of HO_2 formed

53

would react with NO, with the resulting net effect being the observed conversion of one molecule of NO to NO_2.

Another pathway for the loss of N_2H_4 during hydrazine-NO_x-air photolysis is the reaction of N_2H_4 with HNO_3 to form hydrazinium nitrate ($N_2H_4 \cdot xHNO_3$), a product which was observed directly during the experiment. Nitric acid is formed from the reaction of OH with NO_2 at a rate that is probably slower than the rate of OH + N_2H_4 reaction. The extent of N_2H_4 stabilization to the nitric acid salt could not be quantitatively determined by infrared spectroscopy, since the bulk of this product is in the aerosol phase. The formation of hydrazinium nitrate is expected to parallel that of NH_4NO_3 formation. The decrease in NH_3 during the later stage of irradiation is attributed mainly to its reaction with HNO_3, since the reaction NH_3 + OH is known to be slow (References 40 and 41). [HNO_3 was not observed directly due to remaining excess NH_3 (Table 10); it was detected in the UDMH + NO_x and MMH + NO_x systems (Tables 11 and 12) following complete consumption of NH_3.] From the comparative depletion rates of N_2H_4 and NH_3 (see Figure 9), it can be concluded that the dominant pathway in the hydrazine-NO_x-air photolysis is the reaction of N_2H_4 with the OH radical.

The chemistry of the hydrazine-NO_x-air photolysis has many features in common with the hydrazine-O_3-air system, and hydrazine consumption by reaction with O_3 will probably dominate when O_3 is present. However, there are a number of additional uncertainties for the N_2H_4-NO_x photolysis system relating to the relative importance of diimide photolysis and N_2H_3 + NO_x reactions, which must be resolved before this system is adequately understood.

Atmospheric Reactions of Monomethylhydrazine (MMH)

There appears to be little prior work done concerning the atmospheric reactions of monomethylhydrazine (MMH). The results of this study indicate that MMH is even more reactive in atmospheric systems than hydrazine and that a variety of unusual products are observed. The specific systems for which information was obtained were: reactions of MMH in air in the presence and absence of NO_x; reaction of MMH with O_3 in air; and MMH-NO_x-air

irradiations. Possible mechanisms accounting for the results observed are discussed below.

MMH-Air and MMH-NO$_x$-Air Dark Reactions. The products slowly formed in the dark decay of MMH in air are NH$_3$, N$_2$O, and CH$_3$N=NH. The initiating process in this decay could be heterogeneous in nature, since it is unlikely that a significant homogeneous reaction between O$_2$ and MMH could occur at the temperatures in which the experiments were conducted.

The dark decay of MMH in the presence of NO$_x$ (Table 12) is estimated to have a half-life of ~70 minutes, about 3.5 times faster than the corresponding decay in dry air (Table 2) without added NO$_x$. The same products were observed as in air alone but at higher yields. As indicated by the chemiluminescent instrument's readings (Table 12), no decrease in total NO$_x$ took place in the dark. However, the monitor's readings for NO$_2$ (Reference 27) are known to include -NO and -NO$_2$ group-bearing species (e.g., HNO$_3$, organic nitrates) and may possibly include products not detected by the infrared method under the conditions of our experiments. Thus, the decrease in the NO values may actually reflect reactions occurring rather than the apparent total conversion of NO to NO$_2$. These reactions possibly include those with intermediates that form even in the absence of NO$_x$. Product identification and quantification are currently insufficient to provide a clear understanding of the MMH dark decay mechanism.

MMH + O$_3$ Reactions. When O$_3$ is injected into MMH-air mixtures, the consumption of O$_3$ or MMH goes to completion in less than 2 minutes with formation of a variety of products, whose yields depend on the initial MMH/O$_3$ ratio. The major products observed are methylhydroperoxide, methyldiazene, diazomethane, formaldehyde, methanol, and H$_2$O$_2$. In the presence of excess O$_3$, methyldiazene and diazomethane are not observed and higher yields of HCHO, CH$_3$OH, and CH$_3$OOH are seen, accounting for essentially all the carbon in the initial MMH. The rapidity of the MMH + O$_3$ reaction indicates that it is primarily homogeneous in nature, and possible mechanisms which could account for obtained experimental results are discussed below.

The initial reactions occurring in the MMH-O$_3$ system are reasonably analogous to those occurring in the N$_2$H$_4$-O$_3$ system discussed previously and shown in Figure 15. In the subsequent discussion the initial O$_3$ + MMH

55

reaction is assumed to be H-abstraction rather than N-oxide formation, since the latter mechanism is inconsistent with the stoichiometry and H_2O_2 yields yields observed in the N_2H_4 system. Thus, the initial attack of O_3 on MMH could be either via reaction (29) or reaction (30):

$$\begin{array}{c} CH_3 \quad H \\ \diagdown \quad \diagup \\ N-N \\ \diagup \quad \diagdown \\ H \quad\quad H \end{array} + O_3 \rightarrow \begin{array}{c} CH_3 \quad H \\ \diagdown \quad \diagup \\ N-N \\ \bullet \quad \diagdown \\ \quad\quad H \end{array} + OH + O_2 \qquad (29)$$

$$\begin{array}{c} CH_3 \quad H \\ \diagdown \quad \diagup \\ N-N \\ \diagup \quad \diagdown \\ H \quad\quad H \end{array} + O_3 \rightarrow \begin{array}{c} CH_3 \quad\quad H \\ \diagdown \quad \diagup \\ N-N\bullet \\ \diagup \\ H \end{array} + OH + O_2 \qquad (30)$$
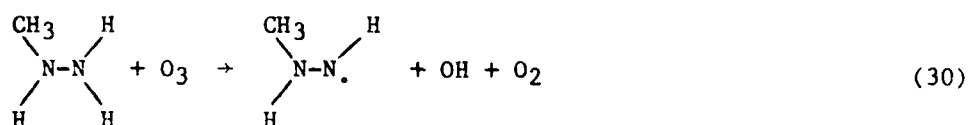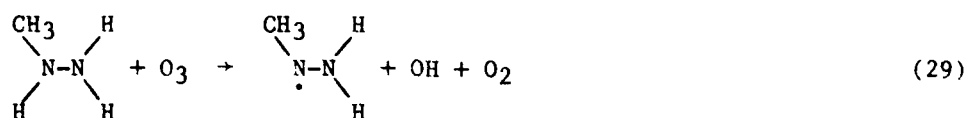
The hydroxyl radical formed would cause additional MMH consumption,

$$\begin{array}{c} CH_3 \quad H \\ \diagdown \quad \diagup \\ N-N \\ \diagup \quad \diagdown \\ H \quad\quad H \end{array} + OH \rightarrow H_2O + \begin{array}{c} CH_3 \quad H \\ \quad \diagup \\ \bullet N-N \\ \quad \diagdown \\ \quad\quad H \end{array} \qquad (31)$$

$$\begin{array}{c} CH_3 \quad H \\ \diagdown \quad \diagup \\ N-N \\ \diagup \quad \diagdown \\ H \quad\quad H \end{array} + OH \rightarrow H_2O + \begin{array}{c} CH_3 \quad\quad H \\ \diagdown \quad \diagup \\ N-N\bullet \\ \diagup \\ H \end{array} \qquad (32)$$
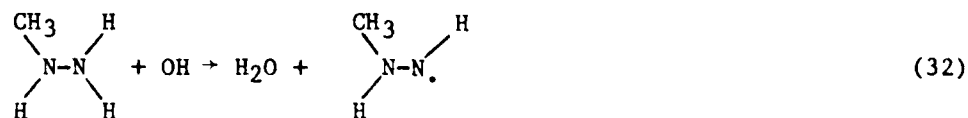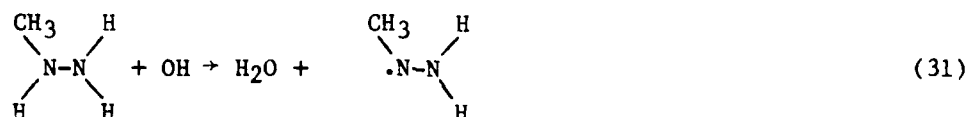
and in view of the fact that the OH + hydrazine and the OH + MMH rate constants are similar (see Section II), it is probable that reactions (31) and (32) occur at comparable rates. For this reason, the subsequent reactions of both these N-amino radicals must be considered.

As with the N_2H_3 radicals formed in the O_3 + hydrazine system, there are three possible fates for the radicals formed in reactions (31) and (32) under the conditions of these runs. They could react with O_2 to form methyldiazene:

$$\begin{array}{c} CH_3 \quad H \\ \diagdown \quad \diagup \\ \bullet N-N \\ \quad \diagdown \\ \quad\quad H \end{array} + O_2 \rightarrow HO_2 + CH_3-N=N-H \qquad (33)$$

56

$$\begin{array}{c} CH_3 \quad H \\ \diagdown \quad \diagup \\ N-N_{\bullet} \\ \diagup \\ H \end{array} + O_2 \rightarrow HO_2 + CH_3-N=N-H \qquad (34)$$
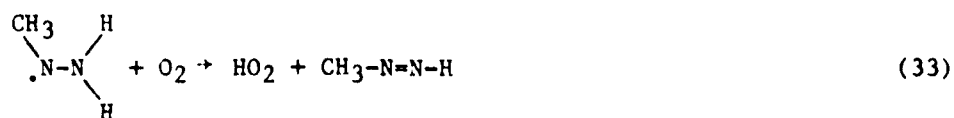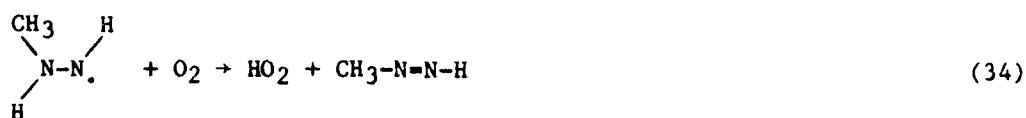
They could react with O_3 to form methyl radicals and nitrosamine (which subsequently decomposes to $N_2 + H_2O$)

$$\begin{array}{cc} CH_3 \quad H & CH_3 \quad H \\ \diagdown \quad \diagup & \diagdown \quad \diagup \\ {}_{\bullet}N-N & + O_3 \rightarrow \quad N-N \\ \diagdown & \diagup \quad \diagdown \\ H & {}_{\bullet}O \quad H \end{array} \qquad (35)$$

$$\begin{array}{c} CH_3 \quad H \\ \diagdown \quad \diagup \\ N-N \\ \diagup \quad \diagdown \\ {}_{\bullet}O \quad H \end{array} \rightarrow C\overset{\bullet}{H}_3 + H_2N-NO \rightarrow CH_3{}^{\bullet} + H_2O + N_2$$
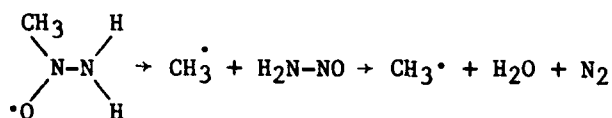
or to form HO_2 and methylnitrosamine

$$\begin{array}{cc} CH_3 \quad H & CH_3 \quad H \\ \diagdown \quad \diagup & \diagdown \quad \diagup \\ N-N_{\bullet} + O_3 \rightarrow \quad N-N \\ \diagup & \diagup \quad \diagdown \\ H & H \quad O{\bullet} \end{array} + O_2$$

$$(36)$$

$$\begin{array}{cc} CH_3 \quad H & CH_3 \\ \diagdown \quad \diagup & \diagdown \\ N-N + O_2 \rightarrow HO_2 + \quad N-N=O \\ \diagup \quad \diagdown & \diagup \\ H \quad O{\bullet} & H \end{array}$$
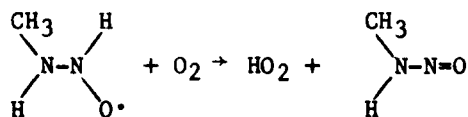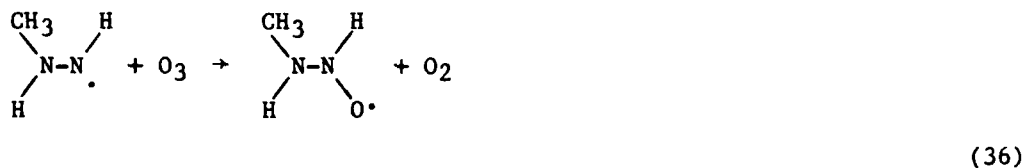
or they could add O_2 to form N-peroxy radicals. The fact that methyldiazene is directly observed indicates that O_2 abstraction [reactions (33) and (34)] is probably an important, and perhaps the dominant, pathway in the MMH-O_3 system.

Methyldiazene appears to be reasonably stable in the absence of O_3 (having a half life of ~6.5 hours, Table 8), but it disappears rapidly in the presence of O_3 (Tables 8 and 9) suggesting that the other products observed could be due to secondary reactions of this compound. The most probable mode of reaction of methyldiazine with O_3 is reaction (37)

57

$$CH_3-N=N-H + O_3 \rightarrow CH_3-N=N^{\bullet} + OH + O_2 \qquad (37)$$

$$CH_3-N=N^{\bullet} \rightarrow CH_3^{\bullet} + N_2$$
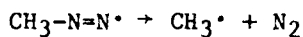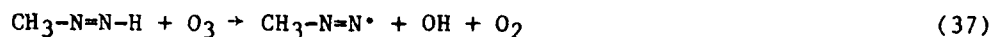
with the subsequent reaction of the methyl radicals accounting for the observed methylhydroperoxide, formaldehyde, and methanol.

$$CH_3^{\bullet} + O_2 \overset{M}{\rightarrow} CH_3O_2 \qquad (38)$$

$$CH_3O_2 + HO_2 \rightarrow CH_3OOH + O_2 \qquad (39)$$

$$CH_3O_2 + CH_3O_2 \rightarrow CH_3OH + HCHO + O_2 \qquad (40)$$

$$CH_3O_2 + CH_3O_2 \rightarrow 2CH_3O + O_2 \qquad (41)$$

$$CH_3O + O_2 \rightarrow HCHO + HO_2 \qquad (42)$$
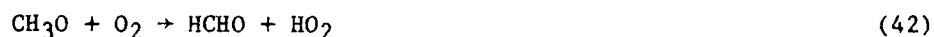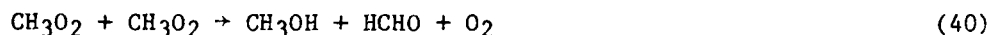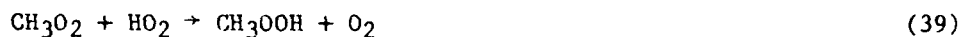
Other modes of reaction of O_3 with methyldiazene are possible, but they predict formation of products which are not observed. Furthermore, the good carbon balance obtained in the 16 June 1980 run (Table 9) means that there is no significant formation of undetected carbon-containing products.

The reaction of methyldiazene with the hydroxyl radicals formed in the MMH + O_3 system is likely to be fast, based on known OH + organic rate constants (Reference 42). Two possible modes of attack can occur:

$$CH_3N=NH + OH \rightarrow H_2O + CH_3N=N^{\bullet} \qquad (43)$$

$$CH_3N=N^{\bullet} \rightarrow CH_3^{\bullet} + N_2$$

$$CH_3N=NH + OH \rightarrow H_2O + \overset{\bullet}{C}H_2N=NH \qquad (44)$$

$$\overset{\bullet}{C}H_2N=NH + O_2 \rightarrow HO_2 + CH_2N_2$$
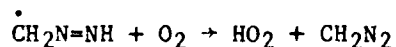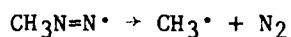
Reaction (44) appears to be the most probable reaction which accounts for the observed formation of diazomethane. The relatively large yields of diazomethane (up to 13% of the MMH consumed) suggests that reaction ofOH with methyldiazene is a significant process in the MMH-O_3 system. However, the possibility of diazomethane formation by means of other routes, such as from reaction of O_3 + methyldiazene, has not been eliminated.

When additional excess O_3 is added to the MMH-O_3 system, diazomethane is observed to disappear (Table 9), probably by means of the following reaction with O_3:

$$CH_2N_2 + O_3 \rightarrow CH_2O + O_2 + N_2 \tag{45}$$

This reaction can contribute to the observed formation of formaldehyde in higher yields than methanol.

H_2O_2 is produced in the O_3 + MMH runs, although at a lower yield than that in the O_3 + hydrazine system. The mechanism for H_2O_2 formation is probably the same in both systems (reaction of HO_2 with itself or perhaps with a hydrazine), but the lower H_2O_2 yield in the MMH system can be explained by the competing reaction of HO_2 with CH_3O_2 to form the observed methylhydroperoxide.

Most of the products observed in the MMH + O_3 system can be accounted for by assuming the formation of methyldiazene and its subsequent reactions with OH and O_3. The MMH + O_3 mechanism is probably similar in its main features to the hydrazine + O_3 system, although it is unclear which reactions in the MMH system would be analogous to those forming the traces of N_2O in the hydrazine system. The mechanisms for both systems are still uncertain, and more studies are required to unambiguously determine the exact pathways.

MMH-NO_x-Air Photolysis. When photolyzed in the presence of NO_x in air, MMH is consumed at a rate at least an order of magnitude faster than both hydrazine and UDMH. During this process NO is converted to NO_2 and large yields of formaldehyde, HNO_3, and O_3 are observed (Table 12). Probable mechanisms accounting for these observations are discussed below.

The high reactivity observed in the MMH-NO_x photolysis can be attributed to the presence, at the start of the photolysis, of highly photoreactive impurities previously formed during the initial MMH-NO_x dark reactions. In particular, both HONO and methyldiazene were initially present, and both will undergo rapid photolysis, resulting in hydroxyl radical formation.

$$HONO + h\nu \rightarrow OH + NO \tag{28}$$

$$CH_3N{=}NH + h\nu \xrightarrow{O_2} CH_3O_2^{\cdot} + HO_2 + N_2 \tag{46}$$

$$CH_3O_2^{\cdot} + NO \rightarrow CH_3O^{\cdot} + NO_2 \tag{47}$$

$$CH_3O^{\cdot} + O_2 \rightarrow HO_2 + HCHO \tag{42}$$

$$HO_2 + NO \quad OH + NO_2 \tag{29}$$
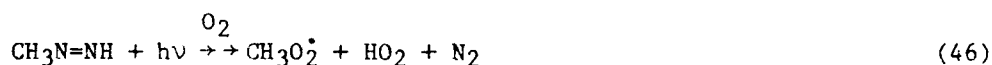
The hydroxyl radicals so formed would contribute to the initiation of the chain reactions causing the observed MMH and NO_x oxidation.

During the initial stages of the photolysis, the primary mode of MMH decay is probably reaction with OH [reactions (31) and (32)], resulting in the formation of N-amino radicals. Later, consumption of MMH by reaction with O_3 to form N-amino radicals is expected. The N-amino radicals formed in this system could react with NO, NO_2, or O_2. Reaction with O_2 is expected to give rise to methyldiazene [by means of reactions (33) and (34)], as discussed previously. Reaction of either radical with NO_2, if it occurs, probably also would give rise to methyldiazene.

$$\begin{array}{c} CH_3 \quad\;\; H \\ \diagdown \;\; \diagup \\ N{-}N \\ \diagup \quad\; \cdot \\ H \end{array} + NO_2 \xrightarrow{M} \begin{array}{c} CH_3 \quad\; H \\ \diagdown \;\; \diagup \\ N{-}N \\ \diagup \quad\; \diagdown \\ H \quad\;\;\; NO_2 \end{array} \rightarrow CH_3{-}N{=}N{-}H + HONO \tag{48}$$
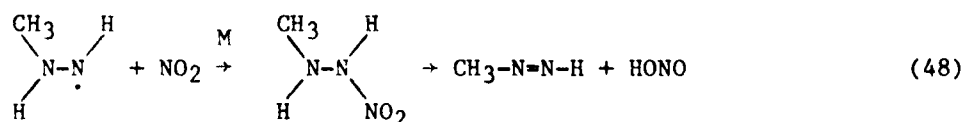
Reaction with NO is probably not significant, since, if it occurs, it would be expected to be rapidly reversed by photolysis.

60

Methyldiazene formed in this system is expected to be consumed either by photolysis [reaction (46)] or by reaction with OH radicals [reactions (43) and (44)]. These reactions should result ultimately in the formation of N_2, formaldehyde, and the conversion of NO to NO_2. Formaldehyde can be formed either from methyl radicals [by means of reactions (38), (47), and (42), formed in reactions (43) and (46)], or from the photolysis of diazomethane formed in reaction (44).

$$CH_2N_2 + h\nu \rightarrow CH_2 + N_2$$
$$CH_2 + O_2 \rightarrow CH_2O + O$$
(49)

In addition to formation of formaldehyde and NO conversion, consumption of NH_3 and formation of HNO_3, HONO, formic acid, and methylnitrate is observed. HONO and HNO_3 formation (the latter causing NH_3 consumption) can be attributed to reaction of OH with NO and NO_2, respectively. Methylnitrate is expected to be formed in trace amounts as a side product of the oxidation of methyl radicals by means of reaction (50).

$$CH_3O\cdot + NO_2 \overset{M}{\rightarrow} CH_3ONO_2$$
(50)

The observation of formic acid as a secondary product is attributed to the reaction of HO_2 with formaldehyde (Reference 43).

Therefore, the data obtained in the irradiation of $MMH-NO_x$-air mixtures (with HONO and methyldiazene impurities) can be accounted for by assuming methyldiazene formation and its subsequent photolysis or reaction with OH. The steady N_2O buildup which occurs even after all the MMH is consumed suggests that other reactions may be occurring. Thus, additional studies are required to adequately characterize and validate the mechanism.

Atmospheric Reactions of Unsymmetrical Dimethylhydrazine

Like hydrazine and monomethylhydrazine, unsymmetrical dimethylhydrazine (UDMH) appears to be quite reactive in atmospheric systems. However, the results of the $UDMH-O_3$ and the $UDMH-NO_x$ irradiation experiments suggest

61

that its reaction in those systems possibly occurs with different mechanisms than those considered for hydrazine and MMH. These are discussed below.

UDMH-NO_x-Air Dark Reactions. The rate of UDHM decay appears to be unaffected by the addition of NO and NO_2, but formation of HONO and an unidentified product is observed when NO_x is present. This is similar to the results obtained in MMH systems and indicates the probability of heterogeneous processes which form intermediates which are not detected in the UDMH-air system but which subsequently interact with NO_x to form detectable products. Very little is known about the dark decay reactions beyond this point.

UDMH-O_3 Reaction. When O_3 is injected into UDMH-air mixtures, the reaction goes to completion in less than 3 minutes and large yields of dimethylnitrosamine and smaller yields of formaldehyde (up to 12%) and H_2O_2 ($\leq 7\%$) are observed. Probably some NO_2 is also formed; the total NO_x readings (responding to nitrosamine as well as NO_2) increase slightly while nitrosamine decays (see Tables 6 and 7). There is no evidence of formation of nitrosamines in the O_3 + MMH systems indicating that UDMH reacts with O_3 by means of a different type of mechanism than the other hydrazines.

The initial reaction with ozone is assumed to be hydrogen abstraction [reaction (51)] with the OH formed contributing to additional UDMH consumption [reaction (52)]

$$
\begin{array}{c}
CH_3 \\
 \\
N\text{-}N \\
 \\
CH_3 H
\end{array}
\begin{array}{c}
H \\
 \\
 \\
 \\
H
\end{array}
+ O_3 \rightarrow
\begin{array}{c}
CH_3 \\
 \\
N\text{-}N_{\bullet} \\
 \\
CH_3
\end{array}
\begin{array}{c}
H \\
 \\
 \\

\end{array}
+ OH + O_2 \qquad (51)
$$

$$
\begin{array}{c}
CH_3 \\
 \\
N\text{-}N \\
 \\
CH_3 H
\end{array}
\begin{array}{c}
H \\
 \\
 \\
 \\
H
\end{array}
+ OH \rightarrow
\begin{array}{c}
CH_3 \\
 \\
N\text{-}N_{\bullet} \\
 \\
CH_3
\end{array}
\begin{array}{c}
H \\
 \\
 \\

\end{array}
+ H_2O \qquad (52)
$$
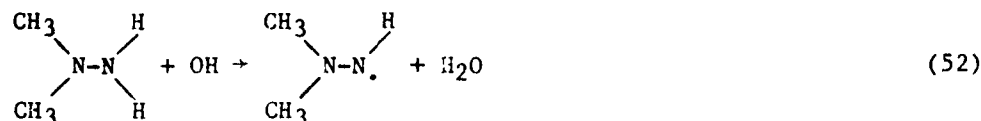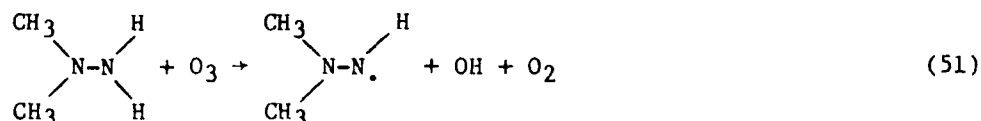
However, in this case subsequent formation of a diazene by means of β-hydrogen abstraction, probably the major process in the O_3 + N_2H_4 and the O_3 + MMH systems, is not possible. Instead, the N-amino radical could either react with O_3 [reaction (53)] or add O_2 [reaction (54)].

62

$$\begin{array}{c} CH_3 \\ \diagdown \\ N-N \\ \diagup \quad \cdot \\ CH_3 \end{array} \overset{H}{} + O_3 \rightarrow \begin{array}{c} CH_3 \\ \diagdown \\ N-N \\ \diagup \quad \diagdown \\ CH_3 \quad O. \end{array} \overset{H}{} + O_2 \qquad (53)$$

$$\begin{array}{c} CH_3 \\ \diagdown \\ N-N \\ \diagup \quad \cdot \\ CH_3 \end{array} \overset{H}{} + O_2 \overset{M}{\rightarrow} \begin{array}{c} CH_3 \\ \diagdown \\ N-N \\ \diagup \quad \diagdown \\ CH_3 \quad OO \cdot \end{array} \overset{H}{} \qquad (54)$$
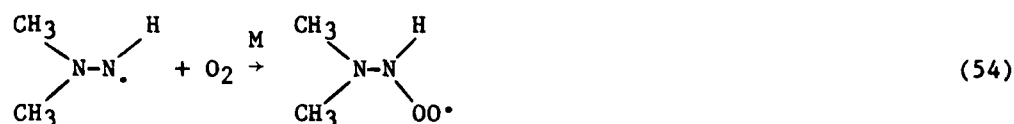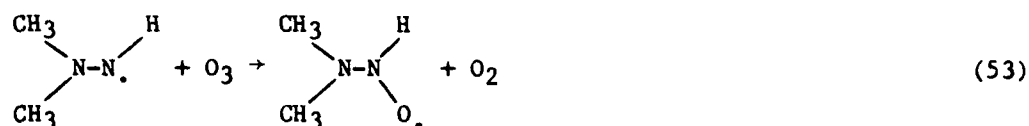
Subsequent reactions of the intermediates formed in either of these reactions can account for the observed formation of dimethylnitrosamine in this system.

If reaction of the N-amino radical with O_3 occurred [Reaction (53)], formation of dimethylnitrosamine and HO_2 is expected [Reaction (55)].

$$\begin{array}{c} CH_3 \\ \diagdown \\ N-N \\ \diagup \quad \diagdown \\ CH_3 \quad O \cdot \end{array} \overset{H}{} + O_2 \rightarrow \begin{array}{c} CH_3 \\ \diagdown \\ N-NO \\ \diagup \\ CH_3 \end{array} + HO_2 \qquad (55)$$
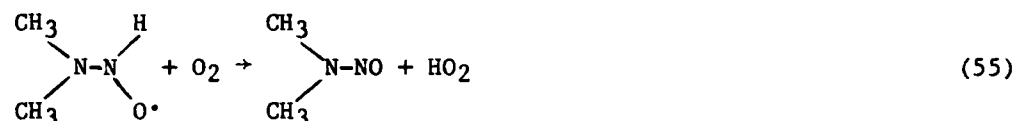
As with other hydrazine-O_3 systems, the HO_2 formed will give rise to H_2O_2 either by means of self-reaction [reaction (13)], or by means of consumption of an additional UDMH molecule [reaction (56)]. The latter reaction, if important, gives rise to a chain reaction mechanism consuming both UDMH and O_3, with HO_2 as the carrier.

$$\begin{array}{c} CH_3 \\ \diagdown \\ N-N \\ \diagup \quad \diagdown \\ CH_3 \quad H \end{array} \overset{H}{} + HO_2 \rightarrow \begin{array}{c} CH_3 \\ \diagdown \\ N-N \\ \diagup \quad \cdot \\ CH_3 \end{array} \overset{H}{} + H_2O_2 \qquad (56)$$
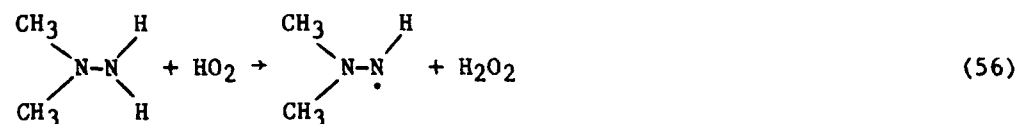
If the addition of O_2 to the N-amino radical was the major process, dimethylnitrosamine formation would occur through a series of radical-radical reactions as shown below:

$$2 \begin{array}{c} CH_3 \\ \diagdown \\ N-N \\ \diagup \quad \diagdown \\ CH_3 \quad OO \cdot \end{array} \overset{H}{} \rightarrow 2 \begin{array}{c} CH_3 \\ \diagdown \\ N-N \\ \diagup \quad \diagdown \\ CH_3 \quad O \cdot \end{array} \overset{H}{} \overset{O_2}{\rightarrow} \rightarrow 2HO_2 + 2 \begin{array}{c} CH_3 \\ \diagdown \\ N-NO \\ \diagup \\ CH_3 \end{array} \qquad (57)$$

$$2 \quad \underset{CH_3}{\overset{CH_3}{>}}N-N\underset{OO\cdot}{\overset{H}{<}} \quad \rightarrow \quad \underset{CH_3}{\overset{CH_3}{>}}N-N\underset{O\cdots O-O}{\overset{\cdot H\cdots H}{\cdots}}O-N\underset{CH_3}{\overset{CH_3}{<}}$$

$$\rightarrow \quad \underset{CH_3}{\overset{CH_3}{>}}N-NO \;+\; \underset{CH_3}{\overset{CH_3}{>}}N-N\underset{OH}{\overset{H}{<}} \;+\; O_2 \qquad (58)$$

$$\underset{CH_3}{\overset{CH_3}{>}}N-N\underset{OO\cdot}{\overset{H}{<}} \;+\; HO_2 \;\rightarrow\; \underset{CH_3}{\overset{CH_3}{>}}N-N\underset{OOH}{\overset{H}{<}} \;+\; O_2 \qquad (59)$$

$$\underset{CH_3}{\overset{CH_3}{>}}N-N\underset{OOH}{\overset{H}{<}} \;\rightarrow\; \underset{CH_3}{\overset{CH_3}{>}}N-NO \;+\; H_2O$$
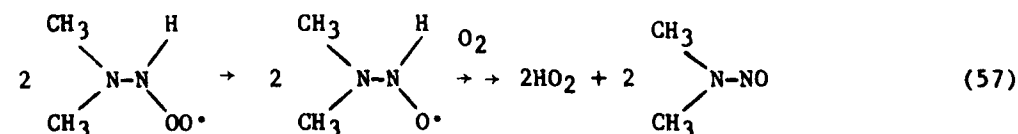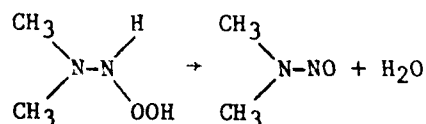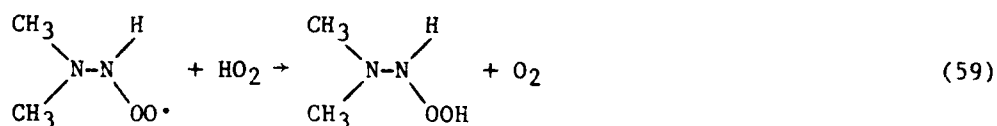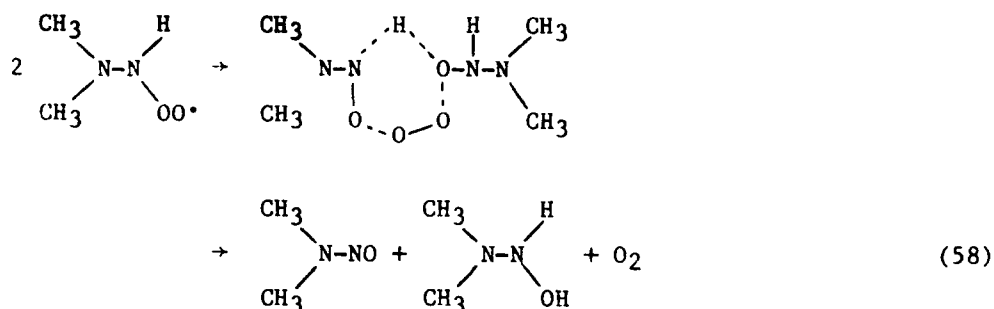
Note that reaction (58) predicts the formation of an N-hydroxylamine which is not observed. However, in view of the rapid reaction of hydrazine with O_3, it is probable that, if formed, the N-hydroxylamine also reacts too quickly with O_3 to allow its detection. This reaction is also expected to give rise to dimethylnitrosamine.

$$\underset{CH_3}{\overset{CH_3}{>}}N-N\underset{OH}{\overset{H}{<}} \;+\; O_3 \;\rightarrow\; \underset{CH_3}{\overset{CH_3}{>}}N-N\underset{OH}{\overset{\cdot}{<}} \;+\; OH \;+\; O_2 \qquad (60)$$

$$\underset{CH_3}{\overset{CH_3}{>}}N-N\underset{OH}{\overset{\cdot}{<}} \;+\; O_2 \;\rightarrow\; \underset{CH_3}{\overset{CH_3}{>}}N-NO \;+\; HO_2$$
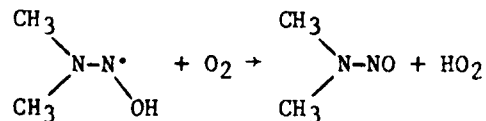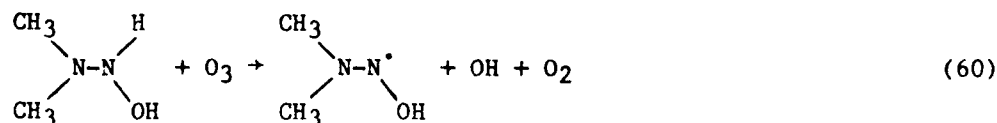
In addition to dimethylnitrosamine, formation of formaldehyde, H_2O_2, NO_2, and methylnitrate are observed; NH_3 levels decline, indicating probable HNO_3 formation. H_2O_2 is expected to result from the HO_2 radicals formed in either reaction (55) or reaction (57), and the other products

64

probably result from secondary reactions of dimethylnitrosamine with OH radicals. However, it is unclear exactly what mechanism will account for the formation of these products.

Although the results of the experiments reported clearly indicate that dimethylnitrosamine formation is the dominant process in the UDMH-O_3 system, the data are insufficient to determine definitively the exact mechanism for either its formation or that of the minor products observed. It is probable, however, that the major reactions occurring in this system are different from those occurring when O_3 reacts with hydrazines which have N-H bonds on both nitrogens.

UDMH-NO_x Irradiation. When UDMH-NO_x mixtures are irradiated, UDMH is consumed, and dimethylnitrosamine, dimethylnitramine, N_2O, formaldehyde, formic acid, nitrous acid, nitric acid, and O_3 are formed (Table 11). The rate of UDMH consumption is comparable to that of hydrazine in the N_2H_4-NO_x irradiation, and far slower than MMH consumption when it is irradiated in a NO_x mixture. Unlike the other hydraz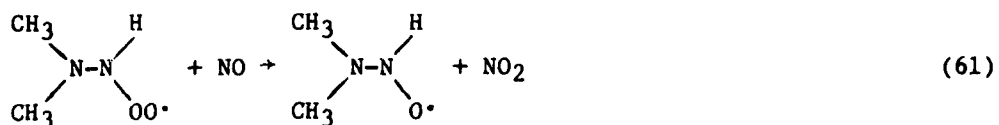ines, NO is apparently not converted to NO_2 in the UDMH-NO_x photooxidation, since the NO levels remain relatively constant until UDMH is mostly consumed. Later in the run NO conversion is observed, apparently as a result of the photooxidation of the product formed. Possible mechanisms accounting for these results are discussed below.

The primary reaction consuming UDMH is probably reaction with OH generating the corresponding N-amino radical [reaction (52)]. Ozone formation does not occur until after the UDMH is depleted, so consumption by reaction with O_3 is not significant in this experiment. The N-amino radical can either add O_2 [reaction (54)] or react with NO or NO_2 (discussed below). If O_2 addition occurs, the subsequent reactions of the N-peroxy radical will result in nitrosamine formation and conversion of 2 molecules of NO to NO_2:

$$
\begin{array}{c}
CH_3 \\
{}^{\diagdown}N-N{\diagdown}^H \\
CH_3{}^{\diagup} \quad {}^{\diagdown}OO\cdot
\end{array}
+ \; NO \; \rightarrow \;
\begin{array}{c}
CH_3 \\
{}^{\diagdown}N-N{\diagdown}^H \\
CH_3{}^{\diagup} \quad {}^{\diagdown}O\cdot
\end{array}
+ \; NO_2 \qquad (61)
$$

65

$$\text{(CH}_3)_2\text{N–N(H)(O}\cdot) + O_2 \rightarrow (CH_3)_2\text{N–NO} + HO_2 \tag{55}$$

$$HO_2 + NO \rightarrow OH + NO_2 \tag{20}$$
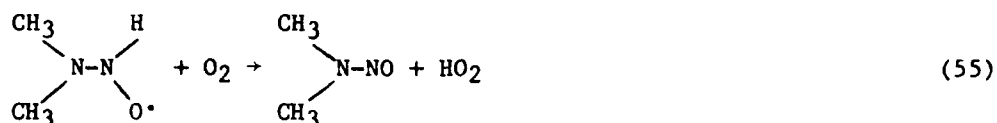
Since NO is not converted to NO_2 in the initial phase of the UDMH-NO_x irradiation, this mechanism is inconsistent with the data. For this reason the data appear to indicate that rather than undergoing O_2 addition, the N-amino radicals must react with NO and NO_2.

The reaction of N-amino radicals with NO is probably rapidly reversed by photolysis of the N-nitroso compounds formed, so it will not be considered. Two modes of reaction with NO_2 are possible:

$$\text{(CH}_3)_2\text{N–N(H)}\cdot + NO_2 \xrightarrow{M} (CH_3)_2\text{N–N(H)(NO}_2) \tag{62}$$

$$\text{(CH}_3)_2\text{N–N(H)}\cdot + NO_2 \xrightarrow{M} (CH_3)_2\text{N–N(H)(O–N–O)} \tag{63}$$
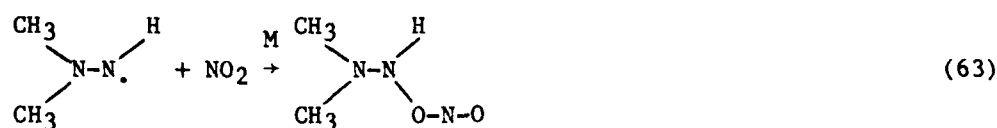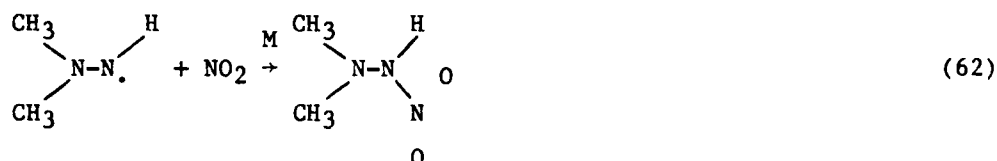
If reaction (62) dominates, the subsequent reactions of the nitramine species formed are uncertain, and it is difficult to see how subsequent reactions of this compound could give rise to the observed products. Therefore, it must be assumed either that reaction (63) dominates, or that reaction (62) occurs with the adduct rearranging to form the same species as in reaction (63). That species can undergo either a molecular elimination or photolyze, in either case giving rise to dimethylnitrosamine, HO_2 and NO.

66

$$\begin{array}{c}CH_3 \\ | \\ N-N \\ | \quad \backslash \\ CH_3 \quad NO_2\end{array} \quad H \rightarrow \left[\begin{array}{c}CH_3 \quad H \\ | \quad | \\ N-N \quad O\cdot \\ | \quad | \\ CH_3 \quad O\cdots N\end{array}\right] \rightarrow \begin{array}{c}CH_3 \\ \backslash \\ N-NO + HNO \\ / \\ CH_3\end{array} \qquad (64)$$

$$HNO + O_2 \rightarrow HO_2 + NO$$

$$\begin{array}{c}CH_3 \quad H \\ \backslash \quad | \\ N-N \\ / \quad \backslash \\ CH_3 \quad ONO\end{array} + h\nu \rightarrow \begin{array}{c}CH_3 \quad H \\ \backslash \quad | \\ N-N \\ / \quad \backslash \\ CH_3 \quad O.\end{array} + NO \xrightarrow{O_2} \begin{array}{c}CH_3 \\ \backslash \\ N-NO + HO_2 + NO \\ / \\ CH_3\end{array} \qquad (65)$$
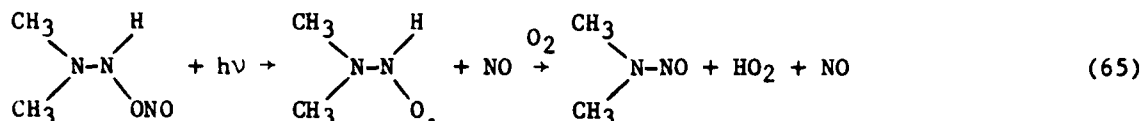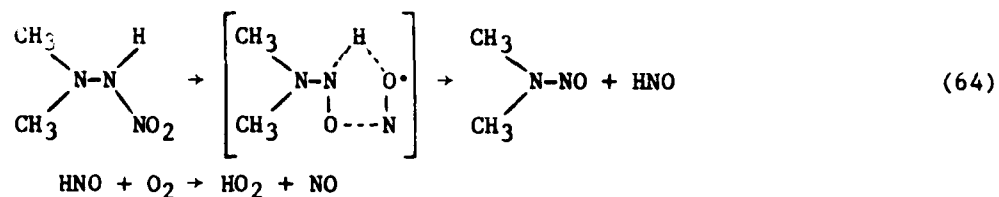
Note that the overall formation of nitrosamine in this mechanism results in no net conversion of NO to NO_2, which is consistent with the data.

The dimethylnitrosamine formed is expected to undergo either rapid photolysis producing the nitramine [reactions (66) and (67)], or reaction with OH producing the observed N_2O, formaldehyde, and methylnitrate [reactions (68) through (73)].

$$\begin{array}{c}CH_3 \\ \backslash \\ N-NO \\ / \\ CH_3\end{array} \underset{\gets}{\overset{h\nu}{\rightleftharpoons}} \begin{array}{c}CH_3 \\ \backslash \\ N\cdot + NO \\ / \\ CH_3\end{array} \qquad (66)$$

$$\begin{array}{c}CH_3 \\ \backslash \\ N\cdot + NO_2 \rightarrow \\ / \\ CH_3\end{array} \begin{array}{c}CH_3 \\ \backslash \\ N-NO_2 \\ / \\ CH_3\end{array} \qquad (67)$$

$$\begin{array}{c}CH_3 \\ \backslash \\ N-NO + OH \rightarrow H_2O + \\ / \\ CH_3\end{array} \begin{array}{c}CH_3 \\ \backslash \\ N-NO \\ / \\ \cdot CH_2\end{array} \qquad (68)$$

$$\begin{array}{c}CH_3 \\ \backslash \\ N-NO + O_2 \xrightarrow{M} \\ / \\ \cdot CH_2\end{array} \begin{array}{c}CH_3 \\ \backslash \\ N-NO \\ / \\ \dot{O}OCH_2\end{array} \qquad (69)$$

$$\underset{\cdot OOCH_2}{\overset{CH_3}{\diagdown}} N\text{--}NO + NO \rightarrow \underset{\cdot OCH_2}{\overset{CH_3}{\diagdown}} N\text{--}NO + NO_2 \qquad (70)$$

$$\underset{\cdot OCH_2}{\overset{CH_3}{\diagdown}} N\text{--}NO \rightarrow HCHO + CH_3\text{--}\overset{\cdot}{N}\text{--}NO \qquad (71)$$

$$CH_3\text{--}\overset{\cdot}{N}NO \rightarrow \cdot CH_3 + N_2O \qquad (72)$$

$$\cdot CH_3 \xrightarrow{O_2, \ NO_x} \rightarrow HCHO + HO_2 \quad \text{or} \quad CH_3ONO_2 \qquad (73)$$
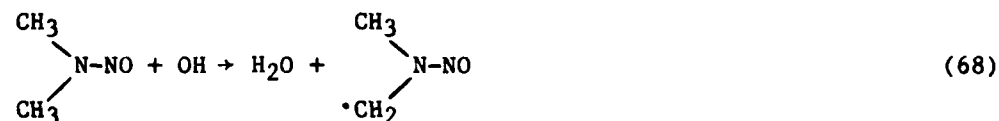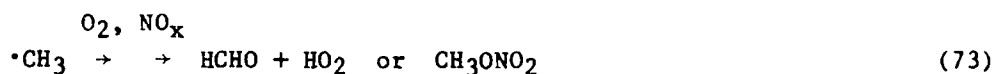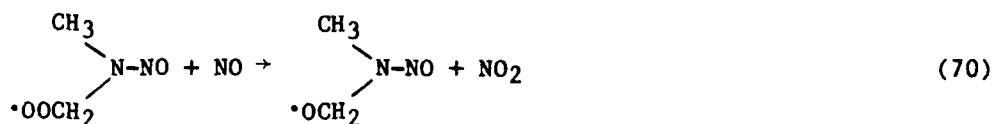
The continued formation of these products after the UDMH has been consumed indicates that the products are unlikely to arise directly from the oxidation of UDMH itself.

Thus, the major fate of UDMH when photolyzed in the presence of NO_x is dimethylnitrosamine formation, with the subsequent reactions of this highly reactive product accounting for the other products observed. Dimethylnitrosamine is also formed when UDMH is reacted with O_3, but the mechanism appears to be different. However, the mechanism proposed for the formation of the nitrosamine from UDMH in the NO_x-air photolysis is highly speculative in nature, and additional research is clearly needed. Further studies are also required to determine the ultimate atmospheric fate of nitramines, which are formed in large yields in this system.

SECTION IV

CONCLUSIONS AND RECOMMENDATIONS

CONCLUSIONS

The results of the studies reported here clearly show that, upon re-
lease into the atmosphere, the hydrazines (hydrazine, monomethylhydrazine,
and unsymmetrical dimethylhydrazine) could be rapidly consumed by reaction
either with ozone (O_3) or with hydroxyl radicals (OH), depending upon the
nature of the atmosphere into which the emissions occur. With respect to
reaction with OH, the tropospheric half-lives for hydrazine is expected to
range from < 1 hour in polluted urban atmospheres up to 3 to 6 hours in the
unpolluted atmospheres, with substituted hydrazines being consumed at about
the same rate. With respect to reaction with O_3, the half-life for unsub-
stituted hydrazine would range from less than 10 minutes during O_3 pollution
episodes to less than ~2 hours in the natural troposphere, with the half-
lives for the substituted hydrazines (MMH and UDMH) being at least 10 times
shorter. Therefore, under most conditions, reaction with ozone will be the
major fate of hydrazines released into the atmosphere and their lifetimes are
unlikely to be longer than 2 to 3 hours at most.

In terms of long-range impact, beyond the inherent toxicity of the
hydrazines themselves, the release of N_2H_4, MMH (and by extrapolation
other hydrazines with N-H bonds on both nitrogen atoms) will probably have
relatively little effect on the levels of NO_x, nitrates or other forms of
active nitrogen in the atmosphere, since the hydrazine nitrogen appears to be
efficiently converted to N_2. A qualification to this, however, is that a
major release of MMH in an area of high O_3 pollution, particularly during
late afternoon or early evening hours, could subject any industrial environ-
ment or nearby downwind region to possibly significant levels of potentially
toxic methylhydroperoxide and methyldiazene, as well as highly poisonous
diazomethane.

A similar scenario for UDMH and other unsymmetrically disubstituted
hydrazines could have even more far-reaching health implications, since
their reactions with O_3 would form high yields of nitrosamines, species
which are known to be potent carcinogens (References 44 and 45).

69

Although nitrosamines react in sunlight to form the relatively more stable nitramines (References 23 and 24), the latter class of compounds may also be classified as a health hazard, since dimethylnitramine has been demonstrated to induce carcinogenic activity in test animals (References 46 and 47).

The mechanisms for the atmospheric reactions of the unsubstituted and monosubstituted hydrazines appear to be similar in their overall features. Reaction with O_3 appears to occur by means of a radical chain mechanism, but the chain length and the relative importance of OH and HO_2 radicals as chain carriers are uncertain. The data obtained in most of the dark O_3 and NO_x irradiation systems are best explained by assuming that both OH and O_3 abstract a hydrogen from the weak N-H bond, with the resulting N-amino radical reacting with O_2 to form HO_2 and a diazene. Diazenes are highly reactive in atmospheric systems, and their photolysis, reaction with O_3, and/or reaction with OH will give rise ultimately to N_2, radicals, and, for carbon-containing compounds, oxygenated organics. Again, the details of mechanisms and the relative importance of these processes are uncertain.

Although unsymmetrical dimethylhydrazine appears to be converted to the corresponding nitrosamine with high efficiency in both the UDMH plus O_3 and UDMH plus NO_x photolysis sytems (with other products observed being attributed to secondary reactions of the nitrosamines), the mechanism is highly uncertain, and is probably different in both systems. The subsequent reactions of nitramines, produced when the initially-formed nitrosamines are photolyzed in the presence of NO_2, are unknown and must be elucidated before the ultimate impact of the release of UDMH on the atmospheric environment can be determined.

RECOMMENDATIONS

The results of the experiments reported here provide evidence concerning the possible mechanisms of atmospheric reactions of the hydrazines and hence the environmental impact of these compounds. It is clear, however, that more research is required before these mechanisms can be considered to be firmly established and before quantitative predictions of the effect of release of hydrazine compounds on the immediate environment can be made.

70

Additional areas of study which could help elucidate and validate the proposed mechanisms are briefly indicated below.

● The elementary rate constants for the reactions of O_3 with hydrazines should be accurately determined. The present FT-IR method could only provide a rough estimate of the N_2H_4 plus O_3 reaction rate and is unsuitable for investigating the much faster reactions of MMH and UDMH with O_3. It should be possible to devise a dynamic flow system that will permit measurement of these fast reactions.

● The hydrazine-O_3 system should be studied in an environmental chamber under a variety of conditions much wider than those utilized in the experiments reported here. The effects on the products of carrying out the reactions in a large excess of hydrazine or of ozone should be determined. Such experiments should be done with added tracers with known OH rate constants so that OH radical levels can be calculated. The effect of adding radical traps should also be examined.

More extensive product identification by FT-IR spectroscopy will be facilitated by conducting the experiments under ultra-dry conditions so as to minimize H_2O interferences which possibly mask critical infrared absorptions, such as those of the predicted species HN=NH.

● The assumption that the initial O_3-hydrazine reaction is hydrogen abstraction forming OH and N-amino radicals and not O-atom transfer forming unstable N-oxides needs to be validated. Photoionization mass spectrometry could be potentially useful in this regard.

● Information is needed as to what products are formed when nitrosamines react with OH and whether the nitrosamines react with O_3. It is assumed that the reaction of N-nitrosodimethylamine with O_3 is negligible and that its reaction with OH results in N_2O and aldehyde formation. These assumptions should be verified through studies examining nitrosamines in cleaner systems.

● Nitramine formation has been shown to be significant in UDMH-NO_x photolysis, but its subsequent reactions are unknown. Nitramines are known not to photolyze in the actinic region, and they probably do not react rapidly with O_3 (although this has not been directly verified), so their probable major fate is reaction with OH. However, the rate of OH plus nitramine

reactions and the products formed are not known. It is particularly important to determine whether relatively inert compounds such as N_2 and N_2O are formed or whether reactive nitrogen compounds are produced.

● Diazenes are believed to be the initially formed intermediates in the atmospheric reactions of unsubstituted, monosubstituted, and probably symmetrically disubstituted hydrazines. Thus, the rate constants for the reactions of diazenes with OH and O_3 should be determined so that the importance of these reactions relative to each other and to photolysis in atmospheric systems can be calculated.

● The rate constant for the reaction of HO_2 radicals with hydrazines must be determined so that the role of HO_2 as a chain carrier in the O_3-hydrazine system can be either verified or ruled out. If the reaction with HO_2 is sufficiently fast, it could be another, previously unconsidered, sink for hydrazine in the atmosphere.

● The relative rate constants for the reactions of N-amino radicals with O_3, O_2, NO, and NO_2 should be determined. N-amino radicals should be generated under conditions such that their major fate has to be either reaction with NO or, in separate experiments, reaction with NO_2, so that the resulting products can be determined. It would be useful to know whether species such as $R_2N-NH-NO_2$ are formed and whether they are stable or readily decompose.

● In the present investigation, the effect of the presence of, and possible interactions with, atmospheric pollutants other than NO_x were not examined. In particular, the effects of organic compounds, SO_2, and perhaps other pollutants, on the products of dark O_3 reactions and on NO_x-air photooxidation reactions with the hydrazines need to be determined.

The above represents a partial list of the types of studies which would be useful in elucidating the atmospheric chemistry of hydrazines. Results from such investigations would not only provide a better understanding of the atmospheric chemistry of hydrazines, but also would be of fundamental scientific interest as well, leading to an increased ability to predict the atmospheric reactions of other classes of compounds as well as of the hydrazines.

REFERENCES

1. Audrieth, L. F. and B. Ogg, _The Chemistry of Hydrazine_, John Wiley and Sons, New York, 1951, and references therein.

2. Saad, M. A., M. B. Detweiler and M. A. Sweeney, "Analysis of Reaction Products of Nitrogen Tetroxide with Hydrazines under Nonignition Conditions," AIAA Journal, 10, 1073 (1972).

3. Branch, M. C. and R. F. Sawyer, "Review and Evaluation of Rate Data for Gas Phase Reactions of the N-H System," AFSUR-TR-72-0020, Report No. TS-71-1, June 1971, and references therein.

4. Sawyer, R. F. and I. Glassman, "Gas-Phase Reactions of Hydrazine with Nitrogen Dioxide, Nitric Oxide and Oxygen," Symposium (Intl.) on Combustion, 11, 861 (1967).

5. Stone, D. A., "The Autooxidation of Hydrazine Vapor," Report No. CEEDO-TR-78-17, January 1978; "The Vapor-Phase Autooxidation of Unsymmetrical Dimethylhydrazine and 50-percent Unsymmetrical Dimethylhydrazine-50-percent Hydrazine Mixtures," Report No. ESL-TR-80-21, April 1980.

6. Levy, H., II, "Photochemistry of Minor Constituents in the Troposphere," Planetary and Space Sci., 21, 575 (1973).

7. Crutzen, P. J., "Photochemical Reactions Initiated by and Influencing Ozone in Unpolluted Tropospheric Air," Tellus, 26, 47 (1974).

8. Levy H., II, "Photochemistry of the Troposphere," in _Adv. Photochem._, Wiley-Intersicence, New York, 9, 369 (1974).

9. Wofsy, S. C., "Interactions of CH_4 and CO in Earths Atmosphere," Ann. Rev. Earth Planetary Sci., 4, 441 (1976).

10. Crutzen, P. J. and J. Fishman, "Average Concentrations of OH in Troposphere, and Budgets of CH_4, CO, H_2, and CH_3CCl_3," Geophys. Res. Lett., 4, 321 (1977).

11. Atkinson, R. D. A. Hansen and J. N. Pitts, Jr., "Rate Constants for the Reaction of the OH Radical with H_2 and NO (M = Ar and N_2)," J. Chem. Phys., 62, 3284 (1975); "Rate Constants for the Reaction of OH Radicals with CHF_2Cl, CF_2Cl_2, $CFCl_3$ and H_2 over the Temperature Range 297-434 K," 63, 1703 (1975).

12. Atkinson, R., R. A. Perry and J. N. Pitts, Jr., "Rate Constants for Reaction of OH Radical with CH_3SH and CH_3NH_2 over the Temperature Range 299-426 K," J. Chem. Phys., 66, 1578 (1977).

13. Atkinson, R., R. A. Perry and J. N. Pitts, Jr., "Rate Constants for Reactions of OH Radical with $(CH_3)_2NH$, $(CH_3)_3N$, and $C_2H_5NH_2$ over the Temperature Range 298-426 K," J. Chem. Phys., 68, 1850 (1978).

14. Atkinson, R., R. A. Perry and J. N. Pitts, Jr., "Rate Constants for Reactions of OH Radicals with COS, CS_3 and CH_3SCH_3 over Temperature Range 299-430 K," Chem. Phys. Lett., 54, 14 (1978).

15. Hack, W., K. Hoyerman and H. G. Wagner, "Gas-Phase Reactions of Hydroxyl Radical with Ammonia and Hydrazine," Ber. Bun. Ges., 78, 386 (1974).

16. Hamilton, Jr. E. J. and C. A. Naleway, "Theoretical Calculation of Strong Complex Formation by HO_2 Radical: $HO_2 \cdot H_2O$ and $HO_2 \cdot NH_3$," J. Phys. Chem., 80, 2037 (1976).

17. Perry, R. A., R. Atkinson and J. N. Pitts, Jr., "Rate Constants for the Reactions $OH + H_2S \rightarrow H_2O + SH$ and $OH + NH_3 \rightarrow H_2O + NH_2$ over the Temperature Range 297-427 K," J. Chem. Phys., 64, 3237 (1976).

18. Calvert, J. G. and J. N. Pitts, Jr., Photochemistry, John Wiley and Sons, New York (1966).

19. Horn, D. and G. C Pimentel, "2.5-Km Low-Temperature Multiple-Reflection Cell," Applied Optics, 10, 1892 (1971).

20. Dibeler, V. H., J. L. Franklin and R. M. Pease, "Electron Impact Studies of Hydrazine and the Methyl-Substituted Hydrazines," J. Am. Chem. Soc., 81, 1 (1958).

21. Eberstein, I. J., "Gas-Phase Decomposition of Hydrazine Propellants," Report No. AD 607334, AFOSR Contract No. AF 49(638)-1268 (1964).

22. Ackerman, M., J. Burdge and N. Craig, "Infrared Spectra and Vibrational Assignments of trans-CH_3N-NH, CH_3N-ND, CD_3N-NH, and CD_3N-ND," J. Chem. Phys., 58, 203 (1973).

23. Tuazon, E. C., A. M. Winer, R. A. Graham, J. P. Schmid and J. N. Pitts, Jr., "Fourier Transform Infrared Detection of Nitramines in Irradiated Amino-NO_x Systems," Environ. Sci. Technol., 12, 954 (1978).

24. Pitts, J. N., Jr., D. Grosjean, K. Van Cauwenberghe, J. P. Schmid and D. R. Fitz, "Photooxidation of Aliphatic Amines under Simulated Atmospheric Conditions: Formation of Nitrosamines, Nitramines, Amides and Photochemical Oxidant," Environ. Sci. Technol., 12, 946 (1978).

25. Urry, W. H., A. L. Olsen, E. M. Eens, H. W. Kruse, C. Ikoku and Z. Gaibel, "Autooxidation of 1,1-Dimethylhydrazine," NAVWEPS Report 8798 (NOTS-TP3900) September (1965).

26. Niki, H., P. L. Maker, C. M. Savage and L. P. Breitenbach, "FTIR Spectroscopic Observation of Peroxyalkyl Nitrates Formed Via $ROO + NO_2 \rightarrow ROONO_2$," Chem. Phys. Lett., 55, 289 (1978).

27. Winer, A. M., J. W. Peters, J. P. Smith and J. N. Pitts, Jr., "Response of Commercial Chemiluminescent NO-NO_2 Analyzers to other Nitrogen-Containing Compounds," Environ. Sci. Technol., 8, 1118 (1974).

28. Saunders, R. and J. Larkins, "Detection and Monitoring of Hydrazine, Monomethylhydrazine and their Decomposition Products," NRL Memorandum Report 3313 (1976).

29. Foner, S. N. and R. L. Hudson, "Mass Spectrometric Detection of Triazene and Tetrazene and Studies of the Free Radicals NH_2 and N_2H_3," J. Chem. Phys., 29, 442 (1958).

30. Dibeler, V. H., J. L. Franklin and R. M. Reese, "Electron Impact Studies of Hydrazine and the Methyl-Substituted Hydrazines," J. Am. Chem. Soc., 81, 68 (1959).

31. Benson, S. W., Thermochemical Kinetics, 2nd Ed., John Wiley and Sons, New York (1976).

32. Jayanty, R. K. M., R. Simonaitis and J. Heicklen, "Reaction of NH_2 with NO and O_2," J. Phys. Chem., 80, 433 (1976).

33. Harris, G. W., R. Atkinson and J. N. Pitts, Jr., "Kinetics of the Reactions of the OH Radical with Hydrazine and Methylhydrazine," J. Phys. Chem., 83, 2557 (1979).

34. Ravishankara, A. R., P. H. Wine and A. O. Langford, "Absolute Rate Constant for the Reaction OH ($v = 0$) + O_3 HO_2 + O_2 over the Temperature Range 238-387 K," J. Chem. Phys., 70, 984 (1979).

35. Kurasawa, H. and R. Lesclaux, "Kinetics of the Reaction of NH_2 with NO_2," Chem. P. Lett., 66, 602 (1979).

36. Lindley, C. R. C., J. G. Calvert and J. H. Shaw, Rate Studies of the Reactions of the $(CH_3)_2N$ Radical with O_2, NO and NO_2," Chem. P. Lett., 67, 57 (1979).

37. Barker, J. R., S. W. Benson and D. M. Golden, "Decomposition of Dimethyl Peroxide and Rate Constant for CH_3O + O_2 + CH_2O + HO_2," Int. J. Chem. Kinetics, 9, 31 (1977).

38. Willis, C. and R. A. Back, "Di-imide: Some Physical and Chemical Properties, and the Kinetics and Stoichiometry of the Gas-Phase Decomposition," Can. J. Chem., 51, 3605 (1973).

39. Lesclaux, R. and M. Demissy, "On the Reaction of NH_2 Radical with Oxygen," Nouveau Journal de Chemie, 1, 443 (1977).

40. Kurylo, M. J., "Kinetics of Reactions OH($v = 0$) + NH_3 → H_2O + NH_2 and OH ($v = 0$) + O_3 → HO_2 + O_2 at 298 K," Chem. P. Lett., 23, 467 (1973).

41. Zellner, R. and I. W. M. Smith, "Rate Constants for Reactions of OH with NH_3 and HNO_3," Chem. P. Lett., 26, 72 (1974).

42. Atkinson, R., K. R. Darnall, A. C. Lloyd, A. M. Winer and J. N. Pitts, Jr., "Kinetics and Mechanisms of the Reactions of the Hydroxyl Radical with Organic Compounds in the Gas Phase," Adv. Photochem., 11, 375 (1979).

43. Su, F., J. G. Calvert and J. H. Shaw, "Mechanism of the Photooxidation of Gaseous Formaldehyde," J. Phys. Chem., 83, 3185 (1979).

44. Searle, C. E., Ed., "Chemical Carcinogens," ACS Monograph 173, American Chemical Society, Washington, DC (1976).

45. Fahmy, O. G. and M. J. Fahmy, "Mutagenicity of N-alpha Acetoxyethyl-N-Ethylnitrosamine and N,N-Dimethylnitrosamine in Relation to Mechanisms of Metabolic Activation of Dialkylnitrosamines," Cancer Research, 36, 4505 (1976).

46. Goodall, C. M. and T. H. Kennedy, "Carcinogenicity of Dimethylnitramine in NZR Rats and NZO Mice," Cancer Lett., 1, 295 (1976).

47. Druckrey, H., R. Preussman, D. Schmahl and M. Muller, "Chemical Constitution and Carcinogenic Action of Nitrosamines," Naturwissenschaften, 48, 134 (1961).

48. Hanst, P. L., W. E. Wilson, R. K. Patterson, B. W. Gay, L. W. Chaney and C. S. Burton, "A Spectroscopic Study of California Smog," EPA Publication No. 650/4-75-0006, Research Triangle Park, NC (1975).

49. Molina, L. and M. Molina (private communication).

50. Crawford, B. L., Jr., W. H. Fletcher and D. A. Ramsey, "Infrared Spectra of CH_2N_2 and CD_2N_2," J. Chem. Phys., 19, 406 (1951).

51. McAfee, J. M., E. R. Stephens, D. R. Fitz and J. N. Pitts, Jr., "Infrared Absorptivity of the 9.6 ;m Ozone Band as a Function of Spectral Resolution and Abundance," J. Quant. Spectrosc. Radiat. Transfer, 16, 829 (1976).

APPENDIX A

FOURIER TRANSFORM-INFRARED SPECTROSCOPIC ANALYSIS
OF HYDRAZINES AND THEIR REACTION PRODUCTS

The absorption coefficients corresponding to the measurement frequencies used in the analysis of reactant and product spectra of the hydrazine reactions are listed in Table A-1. Where possible, measurements are made from strong Q-branch features (e.g., 1034.14 cm^{-1} Q-branch of CH_3OH) and/or other well-resolved fine structures (such as those of N_2H_4) as they provide values with least interference from underlying unknown bands. Relatively broader bands are measured from the baseline [e.g., 1015.8 cm^{-1} band of $(CH_3)_2NNO$].

In some cases, the overlap of two or more absorption bands requires a detailed comparison of the spectral features of the pure compounds before reliable values of concentrations can be derived by spectral desynthesis. A good example is the interference between the heavily structured band system of N_2H_4 centered at ~940 cm^{-1} with the well-resolved vibration-rotation lines of the NH_3 inversion doublet at ~950 cm^{-1}. No baseline-to-peak measurement of N_2H_4 can be made in the presence of significant NH_3 interference. In this case, the most appropriate procedure found is to measure the intensity of the fine structure at 974.36 cm^{-1}, which has been verified to be the least interfered feature that has an acceptable absorption coefficient. Peak-to-peak valley measurement is made between points corresponding to 974.36 cm^{-1} and 973.39 cm^{-1}. Despite the higher detection limit (Table A-1), concentration measurements of N_2H_4 by this procedure are more reliable than those evaluated by baseline-to-peak determinations. The concentration of NH_3 is then determined by subtracting the N_2H_4 absorptions based on the peak-to-valley (974.36 cm^{-1} to 973.39 cm^{-1}) intensity. The spectral stripping procedure is most conveniently done through the in-house interactive display feature of the data system.

Low-noise reference spectra of the known stable species were generated for use in the spectral subtraction process. The most desirable reference spectra are those recorded at the highest concentrations possible that still allow linear subtraction to be made. Since the subtraction process is purely

TABLE A-1. INFRARED MEASUREMENT FREQUENCIES AND ABSORPTION COEFFICIENTS OF THE HYDRAZINES AND THEIR REACTION PRODUCTS

Compound	Analytical Frequency (cm^{-1})	Absorption Coefficient $(cm^{-1}\ atm^{-1}$, base e)		Detection Limit at 460 m, 1 cm^{-1} Resolution (ppm)
N_2H_4	974.36	5.0	Present work	0.043
	$(974.36-973.39)$[a]	2.9	Present work	0.075
UDMH	909.75	7.0	Present work	0.031
	1144.55 (Q)[b]	3.0	Present work	0.072
MMH	772.35	8.8	Present work	0.025
	772.35 (Q)	6.4	Present work	0.035
H_2O_2	1251.58	9.0	Refs. 48 and 49	0.025
N_2O	2224 (P-branch max)	16	Present work	0.014
$(CH_3)_2N-NO$	1015.8	20	Present work	0.011
$(CH_3)_2N-NO_2$	1307	37	Reference 23	0.006
$CH_2=\overset{+}{N}=\bar{N}$	2087 (P-branch max)	11	Reference 50	0.020
CH_3OH	1034.14 (Q)	19	Present work	0.011
NH_3	931.45	24	Present work	0.009
	967.61	28	Present work	0.008
	993.16	17	Present work	0.013
O_3	1055.35	9.7	Reference 51	0.022
HONO(cis)	852.86 (Q)	71	Reference 48	0.010 (cis + trans)
HNO_3	879.38 (Q)	29	Present work	0.010
HCOOH	1105.49 (Q)	64	Present work	0.004

[a]Peak-to-valley measurement of fine structure
[b]Q-branch intensity only

78

arithmetic, the low factors allowed also reduce to a minimum the noise added to the residual spectrum.

The theoretical detection limits given in Table A-1 are based on 1% absorption (0.01 absorbance unit, base e) at a pathlength of 460 meters and 1 cm^{-1} resolution. For absorption bands located in the region of heavy H_2O interference [e.g., the 1307 cm^{-1} band of $(CH_3)_2NNO_2$], the detection limit can be as much as three times that of the value indicated. The detection sensitivity also varies according to the number of subtraction stages (which generate accumulative noise) incurred in arriving at a clear estimate of a species in the residual spectrum.

(The reverse of this page is blank.)

INITIAL DISTRIBUTION LIST

OASD(I&L)EES	1	SAALC/SFQT	1
OUSDR&E	1	SA-ALC/SFQ	1
OSAF/MIQ	1	Ch, Pollution Abatement Br	1
DTIC/DDA	12	NAVFAC Code 111	
ARPA	1	NESO	1
OSAF/PA	1	NCEL, Code 15111	1
HQ USAF/LEEV	2	U S Navy Ord Station/Code MEZ	1
HQ USAF/SGES	1	Commandant/GDD, USCG	1
AFMSC/SGPA	1	HQ NASA, Code MAS-7	1
HQ AFSC/DLWM	1	NASA/DL-DED-32	1
HQ AFSC/SD	1	DD-MED-41	1
HQ AFSC/DEV	1	NASA/MD-E	1
HQ AFSC/SGB	1	Library, Chemical Abstracts Service	1
AMD/RD	1	Toxic Matls Information Ctr	1
AMD/RDB	1	HQ AFESC/DEV	4
USAFOEHL/CC	3	HQ AFESC/TST	1
USAFSAM/EDE	2	HQ AFESC/RDV	10
USAFSAM/VNL	2	EPA/ORD	1
USAFSAM/CC	1	EPA Env Res Lab	1
AFOSR/CC	1	MIT Lincoln Laboratory	1
AFOSR/NL	1	AFWAL/THE	3
AFOSR/NA	1	AFIT/Library	1
AFOSR/NC	1	AFIT/DE	1
SD/SGX	1	HQ AFESC/RDVC	5
SD/DEV	2	Statewide Air Pollution Res Ctr	2
SD/LV-1	5		
OL-AD; USAF OEHL	1		
HQ AFISC/SG	1		
USAF Hospital Wiesbaden/SGB	3		
AUL/LSE 71-249	1		
HQ USAFA/Library	1		
USAFRCE/WR/DEEV	3		
USAFRCE/CR/DEEV	3		
USAFRCE/ER/DEEV	3		
U S Army, MIRADCOM	1		
Ch, Environmental Chem Div,USAEHA	1		
Cmdr, USA Med Bioengrg R&D Lab	2		
Ch, Industrial Hyg Div/USAEHA	2		
USA Chief, R&D/EQ	1		
SDSANQ-QS	1		
USN, Chief R&D/EQ	1		
SAMTEC/SEM	1		
6595 STESTG/SZ	1		
6595 STESTG/TS	1		
AFRPL/Library	1		
AFRPL/LKDP	1		
AFRPL/LKCP	1		
USAF Hospital Edwards/SGP	1		
AFATL/DLODL	1		
AFWL/SUL	1		
AFTEC/SG	1		
HQ SAC/DEPA	1		
1 STARD/SEM	1		
USAF Hospital Vandenberg/SGP	2		
6585 Test Group (TKS)	1		

DATE
ILME